Molecular Recognition and Self-Organization of Functionalized Porphyrin via Multi-Point Interactions

Ayato Kawashima

1997

Molecular Recognition and Self-Organization of Functionalized Porphyrin via Multi-Point Interactions

Ayato Kawashima

1997

Preface

The study presented in this thesis has been carried out under the direction of Professor Hisanobu Ogoshi during April, 1991-November, 1996, at the department of Synthetic Chemistry and Biological Chemistry at Kyoto University. This thesis is concerned with a construction of porphyrin assembling system by using molecular recognition and self-organization. The author is very happy that he has encountered with exciting phenomena and respectable persons during his course.

The author would like to express his supreme gratitude to Professor Hisanobu Ogoshi for his kindest guidance, valuable suggestions, and warm encouragement in the laboratory, in the car, on the tennis court, etc. The author also would like to express his sincere gratitude to Professor Yasuhisa Kuroda at Kyoto Institute of Technology for his constant discussions , valuable advice, and warm encouragement with Prince of Wales tea. The author wishes to express his deep gratitude to Associate Professor Tadashi Mizutani and Dr. Takashi Hayashi for their helpful advice and kind suggestions.

The author is thankful to Messrs. Keiji Ikeda, Tadashi Urai, Yuichirou Hayashi, and Takurou Kikuchi for their very active collaborations and all the other members of Ogoshi's group for their friendship, nice considerations, and kind help.

The author wish to thank Mr. Haruo Fujita and Mr. Tadao Kobatake for the measurement of NMR and Mass spectra.

Finally, the author expresses his deep appreciation to his parents, Mr. Yuuji Kawashima, Mrs. Misuzu Kawashima, his grand mother, Mrs. Tuyako Miyata, and his sister, Miss Madoka Kawashima for their affectionate encouragement throughout this work.

Ayato Kawashima

Department of Synthetic Chemistry and Biological Chemistry
Faculty of Engineering
Kyoto University

January, 1997.

Contents

General Introduction

Molecular Recognition and Self-Organization. Organization in biological systems is quite often the result of molecular association phenomena based on noncovalent intermolecular forces. Enzymes, genes, antibodies, ionophores, and other biological systems possess receptor sites that can selectively bind suitable substrates, giving rise to highly specific molecular recognition, transformation, and translocation processes which form the chemical basis of life. The design of artificial molecules capable of displaying processes with highest efficiency and selectivity requires the correct manipulation of the energetic and stereochemical features of the noncovalent intermolecular forces such as electrostatic interactions, hydrogen bonds, van der Waals forces, coordination, hydrophobic interactions, etc, within a defined molecular architecture. The first basic concept to explain such phenomena of enzymatic reactions is " lock and key" by Emil Fischer in 1894.[1] In the middle of this century,1967, C. J. Pedersen found the selective incorporation of metal cations by " crown ether" and this finding has strongly stimulated the imagination and ingenuity of chemist.[2] D. J. Cram and his group started the investigation of the molecular recognition by various kinds of newly synthetic model compounds. He conceptualized the molecular recognition as "preorganization" and "host guest chemistry".[3] Following his work a great variety of receptor molecules have been designed for effecting the recognition of numerous and very diverse types of substrates.[4] In most cases, however, molecular recognition between rigid molecules, i.e., static molecular recognition has been studied and few examples for the study of molecular recognition accompanied by structural changes of

molecules so-called " allosterism" and " induced fit" which is important as a trigger of following function in biological systems, have been investigated. Thus, relationships between structural change and successive chemical reactions or functions of artificial molecules are still unclear.

Recently, based on these many studies of molecular recognition, novel lines of investigation have developed the design of molecular devices and systems displaying higher forms of molecular and supramolecular behavior such as self-organization, regulation, cooperatively, communication, and replication. Well-defined structures in biological systems exist as functional units which are self-assembled with several molecular units. Typical example is DNA. DNA is existing as well-known double helix, but a part of it is sometimes broken. This partial dynamic structural change is essential for characteristic DNA functions such as replication, transcription, and repair. The macro-structure of DNA, however, will be always considered to be double helix. The self-assembled DNA structure determined by the pattern of the multi hydrogen bonding of complementary nucleic acid bases makes it possible that DNA breaks hydrogen bonding of double helix and still at the same time maintain its supramolecular structure. This flexible behaviour of DNA depends on its ability of self organization which involves precise recognition and positive cooperativity of each molecule.

J. M. Lehn developed self-assembling systems with highly defined structures, which led to the formation of "supramolecular chemistry".[5] Supramoecular chemistry is defined as "chemistry beyond the molecule" and this is the chemistry of the intermolecular bond, covering the structures and functions of the entities formed by association of two or more chemical species. According

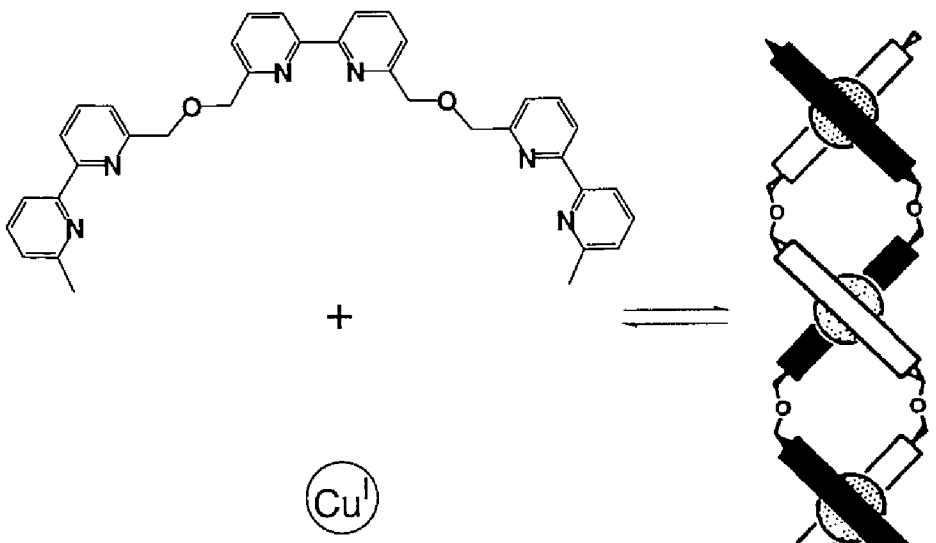

J. M. Lehn *et al.* (1987)

to this concept, he designed oligo-bipyridine-chain ligands incorporating two to five bipy groups.[6] By treatment with Cu(I) ions they underwent a spontaneous assembling into double stranded helicates containing two ligand molecules and one Cu ion per bipy site of each ligand, the two receptor strands being wrapped around the metal ions which hold them together. This spontaneous formation of an organized structure by intermolecular interaction is similar to that of DNA. These control of self organization at the molecular level opens ways to the design and consrtuction of self assembling systems presenting cooperativity, regulation, and amplification features in biology. Such artificial molecular design and engineering now become a field of major interest in chemistry. Various molecular self assembling systems such as helices,[7] macrocycles,[8] cages, [9] tubes,[10] grids,[11] interlocked systems,[12] etc., which are very difficult to be synthesized by normal organic syntheses have been produced according to these

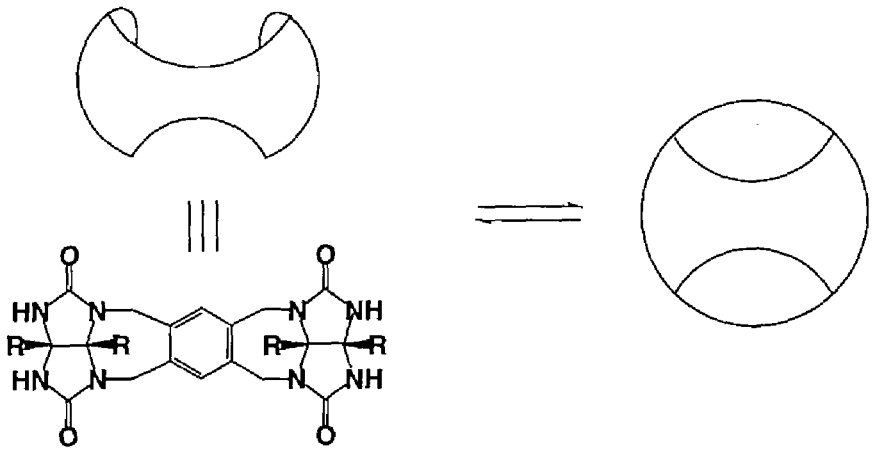

J. Rebek Jr. *et al.* (1993)

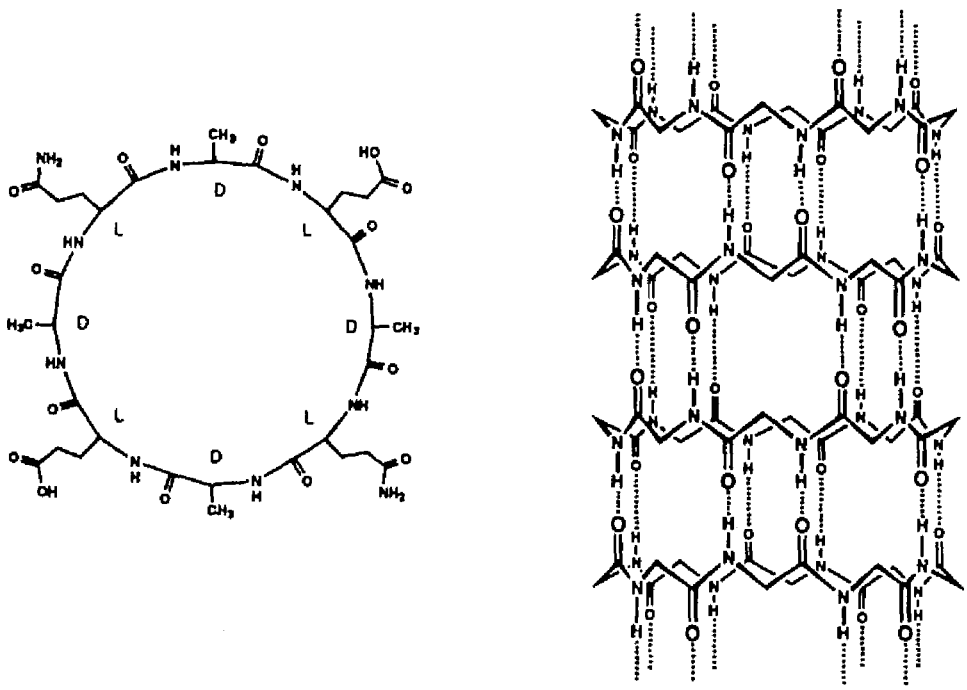

M. R. Ghadiri *et al.* (1994)

novel lines of investigations. In recent years highly well-defined functional structures are also reported. J. Rebek Jr. *et. al.* have reported the bowl-shaped molecule formed by dimerization of self-complementary structure by means of hydrogen bonds.[13] This dimer features a flattened spherical cavity of peculiar symmetry and acts as a host for the encapsulation of guest molecules of complementary shape. M. R. Ghadiri *et. al.* have reported the design of peptide nanotubes which were based on the two central methodology.[14] The first is that cyclic peptides made up of alternating D- and L-amino acid residues can adopt a flat ring-shaped conformation in which the backbone amide groups are approximately perpendicular to the plane of the ring and the second is that intermolecular hydrogen bonding and ring stacking interactions of peptide subunits would be energetically favored under appropriate conditions and would thus produce open-ended tubular ensembles. This peptide tube formed a self-assembled tubular transmembrane channel in a lipid bilayer and shows efficient ion and glucose transport activity. Such self organization as a method to construct artificial functional molecular systems has received much attention in recent years.

Electron and Energy Transfer. Photosynthesis plays a crucial role in biological systems for energy conversion from light into chemical energy. The central part of the photosynthetic molecular device is a noncovalently linked BChl-b dimer so-called "special pair". After its activation by light or by energy transfer from light-harvesting antenna complexes in the membrane, an electron moves from this special pair to an acceptor in almost 100% quantum yield through several electron and energy transfer steps. The recent determination of

the X-ray structures of crystals of the photosynthetic reaction center[15] and the light-harvesting antenna complexes[16] shows that the protein and cofactors such as chlorophyll, quinone, carotenoid, etc., form self assembling structures. First step to clarify the system of biological electron and energy transfer is the dissection of the complex reaction sequence into single steps at the molecular level. Several covalently linked porphyrin-quinone complexes, many of which mimic one or two steps of electron and energy transfer systems in biological systems, have been synthesized during the past two decades.[17] Furthermore, noncovalently linked donor-acceptor systems using hydrogen bonding or hydrophobic interaction have been reported recently.[18] All these model systems have brought a great number of insight into electron and energy transfer in biological systems. Due to their difficulties of synthesis and fixing orientation of each pigment, however, it is very difficult to extend these systems to three- and four- component model systems which are required for construction of more precise mimic of natural photosynthetic complexes composed of self organized multi pigments.

Survey of This Thesis. This thesis describes the construction of novel self-organized molecular systems consisting of two units. One unit is self-organized face-to-face porphyrin dimer formed by dynamic molecular recognition through the eight hydrogen bonds. During the dimer formation a new unique molecular recognition site is formed between the two porphyrin planes. This recognition site has high selectivity for bidentate ligands such as pyrazine. This specific recognition of bidentate ligands make it possible to connect the porphyrin dimer and a second unit which is necessary for further

Scheme 1

meso-tetrakis(2-carboxy-4-nonylphenyl)porphyrin

functionalization. This self-organized system using plural different intermolecular forces is useful for not only one of methods to make highly well-defined structure but also to construct porphyrin assembling system which would be readily extended as a model of photosynthesis.

In chapter 1, synthesis and self-induced porphyrin dimer formation of novel functional porphyrin, *meso*-tetrakis(2-carboxy-4-nonylphenyl) porphyrin (**1**), were investigated. Atropisomerization of porphyrin **1** starting from the mixture of 4 atropisomers in nonpolar solvents such as $CHCl_3$ gives the $\alpha\alpha\alpha\alpha$ isomer exclusively. UV-vis, IR, and NMR investigations of **1** suggest that the porphyrin exists as a face-to-face aggregate in nonpolar solvents. Furthermore, the molecular weight of porphyrin **1** in $CHCl_3$ by the method of vapor pressure osmometry clearly indicated dimer formation. These results show that porphyrin **1** forms self-assembled supramolecular aggregate in nonpolar solvents and the resulting aggregate is face-to-face porphyrin dimer through the eight hydrogen bonds among four pairs of carboxylic acids as shown in Scheme 1.

In chapter 2, computer analyses of unusual TPP atropisomerization containing equilibrium processes are described. Kinetic behavior of atropisomerization were analyzed directly by a non-linear least square optimization method which uses numerical integration of kinetic differential equations. As a plausible mechanism of unusual atropisomerization, four models which contain different rate or association constants are analyzed with new program REDAP (Reaction Dynamics Analysis Program). Analyses show the kinetic model 4 (Scheme 1) determined with one rate and two equilibrium constants gives the smallest residual square sum and excellent agreement with all kinetic traces.

In chapter 3, formation and molecular recognition of self-organized porphyrin dimer Zn complex are described. [5,10,15,20-tetrakis(2-carboxy-4-nonylphenyl)porphyrinato]zinc(II) (**2**) were investigated as the same manner of chapter 1 and these results suggest that the porphyrin aggregates in nonpolar solvents and the resulting aggregate is face-to-face porphyrin dimer through the eight hydrogen bonds among four pairs of carboxylic acids. This self-assembled porphyrin dimer has a cavity between the two porphyrin faces, the distance between the porphyrin planes is 8-9 Å, furthermore, top and bottom end are zinc as the coordination site. So this self-assembled cavity is available for molecular

Scheme 2

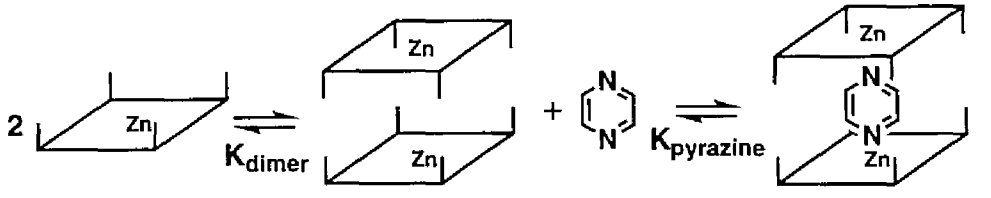

recognition site for bidentate ligands such as pyrazine. The complexations of aromatic amines such as pyrazine, pyridine, and so on with this porphyrin dimer were investigated. These experiments revealed that the incorporation of guests into porphyrin dimer was highly specific for pyrazine. The theoretical fitting for spectroscopic investigation as shown in Scheme 2 suggests that the equilibrium constant of porphyrin dimerization is $5x10^5M^{-1}$ and the binding constant with pyrazine is $1x10^{10}M^{-1}$.

In chapter 4, complex formation between pyrazine derivatives having a large side moiety and dimeric self-assembly of αααα-isomer of **2** to make the inside-outside connection was investigated. ^1H NMR and UV-vis titration experiments for this dimeric assembly with pyrazine derivatives show highly

specific 1:2 complex formation of pyrazine having long alkyl chains. The equilibrium constants for porphyrin dimer formation and 4-(2-pyrazinyl)-*N*-benzoylbutanamide (**5**) binding are estimated to be ca. 5 x 10^5 and ca. 2 x 10^7 M^{-1}, respectively. The most characteristic feature of the present ternary system, $(\mathbf{2})_2$• pyrazine, is that the pyrazine derivative having a large side moiety such as a benzoyl group can coordinate to two zinc atoms inside the dimer cavity by sticking the side moiety out of a window formed between hydrogen bond pillars

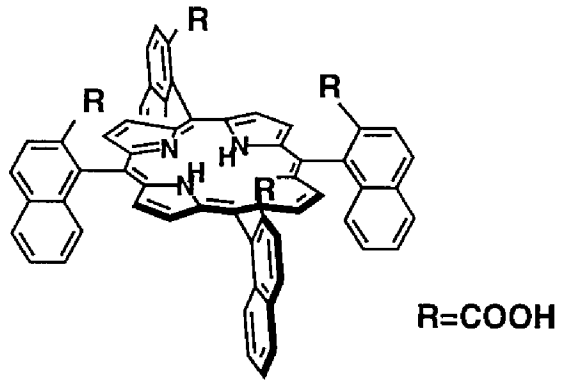

meso-tetrakis(2-carboxy-1-naphthyl)porphyrin

of the complex.

In chapter 5, synthesis and molecular recognition of *meso*-tetrakis(2-carboxy-1-naphthyl) porphyrin (**3**) are described. This porphyrin was designed to have four carboxylic acids as recognition sites. Four carboxylic acids on naphthyl rings were fixed since atropisomerization of porphyrin **3** is prohibited due to the steric hindrance of naphthyl rings at meso position. The interactions of various amines with porphyrin **1** were investigated by UV-vis absorption spectroscopy and association constants were determined by non linear least square optimization analysis of the absorbance changes of Soret band. Three types of

complexation, porphyrin **3** /amine = 1/1, 1/2, and 2/1 , were observed and their relative stability depends on the basicity and structure of each amine.

References

1) Fischer, E. *Ber. Chem.* **1894**, 27, 2985.

2) (a) Pedersen, C. *J. Am. Chem. Soc.* **1967**, 89, 2495. (b) Pedersen, C. *J. Am. Chem. Soc.* **1967**, 89, 7017.

3) Cram, D. J. *Angew. Chem. Int. Ed. Engl.* **1988**, 27, 1009.

4) Dugas, H. *Bioorganic Chemistry* , Springer-Verlag, New York.

5) (a) Lehn, J. M. *Science.* **1985**, 227, 849. (b) Lehn, J. M. *Angew. Chem. Int. Ed. Engl.* **1988**, 27, 89. (c) Lehn, J. M. *Angew. Chem. Int. Ed. Engl.* **1990**, 29, 1304.

6) Lehn, J. M.; Rigault, A.; Siegel, J.; Harrowfield, J.; Chevrier, B.; Moras, D. *Proc. Natl. Acad. Sci. USA* **1987**, 84, 2565.

7) (a) Koert, U.; Harding, M. M.; Lehn, J. M. *Nature* **1990**, 346, 339. (b) Constable, E. C. *Tetrahedron* **1992**, 48, 10013. (c) Constable, E. C.; Edwards, A. J.; Hannon, M. J.; Tocher, D. A. *J. Chem. Soc., Chem. Commun.* **1994**, 1991. (d) Potts, K. T.; Keshavarz-K, M.; Tham, F. S.; Raiford, K. A. G.; Arana, C.; Abruna, H. D. *Inorg. Chem.* **1993**, 32, 5477. (e) Williams, A. F.; Piguet, C.; Bernardinelli, G. *Angew. Chem. Int. Ed. Engl.* **1991**, 30, 1490. (f) Zarges, W.; Hall, J.; Lehn, J. M.; Bolm, C. *Helv. Chim. Acta* **1991**, 74, 1843. (g) Charbonniere, L. J.; Bernardinelli, G.; Piguet, C.; Sargenson, A. M.; Williams, A. F. *J. Chem. Soc., Chem. Commun.* **1994**, 1419.

8) (a) Maverick, A. W.; Klavetter, F. E. *Inorg. Chem.* **1984**, 23, 4129. (b) Fujita, M.; Yazaki, J.; Ogura, K. *J. Am. Chem. Soc.* **1990**, 112, 5645. (c) Drain, C. M.; Lehn, J. M. *J. Chem. Soc., Chem. Commun.* **1994**, 2313. (d) Ruttimann, S.; Bernardinelli, G.; Williams, A. F. *Angew. Chem. Int. Ed. Engl.* **1993**, 32, 392. (e) Yang, J.; Fan, E.; Geib, S. J.; Hamilton, A. D. *J. Am. Chem. Soc.* **1993**, 115,

5314. (f) Mackay, L. G.; Wylie, R. S.; Sanders, J. K. M. *J. Am. Chem. Soc.* **1994**, 116, 3141.

9) (a) Saalfrank, R. W.; Stark, A.; Bremer, M.; Hummel, H. U. *Angew. Chem. Int. Ed. Engl.* **1990**, 29, 311. (b) Lofthagen, M.; Chadha, R.; Siegel, J. S. *J. Am. Chem. Soc.* **1991**, 113, 8785.(c) Fujita, M.; Nagao, J.; Ogura, K. *J. Am. Chem. Soc.* **1995**, 117, 1649. (d) Baxter, P.; Lehn, J. M.; Decian, A. *Angew. Chem. Int. Ed. Engl.* **1993**, 32, 69. (e) Robert, G.; Sherman, J. C. *J. Am. Chem. Soc.* **1995**, 117, 9081.

10) (a) Klufers, P.; Schuhmacher, J. *Angew. Chem. Int. Ed. Engl.* **1994**, 33, 1863. (b) Harada, A.; Li, J.; Kamachi, M. *Nature* **1993**, 364, 516. (c) Li, G.; Mcbown, L. B. *Science* **1994**, 264, 249. (d) Bell, T. W.; Cragg, P. J.; Drew, M. B. G.; Firestone, A.; Kwok, D. I. A. *Angew. Chem. Int. Ed. Engl.* **1992**, 31, 348.

11) (a) Baxter, P. N. W.; Lehn, J. M.; Fischer, J.; Youinou, M. T. *Angew. Chem. Int. Ed. Engl.* **1994**, 33, 2284. (b) Youinou, M. T.; Rahmouni, N.; Fischer, J.; Osborn, J. A. *Angew. Chem. Int. Ed. Engl.* **1992**, 31, 733.

12) (a) Buchecker, C. O. D.; Sauvage, J. P.; Kintzinger, J. P. *Tetrahedron Lett.* **1983**, 24, 5095. (b) Nierengarten, J. F.; Buchecker, C. O. D.; Sauvage, J. P. *J. Am. Chem. Soc.* **1994**, 116, 375. (c) Ashton, P. R.; Goodnow, T. T.; Kaifer, A. E.; Reddington, M. V.; Slawin, A. M. Z.; Spencer, N.; Stoddart, J. F.; Vicent, C.; Williams, D. J. *Angew. Chem. Int. Ed. Engl.* **1989**, 28, 1396. (d) Amabilino, D. B.; Ashton, P. R.; Reder, A. S.; Spencer, N.; Stoddart, J. F. *Angew. Chem. Int. Ed. Engl.* **1994**, 33, 1286. (e) Ogino, H. *J. Am. Chem. Soc.* **1992**, 114, 3136. (f) Bissell, R. A.; Cordova, E.; Kaifer, A. E.; Stoddart, J. F. *Nature* **1994**, 369, 133. (g) Livoreil, A.; Buchecker, C. O. D.; Sauvage, J. P. . *Am. Chem. Soc.* **1994**, 116, 9399.

13) (a) Valdes, C.; Spitz, U. P.; Toledo, L. M.; Kubik, S. W.; Rebek, J., Jr. *J. Am. Chem. Soc.* **1995**, 117, 12733. (b) Grotzfeld, R. M.; Branda, N.; Rebek, J., Jr. *Science*, 1996, 271, 487.

14) (a) Ghadiri, M. R.; Granja, J. R.; Milligan, R. A.; Mcree, D. E.; Khazanovich, N. *Nature* **1993**, 366, 324. (b) Ghadiri, M. R.; Granja, J. R.; Buehler, L. K. *Nature* **1994**, 369, 301. (c) Granja, J. R.; Ghadiri, M. R. *J. Am. Chem. Soc.* **1994**, 116, 10785. (d) Kobayashi, K.; Granja, J. R.; Ghadiri, M. R. *Angew. Chem. Int. Ed. Engl.* **1995**, 34, 95.

15) (a) Deisenhofer, J.;Epp, O.; Miki, K.; Huber, R.; Michel, H. *J. Mol. Biol.* **1984**, 180, 385-398. (b) Allen, J. P.; Feher, G.; Yeates, T. O.; Rees, D. C. ; Deisenhofer, J.; Michel, H.; Huber, R. *Proc. Natl. Acad. Sci. USA.* **1986**, 83, 8589.

16) McDermott, G.; Prince, S. M.; Freer, A. A.; Hawthornthwaite-Lawless, A. M.; Papiz, M. Z.; Cogdell, R. J.; Isaacs, N. W. *Nature* **1995**, 374, 517.

17) (a) Wasielewski, M. R. *Chem. Rev.* **1992**, 92, 435. (b) Balzani, V.; Scandola, F. *Supramolecular Photochemistry* , Ellis Horwood, Chichester, 1991.

18) (a) Tecilla, P.; Dixon, R. P.; Slobodkin, G.; Alavi, D. S.; Waldeck, D. H.; Hamilton, A. D. *J. Am. Chem. Soc.* **1990**, 112, 9408. (b) Harriman, A.; Kubo, Y.; Sessler, J. L. *J. Am. Chem. Soc.* **1992**, 114, 388. (c) Turro, C.; Chang, C. K.; Leroi, G. E.; Cukier, R. I.; Nocera, D. G. *J. Am. Chem. Soc.* **1992**, 114, 4013. (d) Aoyama, Y.; Asakawa, M.; Matsui, Y.; Ogoshi, H. *J. Am. Chem. Soc.* **1991**, 113, 6233. (e) Kuroda, Y.; Ito, M.; Sera. T.; Ogoshi, H. *J. Am. Chem. Soc.* **1993**, 115, 7003.

Self-induced Porphyrin Dimer Formation *via* Unusual Atropisomerization of Tetraphenylporphyrin Derivative

Abstract

A novel functional porphyrin, *meso*-tetrakis(2-carboxy-4-nonylphenyl) porphyrin (**1**), was designed to have four carboxylic acids as recognition sites and long alkyl chains at the phenylrings to provide enough solubility in organic solvents. Atropisomerization of porphyrin **1**, in nonpolar solvents such as $CHCl_3$ gives the αααα isomer exclusively, while the same isomerization in polar solvents such as DMSO proceeds statistically, giving four atropisomers with the ratio αβαβ:ααββ:αααβ:αααα=1:2:4:1. UV-vis, IR, and NMR investigations of a solution of **1** suggest that the porphyrin exists as a face-to-face aggregate in nonpolar solvents. Furthermore, the molecular weight of porphyrin **1** in $CHCl_3$ determined by the method of vapor pressure osmometry undoubtedly indicated dimer formation. These results show that porphyrin **1** forms self-assembled supramolecular aggregate in nonpolar solvents and the resulting aggregate is face-to-face porphyrin dimer through the eight hydrogen bonds among four pairs of carboxylic acids.

Introduction

Porphyrin dimers have been attracting particular attention of chemists for their characteristic chemical and physical properties relating to those of biological systems such as photosynthetic centers.[1] On the basis of such biomimetic interest, various types of synthetic methods have been developed to prepare artificial porphyrin dimers, where two porphyrin molecules were connected with covalent bonds.[2] Another interesting approach to the construction of porphyrin dimers is to utilize self-assembling functions based on molecular recognition. There have been several examples of such spontaneous dimeric porphyrin formation systems designed to use hydrogen bonds or ligand coordination as associative interactions between two porphyrin molecules.[3] These self-assembling systems usually consist of a single equilibrium process and their selectivity for dimer formation is mainly determined by spatial arrangement of interacting groups attached on the porphyrins. We report here a novel self-assembling system for porphyrin dimer formation which is accompanied by conformational change of the monomeric porphyrin. The observed self-assembling process is so highly selective for dimer formation that, even starting from a mixture of undesired monomeric porphyrin isomers, the system gives the practically pure dimer of the single isomer.

Results and Discussion

The porphyrin used in this work is *meso*-tetrakis(2-carboxy-4-nonylphenyl)porphyrin **1**, which was prepared according to Scheme I. Methyl 2-formyl-5-nonylbenzoate (**8**) as a precursor of porphyrin **1** was prepared from p-bromobenzaldehyde (**3**) in five steps. Condensation of **8** and pyrrole gave *meso*-tetrakis(2-methoxycarbonyl-4-nonylphenyl)porphyrin (**2**) as a mixture of 4 atropisomers in 48 % yield. The precursor porphyrin **2**, was easily hydrolyzed in aq. 15M NaOH/THF solution to afford **1** in 70 % yield. Although the analogous porphyrin, *meso*-tetrakis(2-carboxyphenyl)porphyrin having no nonyl group, is known as an intermediate in functionalized porphyrin synthesis, its detailed characteristics such as an atropisomeric distribution has not been studied because of its insolubility in organic solvents.[4] In contrast, the present porphyrin **1** is highly soluble in usual organic solvents and, therefore, may be suitable for

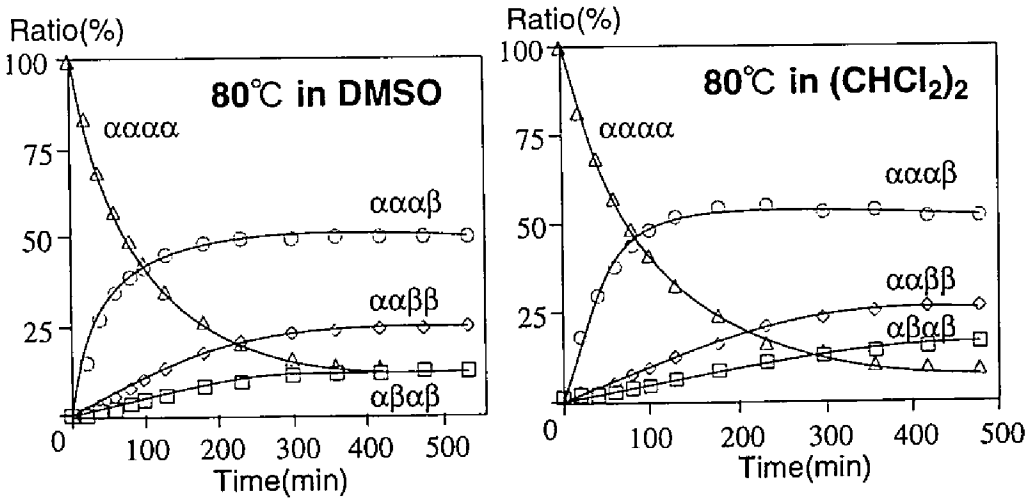

Figure 1. Thermal atropisomerization of $TPP(CO_2CH_3)_4$ in DMSO and $(CHCl_2)_2$ at 80℃.

Scheme I

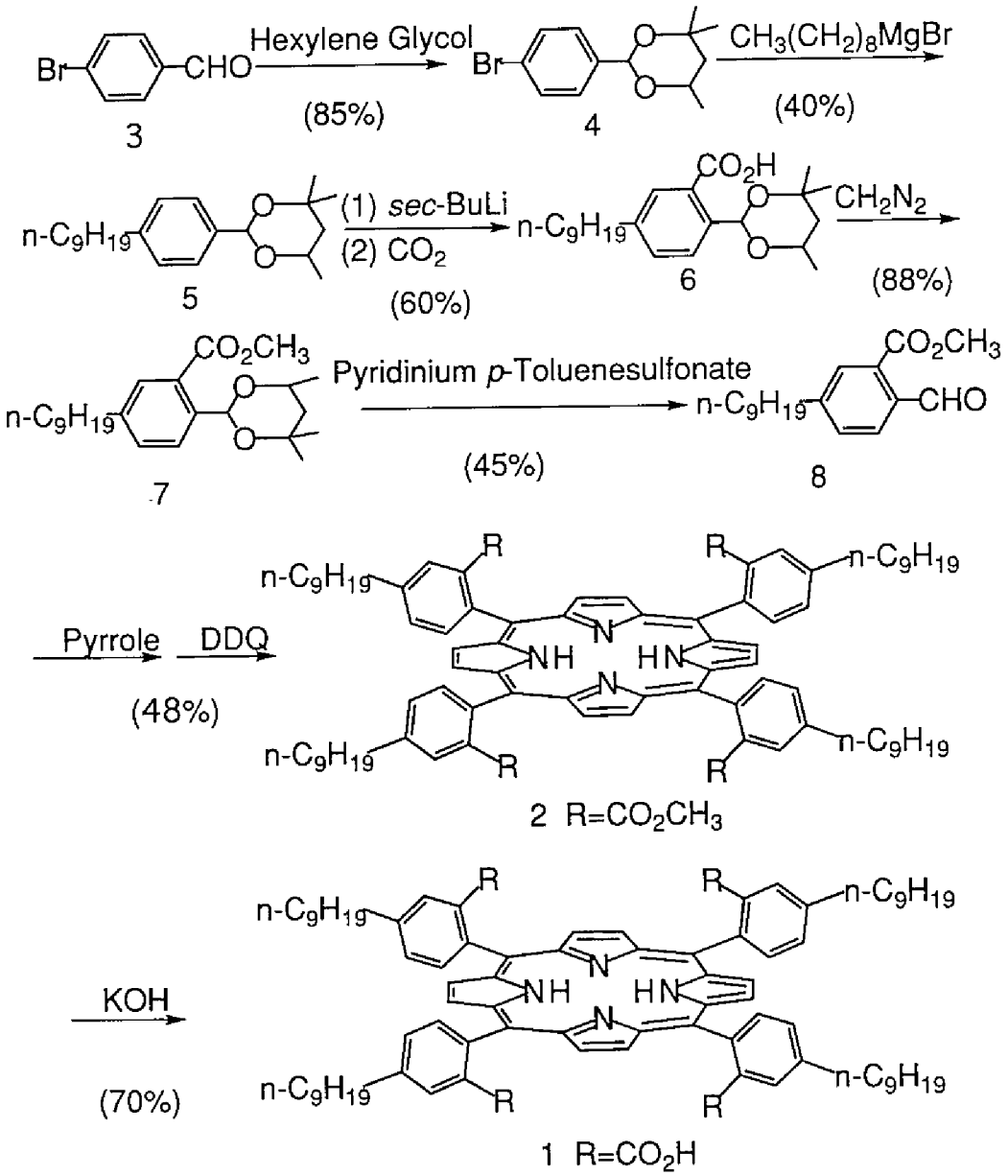
Br
CHO
Hexylene Glycol
(85%)
3
Br
4
$CH_3(CH_2)_8MgBr$
(40%)
$n\text{-}C_9H_{19}$
(1) *sec*-BuLi
(2) CO_2
(60%)
5
CO_2H
6
CH_2N_2
(88%)
CO_2CH_3
Pyridinium *p*-Toluenesulfonate
(45%)
7
CHO
8
Pyrrole
DDQ
(48%)
R
N
NH
HN
2 R=CO_2CH_3
KOH
(70%)
1 R=CO_2H

investigations of its solution properties.

The distribution of atropisomers of **2** was easily determined by using usual reverse phase HPLC column[5] and the equilibrated solution shows the normal statistical distribution, i.e., αβαβ:αααβ:αααα= 1 : 2 : 4 : 1[6] as shown in Figure 1. Although there was no appropriate direct method to analyze an atropisomer distribution of **1**, esterification of **1** with diazomethane at room temperature showed to give **2** quantitatively without any disturbance of the original distribution. Thus, we tried to determine the atropisomer distribution of **1** in various organic solvents.

Experiments of thermal equilibration in sealed tubes at 80 °C for 15 h showed interesting behavior of **1** which was quite different from that of **2**. The most interesting point is that the atropisomerization of **1** is highly solvent-dependent and there are clear two groups of solvents which give distinct results each other; that is, one is the group of relatively polar solvents such as THF, acetone, dioxane and DMSO in which the isomerization proceeds normally to

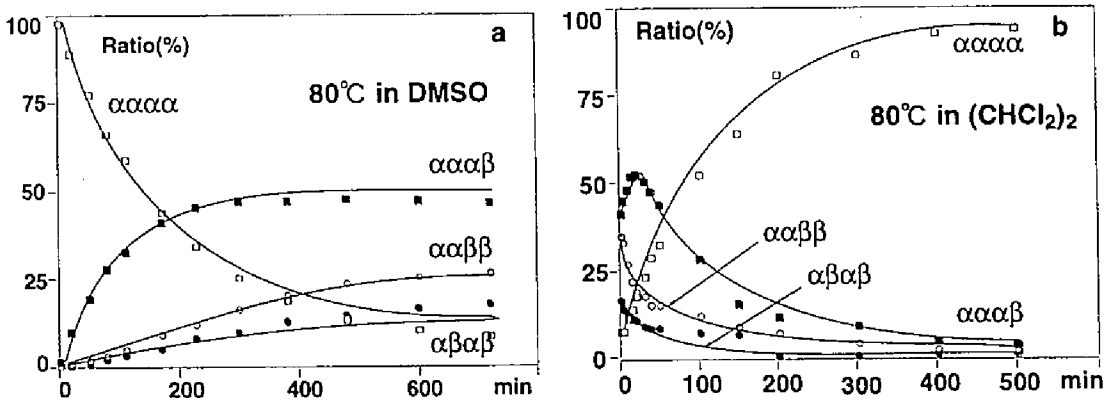

Figure 2. Thermal atropisomerization of $TPP(CO_2H)_4$ in DMSO and $(CHCl_2)_2$ at 80℃.

afford nearly statistical mixture of four isomers, and another is that of relatively nonpolar solvents such as $CHCl_3$, CCl_4, $CHCl_2CHCl_2$ and benzene in which the αααα isomer is unusually enriched after thermal equilibration. The final contents of the αααα isomer in these nonpolar solvents are over 95, 99, 99 and 95 %, respectively. The typical kinetic traces of present atropisomerization are shown in Figure 2. The data clearly show monotonous increase of the αααα isomer in $CHCl_2CHCl_2$, which is in sharp contrast to monotonous decrease of the same isomer in DMSO. These results suggest that the αααα isomer was anomalously stabilized in the nonpolar solvents in spite of its thermodynamic and/or statistic disadvantage.[7] It should be also noted that the system contains no second additive, which is necessary to induce the αααα isomer in previously reported systems showing similar large deviation from statistical atropisomeric equilibration of TPP type porphyrins.[8]

In order to clarify the origin of the present unusual stabilization of the

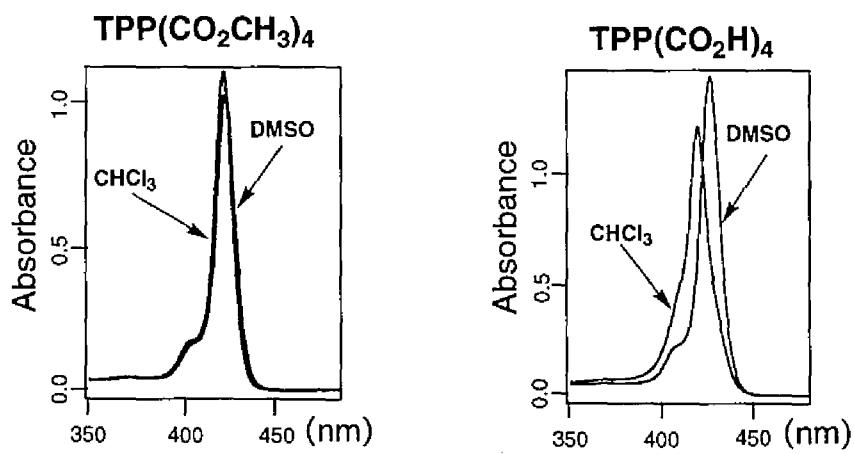

Figure 3. The absorption spectra of αααα-atropisomer of $TPP(CO_2CH_3)_4$ and $TPP(CO_2H)_4$.

αααα isomer of **1**, we investigated its spectroscopic properties in various solvents.

The UV-vis spectra of porphyrin **2** were almost the same in both polar and non-polar solvents as shown in Figure 3. In contrast, the Soret band for **1** in non-polar solvent, $CHCl_3$, shifts from 426nm to 416nm and the shoulder peaks at 400nm-415nm disappears. These spectral changes are in agreement with the features of a face-to-face porphyrin dimer previously reported.[9]

The infrared spectrum of C=O region of the αααα-atropisomer of porphyrin **1** and **2** are shown in Table 1. In THF and CH_2Cl_2, C=O stretching of **2** are not different, while, the stretching of **1** are 1701cm^{-1} and 1727cm^{-1},

Table 1. Infrared spectral data of C=O region for $TPP(CO_2CH_3)_4$ and $TPP(CO_2H)_4$.

	in THF	in CH_2Cl_2
1 $TPP(CO_2CH_3)_4$	1727cm^{-1}	1727cm^{-1}
2 $TPP(CO_2H)_4$	1721cm^{-1}	1701cm^{-1}

respectively. This result strongly indicates hydrogen bond formation between two carboxylic acid moieties in the nonpolar solvent.

The ^{1}H-NMR chemical shift differences between the αααα-atropisomer of porphyrin **1** and **2** in THF, DMSO and $CDCl_3$ are summarized in Figure 4. In DMSO and THF, the chemical shifts of both **1** and **2** behave very similarly and only in $CDCl_3$, the large differences for these chemical shifts were observed. These observations also indicate the aggregation of porphyrin in nonpolar

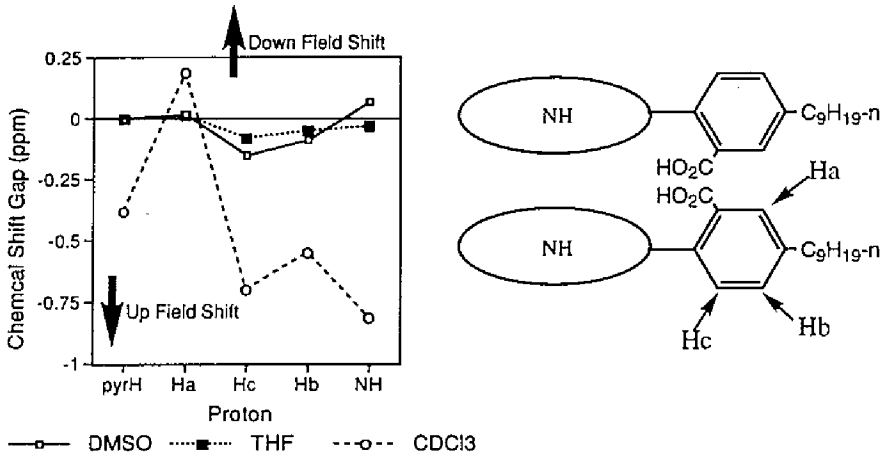

Figure 4. ^{1}H-NMR chemical shift differences between $TPP(CO_2CH_3)_4$ and $TPP(CO_2H)_4$ in $CDCl_3$, THF and DMSO.

solvent.

All of these observations strongly suggest that **1** generates some kind of molecular assembly in nonpolar solvents via hydrogen bond formation between carboxylic acid moieties. Based on these results, we measured molecular weight of **1** in $CHCl_3$ and THF by the method of vapor pressure osmometry. The results undoubtedly indicated dimer formation in $CHCl_3$ and monomeric state in THF, i.e., observed molecular weight of **1** in $CHCl_3$ and THF were 2680 ± 200 and 1260 ± 100 respectively, which are in excellent agreement with those of dimer (M.W.=2588) and monomer (M.W.=1294). Considerations of molecular models reveal the face-to-face dimer of **1** shown in Figure 5 as the most plausible structure.

Base on these observation, we proposed the mechanism for this atropisomerization as shown in Scheme II. The equilibrium constant for dimer formation is estimated to be lager than 10^7 M^{-1} at 80 °C, which corresponds to the stabilization energy of 11 kcal/mol. The eight hydrogen bonds among

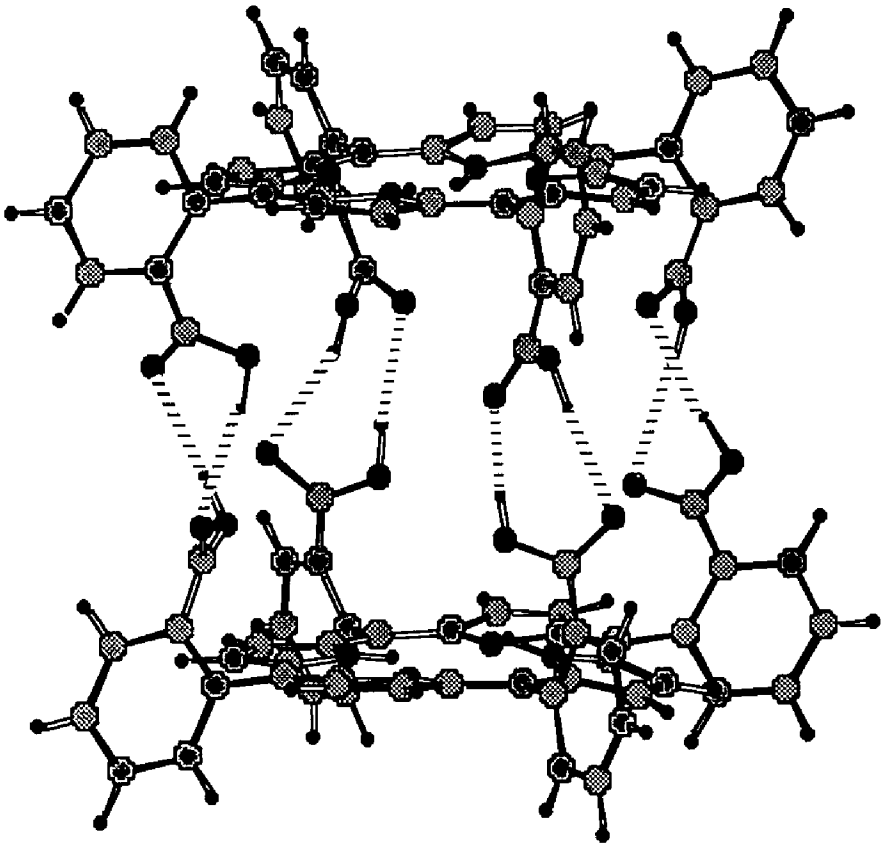

Figure 5. A plausible structure of dimeric **1**. Dashed lines show hydrogen bonds, length of which is 1.9 ± 0.1 Å. The nonyl chains were omitted.

Scheme II

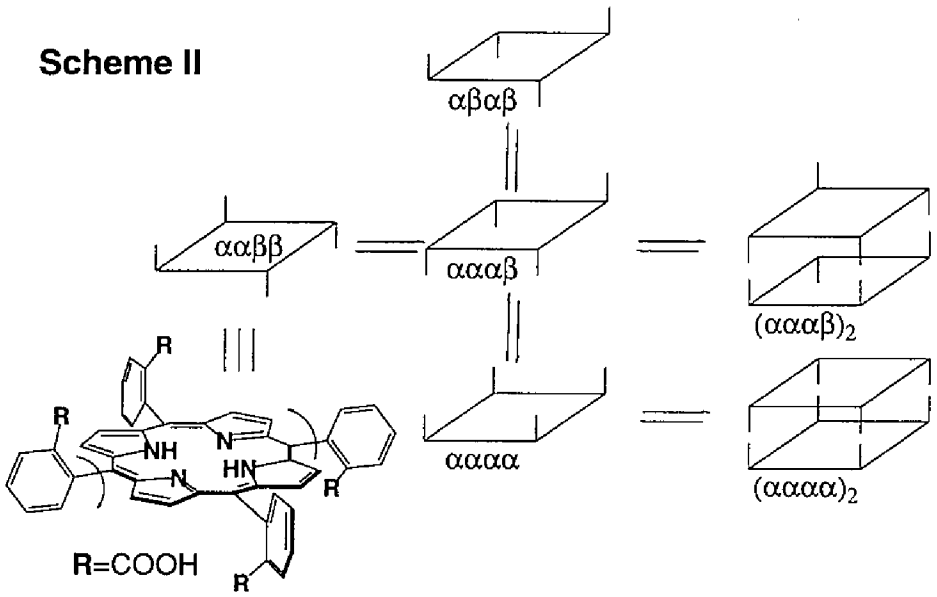

four pairs of carboxylic acids in the dimer not only explain the observed stabilization energy but also give the origin of the driving force for present self-induced dimerization where phase matched atropisomerization to yield the αααα isomer is required.

Experimental Section

General Remarks. ^{1}H-NMR spectra were recorded on a JEOL FX-90Q (90 MHz), a JEOL GX-400 (400MHz) or a JEOL α-500 (500MHz). ^{1}H-NMR chemical shifts are referenced to internal $CDCl_3$ (^{1}H δ7.25 ppm) relative to Me_4Si at 0 ppm. Electronic absorption spectra were performed on a Hitachi U-3410 spectrometer, Multi-channel Photodiode Array Spectrometer, Otsuka Electronics MCPD-100 or Hewlett-Packard HP-8452A, thermostated at given temperatures with a circulation system, NESLAB Instruments, Inc. RTE-9. IR spectra were recorded on PERKIN ELMER System2000 FT-IR. Vapor pressure osmometory measurement were performed on CORONA 117. Mass spectra were obtained with a JEOL JMS DX-300 or a JEOL JMS-SX102A mass spectrometer. HPLC experiments were performed on a TOSOH HLC-837 or Waters M600E equipped with a TOSOH UV-8010 variable-wavelength detector and Waters M991 Photodiode Array Detector.

Materials. Solvents used in spectral measurement were Spectrosol purchased from Nacalai Tesque, Inc.or Dojindo Laboratories. Other commercially available chemicals were purchased from Wako Pure Chemical Industries, Ltd. or Nacalai Tesque, Inc., or Tokyo Kasei Kogyo Co., Ltd. and employed without further purification, unless stated otherwise. Analytical thin-layer chromatography was performed with pre-coated Merck silica gel 60, F254 (0.2mm layers on glass plates). Column chromatography was performed using Merck Kieselgel 60 or WAKOgel LP-40C18.

4,4,6-Trimethyl-2-(4-bromophenyl)-1,3-dioxane (**4**). A 200-ml round-bottomed flask was charged with 50 g(0.27 mmol) of *p*-bromobenzaldehyde, 38ml of 2-methylpentane-2,4-diol, 13 mg of p-toluenesulfonic acid monohydrate, and 58 ml of toluene. The flask was attached to water separator under a reflux condenser fitted with a drying tube. The flask was heated and the reaction mixture was refluxed until close to the theoretical amount of water was collected in the trap. The reaction mixture was cooled to room temperature, extracted several times with ether, washed with 5% sodium hydroxide solution and water. After evaporation, the resulting mixture was loaded on silica gel column eluting with n-hexane: ethyl acetate=5:1 to give 65.72 g (85.4 %) of **4** as a white solid; *Rf*0.55 (*n*-hexane: ethyl acetate=5:1) ; ^{1}H NMR (500 MHz, $CDCl_3$) δ 7.47 (d, 2 H), 7.38 (d, 2 H), 5.69 (s, 1 H), 4.07 (m, 1 H), 1.58-1.49 (m, 2 H), 1.40 (s, 3 H), 1.32 (s, 3 H), 1.27 (d, 3 H) ; MS *m/e* 285 (M^+).

4,4,6-Trimethyl-2-(4-nonylphenyl)-1,3-dioxane (**5**). A 500-ml three-necked flask, equipped with a pressure-equalizing dropping funnel and a reflux condenser attached to a nitrogen inlet was charged with 60 g of **4**, 690 mg of dichloro[1,3-bis(diphenylphosphino)propane]nickel(II), and 103.5 ml of anhydrous ether. The Grignard reagent prepared from 1-bromononane and magnesium was transfered into the dropping funnel and added over 10 min, with stirring, while cooled in an ice bath. The reaction mixture was allowed to warm and refluxed with stirring for 119 h. The progress of reaction was checked with gas chromatography (column SE-30, 3 m, gradient 100 °C-250 °C, flow rate 1.0 ml/min). The retention time of **5** was 15.5 min. The mixture was cooled in an ice

bath and cautiously hydrolyzed with 1 M hydrochloric acid. The organic layer was separated and the aqueous layer extracted with ether. The organic layer and extracts were washed with water and dried. After evaporation the residue was distilled at 2 mmHg 80 °C to remove undesired compounds, then, the mixture is loaded on silica gel column eluting with *n*-hexane: ethyl acetate=7:1 to give 28 g (36.5 %) of **5** as a colorless liquid.; R_f 0.82 (*n*-hexane: ethyl acetate=5:1); ^{1}H NMR (500 MHz, $CDCl_3$) δ 7.38 (d, 2 H), 7.16 (d, 2 H), 5.72 (s, 1 H), 4.08 (m, 6 H), 2.58 (t, 2 H), 1.58-1.22 (m, 25 H), 0.88 (t, 3 H); MS *m/e*332 (M^+).

2-(2,6-Dioxa-3,3,5-trimethylcyclohexyl)-5-nonylbenzoic acid (**6**). A two-necked round bottomed flask equipped with a pressure-equalizing dropping funnel and a nitrogen inlet tube were charged with 10 g of **5** (30 mmol), 10 ml (67 mmol) of tetramethylethylenediamine, and 600 ml of *n*-hexane. The mixture was cooled to -40°C in a liq. nitrogen and tetrahydrofuran bath. Sec-Butyl lithium (67 mmol) was slowly added with maintaining the temperature at -40°C. The reaction mixture was allowed to warm to room temperature and stirring continued until anion formation was complete (2 to 3 h). The preformed orange anion was carefully added to excess dry ice and stirred for 2 h. The solution was washed with 1 M NaOH, brine, and water, dried over Na_2SO_4, filtered, and concentrated in vacuo. The residue was purified by column chromatography (eluted with *n*-hexane:ether=7:2) to give 7.5 g (66 %) of **6** as a white solid.; R_f 0.66 (diethyl ether); ^{1}H NMR (500 MHz, $CDCl_3$) δ 7.79 (d, 1 H), 7.63 (d, 1 H), 7.35(dd, 1 H), 6.25 (s, 1 H), 4.16 (m, 1 H), 2.62 (t, 2 H), 1.7-1.2 (m, 25 H), 0.86 (t, 3 H); MS *m/e* 376 (M^+).

Methyl 2-(2,6-dioxa-3,3,5-trimethylcyclohexyl)-5-nonylbenzoate (**7**). A 100-ml round bottomed flask was charged with 6 g of **6** and 20 ml of ether. Diazomethane ether solution produced in a similar manner as ref.[10] was added until the reaction was complete. The reaction mixture was evaporated and concentrated in vacuo. The residue was purified by column chromatography (eluted with *n*-hexane:diethyl ether=7:3) to give 5.3 g (85.2 %) of **7** as a colorless liquid.; R_f 0.74 (*n*-hexane: diethyl ether=7:3); ^{1}H NMR (500 MHz, CDCl3) δ 7.77 (d, 1 H), 7.58 (d, 1 H), 7.33(dd, 1 H), 6.45 (s, 1 H), 4.10 (m, 1 H), 3.89 (s, 3 H), 2.60 (t, 2 H), 1.6-1.2 (m, 25 H), 0.87 (t, 3 H); MS *m/e* 390 (M^+).

Methyl 2-formyl-5-nonylbenzoate (**8**). A 200-ml flask equipped with a reflux condenser was charged with 5.3 g of **7**, 95 ml of MeOH, 5 ml of H_2O, and 345 mg of pyridinium *p*-toluenesulfonate. The flask was heated and the reaction mixture was refluxed at 60°C under N_2 atmosphere until the reaction was finished (27 h). The reaction mixture was extracted with ether, washed with water, dried over Na_2SO_4, filtered, and concentrated in vacuo. The residue was purified by column chromatography (eluted with *n*-hexane:CH_2Cl_2=1:2) to give 2.32 g (43.8 %) of product as a colorless liquid.; R_f 0.5 (*n*-hexane:CH_2Cl_2=1:2); ^{1}H NMR (500 MHz, $CDCl_3$) δ 10.55 (s, 1 H), 7.88 (d, 1 H), 7.76 (d, 1 H), 7.45 (dd, 1 H), 3.97 (s, 3 H), 2.70 (t, 2 H), 1.7-1.2 (m, 14 H), 0.88 (t, 3 H); MS *m/e* 290 (M^+).

meso-Tetrakis(2-methoxycarbonyl-4-nonylphenyl)porphyrin (**2**). This porphyrin was synthesized with Lindsey's method.[11] A 1-L two-necked round bottomed flask equipped with a septum and nitrogen inlet tube was charged with

1.5 g (5.2 mmol) of **8**, 500 ml of CH_2Cl_2 (distilled from CaH_2), and 0.36 ml (5.2 mmol) of pyrrole. After the solution was purged with N_2 for 5 min, 0.21 ml (1.7 mmol) of $BF_3{\cdot}OEt_2$ was added via syringe. The room temperature reaction was monitored by removing 50 μl aliquots and oxidizing with excess 2,3-dichloro-5,6-dicyano-*p*-benzoquinone, followed by absorption spectroscopy. After 1.5 h, the solution of 0.85 g (3.7 mmol) of DDQ in 30 ml of toluene and 30 ml of MeOH was added. After 10 min (this procedure was also monitored by absorption spectroscopy), 1 equiv of triethylamine was added and the reaction mixture was rotary evaporated to dryness. The residue was purified by column chromatography (eluted with *n*-hexane:ethyl acetate=5:1) to give 841 mg (48.1 %) of **2** as a purple solid.; Rf αβαβ, ααββ=0.62 , αααβ=0.55 αααα=0.38 (*n*-

Table 2. Proton NMR Chemical Shifts for the four Atropisomers of $TPP(CO_2CH_3)_4$.

isomers	H_{pyr}	Hphenyl			$C_1(t)^{1)}$	$CH_3(s)$	$C_2(m)^{1)}$	$NH_{pyr}(s)$
		meta1[1]	ortho(d)	meta2(d)				
α α α α	8.60(s)	8.19(s)	7.96	7.58	2.97	2.84	1.92	-2.43
α α β β	8.58 8.63	8.17(s)	8.03	7.62	2.98	2.65	1.92	-2.47
α α α β	8.61(m)	8.18(m)	8.02	7.62	2.98	2.56 2.69 2.81	1.92	-2.44
α β α β	8.55(s)	8.11(s)	8.06	7.61	2.97	2.82	1.92	-2.46

1) 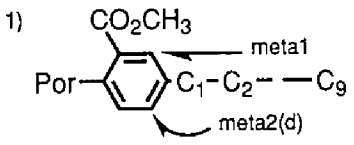

hexane: ethyl acetate=5:1); ^{1}H-NMR (500 MHz, $CDCl_3$) (αααα atropisomer): δ 8.60 (s, 8H), 8.19 (d, J=2.0Hz, 4H), 7.96 (d, J=8.0Hz, 4H), 7.59 (dd, J=8.0,2.0, 4H), 2.97 (t, J=8.0Hz, 8H), 2.84 (s,12H), 1.92 (m, 8H), 1.6-0.9 (several peaks, 60H), -2.43 (s, 2H); FAB MS 1351$(M+H)^+$; UV-vis (CH_2Cl_2) λmax (logε) 424nm (5.53), 520 (4.22), 556 (3.94), 598 (3.73), 658 (3.65).

meso-Tetrakis(2-carboxy-4-nonylphenyl)porphyrin (**1**). A 20 ml of flask fitted with reflux condenser was charged with 57.4 mg of **2**, 5.7 ml of THF, and 5.7 ml of 15 M KOH aq. The reaction mixture was heated at 60°C under N_2 atmosphere with vigorously stirring. After 2 days, the reaction mixture was cooled and the solution was made acidic (pH≈1) with 1 M HCl, extracted with ether, washed with water, dried over Na_2SO_4, and concentrated in vacuo. The residue was purified by reverse phase column chromatography (Wakogel LP-40C18, eluted with MeOH) to give 38.5 mg (70%) of **1** as a purple solid.; **1**(αααα atropisomer):^{1}H-NMR (500 MHz, THF) δ 8.56 (s, 8H), 8.22 (d, J=1.8Hz, 4H), 7.96 (d, j=7.5Hz, 4H), 7.65 (dd, J=7.5,1.8Hz, 4H), 2.99 (t, J=7.8Hz, 8H), 1.95 (m, 8H), 1.6-1.3 (several peaks, 48H), 0.93 (t, J=7.0Hz, 12H), -2.43 (s, 2H); FAB MS 1295$(M+H)^+$; Anal. Calcd for $C_{84}H_{102}N_4O_8$:C, 77.86; H, 7.93; N, 4.32; O, 9.88: Found: C, 77.70; H, 7.96; N, 4.22; O, 9.91; UV-vis (CH_2Cl_2) λmax (logε) 420nm (5.49), 520 (4.13), 554 (3.76), 598 (3.61), 654 (3.51).

HPLC analysis. The polphyrin solution $2x10^{-4}$M was placed in a test

tube with a stirrer bar under N_2 atmosphere. The 50 μl aliquot was removed on each time and in the case of $TPP(COOH)_4$, it was treated with diazomethane ether solution for esterification then evaporated. The sample was dissolved in solvent and injected in HPLC.

References and Notes

1) (a) Deisenhofer, J.;Epp, O.; Miki, K.; Huber, R.; Michel, H. *J. Mol. Biol.* **1984**, 180, 385-398. (b) Allen, J. P.; Feher, G.; Yeates, T. O.; Rees, D. C. ; Deisenhofer, J.; Michel, H.; Huber, R. *Proc. Natl. Acad. Sci. USA.* **1986**, 83, 8589-8593.

2) (a) Collman, J. P.; Elliot, C. M.; Halbert, T. R.; Tovrog, B. S. *Proc. Natl. Acad. Sci. U.S.A.* **1977**, 74, 18-22. (b) Chang, C. K. *J. Chem. Soc., Chem. Commun.***1977**, 800-801. (c) Osuka, A.; Maruyama, K. *J. Am. Chem. Soc.* **1988**, 110, 4454-4456. (d) Sessler, J. L.; Capuano, V. L.; Harriman, A. *Ibid.* **1993**, 115, 4618-4628. (e) Overfield, R. E.; Scherz, A.; Kaufmann, K. J.; Wasielewski, M. R. *Ibid.* **1983**, 105, 4256-4260. (f) Dubowchik, G. M.; Hamilton, A. D. *J. Chem. Soc., Chem. Commun.* **1986**, 1391-1394. (g) Ogoshi, H.; Sugimoto, H.; Yoshida, Z. *Tetrahedron Lett.* **1977**, 169-172.

3) a) Drain, C. M.; Fischer, R.; Nolen, E. G.; Lehn, J. M. *J. Chem. Soc., Chem. Commun.* **1993**, 243-245. (b) Kobuke, Y.; Miyaji, H. *J. Am. Chem. Soc.* **1994**, 116, 4111-4112. (c) Sessler, J. L.; Wang, B.; Harriman, A. *Ibid.* **1995**, 117, 704-714. (d) Aoyama, Y.; Kamohara, T.; Yamagishi, A.; Toi, H.; Ogoshi, H. *Tetrahedron Lett.* **1987**, 28, 2143-2146.

4) (a) Leondiadis, L.; Momenteau, M. *J. Org. Chem.* **1989**, 54, 6135-6138. (b) Fujimoto, T.; Umekawa, H.; Hishino, N. *Chem. Lett.* **1992**, 37-40.

5) HPLC column : YMC-Pack C4 (A-813, 6.0x250 mm), eluent : methanol, flow rate: 1.0 ml/min, detected at 420 nm. Retention time of 4 atropisomers; $\alpha\beta\alpha\beta$=11.5 min, $\alpha\alpha\beta\beta$=12.3 min, $\alpha\alpha\alpha\beta$=13.5 min, $\alpha\alpha\alpha\alpha$=24.8 min.

6) (a) Gottwald, L. K. ; Ullman, E. F. *Tetrahedron Lett.* **1969**, 3071-3074. (b) J. P. Colleman, R. R. Gagne, C. A. Reed, T. R. Halbert, and G. Lang, W. T. Robinson, *J. Am. Chem. Soc.* **1975**, 97, 1427. (c) K. Hatano, K. Anzai, A. Nishino, K. Fujii, *Bull. Chem. Soc. Jpn.* **1985**, 58, 3653. (d) M. J. Crossley, L. D. Field, A. J. Forster, M. M. Harding, and S. Sternhell, *J. Am. Chem. Soc.* **1987**, 109, 341.

7) Recently, interesting thermal conditions which give αβαβ or ααββ atropisomers of meso-tetrakis(o-nitrophenyl)porphyrin exclusively were reported, see (a) Rose, E.; Quelquejeu, M.; Pochet, C.; Julien, N.; Kossanyi, A.; Hamon, L. *J. Org. Chem.* **1993**, 58, 5030-5031. (b) Rose, E.; Pilotaz, A. C.; Quelquejeu, M.; Bernard, N.; Kossanyi, A. *Ibid.* **1995**, 60, 3919-3920.

8) (a) Lindsey, J. *J. Org. Chem.* **1980**, 45, 5215. (b) Elliott, C. M. *Anal. Chem.* **1980**, 52, 666-668. (c) Hayashi, T.; Asai, T.; Hokazono, H.; Ogoshi, H. *J. Am. Chem. Soc.* **1993**, 115, 12210-12211.

9) (a) Osuka, A.; Maruyama, K. *J. Am. Chem. Soc.* **1988**, 110, 4454-4456. (b) Collman, J, P.; Bencosme, C, S.; Barnes, C, E.; Miller, B, D. *J. Am. Chem. Soc.* **1983**, 105, 2704-2710.

10) *Organic Syntheses.* Collect Volume IV, 250.

11) Lindsey, J, S. ; Wagner, R, W. *J. Org. Chem.* **1989**, 54, 828-836.

Computer Analyses of Complex Kinetics Containing Equilibrium Processes (Example of Application for Unusual Atropisomerization of a Tetraphenylporphyrin Derivative)

Abstract

Kinetic behavior of atropisomerization of a tetraphenylporphyrin derivative containing equilibrium processes of dimer formation were analyzed directly by a non-linear least square optimization method using numerical integration of kinetic differential equations. As a plausible mechanism of unusual atropisomerization, four models which contain different rate or association constants are analyzed with a new program REDAP (Reaction Dynamics Analysis Program). Analyses show the kinetic model 4 determined with one rate and two equilibrium constants gives the smallest residual square sum and excellent agreement with all kinetic traces. These results strongly indicate that model 4 is the most plausible mechanism of unusual atropisomerization not only from viewpoint of statistics but also from viewpoint of Ockham's razor.

Chapter 2

Introduction

Chemists have been often encountering difficulties that a kinetic mechanism describing their chemical systems gives no analytically integrated forms of kinetic equations or requires restricted experimental conditions to simplify the kinetic models, though the model itself seems to be quite reasonable from chemical viewpoint without any simplification. In such case, the combination of numerical integration and non-linear least square optimization is a powerful method to analyze dynamic systems, because kinetic differential equations are available and the method makes it possible to analyze and execute a curve fitting procedure for observed data directly. Recently we found an interesting atropisomerization system of *meso*-tetrakis(2-carboxy-4-nonylphenyl)porphyrin (**1**) which gave αααα-atropisomer exclusively at the final equilibrium state.[1] It has been known that the usual atropisomerization process is well explainable by using kinetic model 1 as shown in Figure 2, where each rate constant for the isomerization process is given by a statistically weighted rotational rate of the benzene ring and the isomer ratio of αααα / ααββ / αααβ / αβαβ = 1 / 2 / 4 / 1 is expected at the final equilibrium state. [2] In fact the equilibrium of **1** is attained at 1:4:2:1 ratio in polar solvents such as DMSO. It is evident that this standard model can not explain present unusual atropisomerization where the αααα isomer is practically the sole product at the final state. The observation indicates that a new kinetic model is necessary for further analyses of this system. Since spectroscopic investigations suggest that the αααα isomer of **1** is effectively stabilized via dimer formation, kinetic

models such as model 2 - 4 emerge as the plausible mechanism of the atropisomerization of **1**. We report here procedures and a new program which make it possible to analyze these complex kinetic systems containing equilibrium processes.

Results and Discussion

The differential equations describing reaction dynamics of model 2 - 4 do not give simple analytically integrated forms, in contrast to those for model 1.[3] To analyze these systems, we used a new program REDAP which executes a least square optimization procedure using numerical integration for generation of theoretical kinetic traces.[4] REDAP is able to treat not only kinetic processes described by a set of differential equations but also thermodynamic processes which reach equilibrium much rapidly than the kinetic processes and are described by equilibrium equations.[5] The numerical integration in REDAP was performed with the Runge-Kutta-Gill procedure[6] and the damping Gauss-Newton[7] or Marquardt[8] algorithm was employed as the non-linear least square optimization method. In each cycle of numerical integration, the concentrations of αααα and/or αααβ and their dimers were evaluated with their equilibrium equations.

The atropisomerization of **1** in DMSO (Figure 1) is normal and well

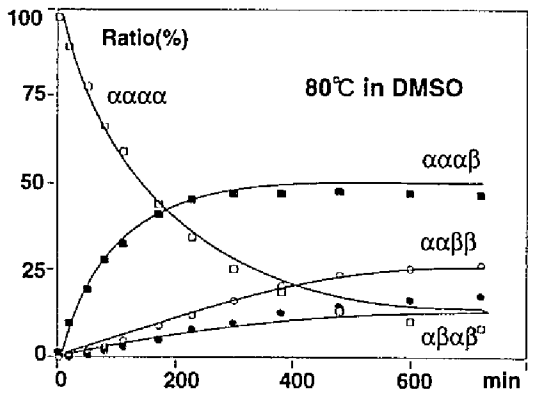

Figure 1. The atropisomerization of $TPP(CO_2H)_4$ in DMSO. The solid lines show the theoretical curves generated by REDAP.

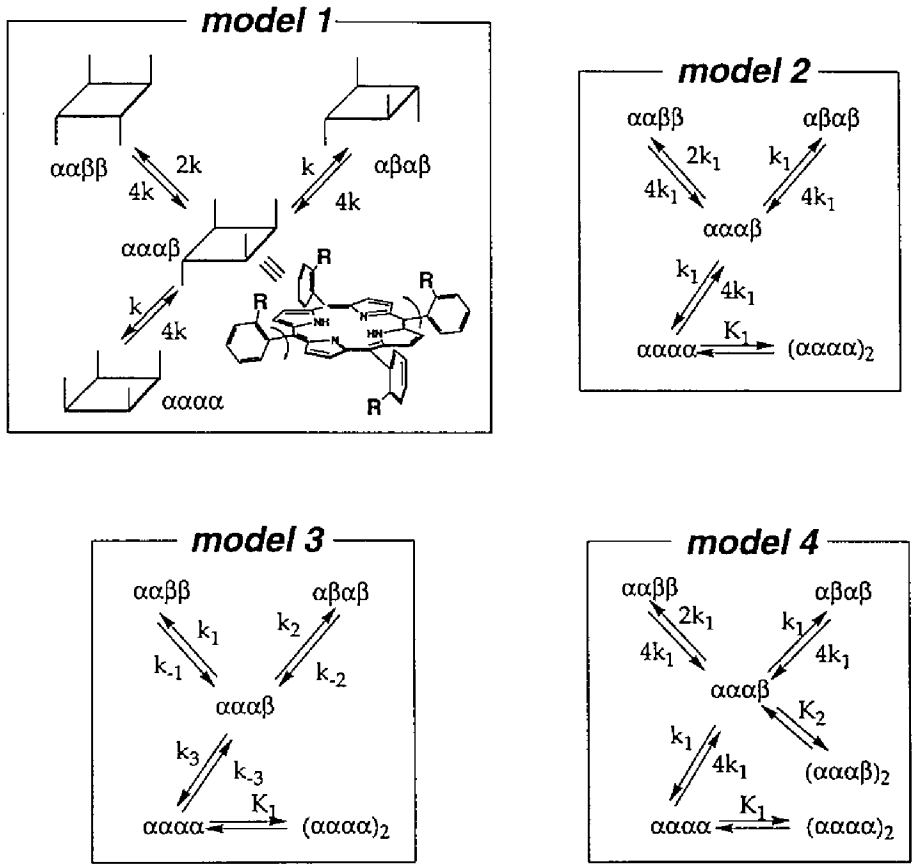

Figure 2. Four different kinetic models for atropisomerization of tetraphenylporphyrin derivatives.

described by model 1. The kinetic equations used for the analysis of the model 1 in REDAP are as follows.

$$d[\alpha\alpha\alpha\beta]/dt = 4k([\alpha\beta\alpha\beta]+[\alpha\alpha\beta\beta]+[\ \alpha\alpha\alpha\alpha]-[\alpha\alpha\alpha\beta]) \quad (1)$$

$$d[\alpha\beta\alpha\beta]/dt = k([\alpha\alpha\alpha\beta]-4[\alpha\beta\alpha\beta]) \quad (2)$$

$$d[\ \alpha\alpha\alpha\alpha]/dt = k([\alpha\alpha\alpha\beta]-4[\ \alpha\alpha\alpha\alpha]) \quad (3)$$

$$d[\alpha\alpha\beta\beta]/dt = 2k([\alpha\alpha\alpha\beta]-2[\alpha\alpha\beta\beta]) \quad (4)$$

When the total concentration of **1** is P and the concentration of each isomer at initial point (t=0) is $[\alpha\alpha\alpha\beta]=aP$, $[\alpha\beta\alpha\beta]=bP$, $[\alpha\alpha\alpha\alpha]=cP$ and $[\alpha\alpha\beta\beta]=P(1-a-b-c)$, respectively, this differential equations (1)-(4) give simple analytically integrated forms as follows.

$$[\alpha\alpha\alpha\beta]=P(a-1/2)e^{-8kt}+1/2P \quad (5)$$

$$[\alpha\beta\alpha\beta]=1/4P(a+4b-1)e^{-4kt}+1/8P(1-2a)e^{-8kt}+1/8P \quad (6)$$

$$[\alpha\alpha\alpha\alpha]=1/4P(a+4c-1)e^{-4kt}+1/8P(1-2a)e^{-8kt}+1/8P \quad (7)$$

$$[\alpha\alpha\beta\beta]=1/2P(1-a-2b-2c)e^{-4kt}+1/4P(1-2a)e^{-8kt}+1/4P \quad (8)$$

Fitting results of REDAP by using (1)-(4) are shown in Figure 1 and these results are almost the same as the result of using integrated forms (5)-(8). Optimized parameter for kinetic model 1 is $k=2.27\times10^{-5}s^{-1}$. Compared with kinetic data of other TPP-type porphyrins as shown in Table 1, this rate constant is reasonable. These results show that REDAP can estimate the parameters by using differential equations without integrated forms.

To explain the unusual atropisomerization of pophyrin **1**, we examined three models in this work. Among the models, model 2 is the most simple system which contains one equilibrium process of $\alpha\alpha\alpha\alpha$ dimer formation in addition to

Table 1. Kinetic data of atropisomerization of tetraphenyl porphyrin derivatives.

substituent at ortho position	T (°C)	k (s^{-1})	$\Delta G^{\ddagger}$ (kcal/mol)	
NH_2	60	——	27.6	2-c)
	81	——	28.0	
CN	60	——	24.6	2-c)
OH	23	——	23.9	2-a)
CO_2Me	80	8.33×10^{-5}	27.5	9)
	90	2.43×10^{-4}	27.4	
CO_2H (*p*-nonyl)	80	2.27×10^{-5}	28.3	

model 1. Model 3 is schematically similar to model 2 but involves with six different rate constants for each kinetic process. Model 4 is presented by the same kinetic system as model 1 having one common rate constant but contains two dimer formation equilibrium processes for αααα and αααβ isomers. The kinetic and equilibrium equations which describe the systems are given as subroutines in REDAP and, for example, the following set of equations is used for the analysis of model 4;

$$d[\alpha\alpha\beta\beta]/dt = 2k([\alpha\alpha\alpha\beta]-2[\alpha\alpha\beta\beta])$$

$$d[\alpha\beta\alpha\beta]/dt = k([\alpha\alpha\alpha\beta]-4[\alpha\beta\alpha\beta])$$

$$d[\alpha\alpha\alpha\beta]/dt = 4k([\alpha\alpha\beta\beta]+[\alpha\beta\alpha\beta]+[\alpha\alpha\alpha\alpha]-[\alpha\alpha\alpha\beta])/(1+4K_2[\alpha\alpha\alpha\beta])$$

$$d[\alpha\alpha\alpha\alpha]/dt = k([\alpha\alpha\alpha\beta]-4[\alpha\alpha\alpha\alpha])/(1+4K_1[\alpha\alpha\alpha\alpha])$$

$$d[\alpha\alpha\alpha\beta]_T/dt = d([\alpha\alpha\alpha\beta]+2[(\alpha\alpha\alpha\beta)_2])/dt = (1+4K_2[\alpha\alpha\alpha\beta]) \cdot d[\alpha\alpha\alpha\beta]/dt$$

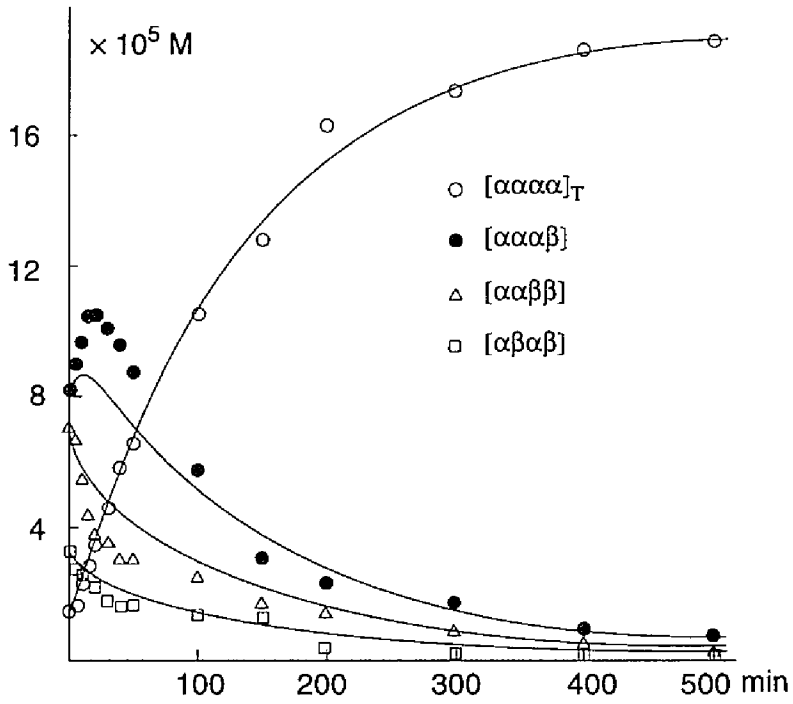

Figure 3. Fitting results for model 2. The solid lines show the theoretical curves generated by REDAP using parameters shown in Table 2.

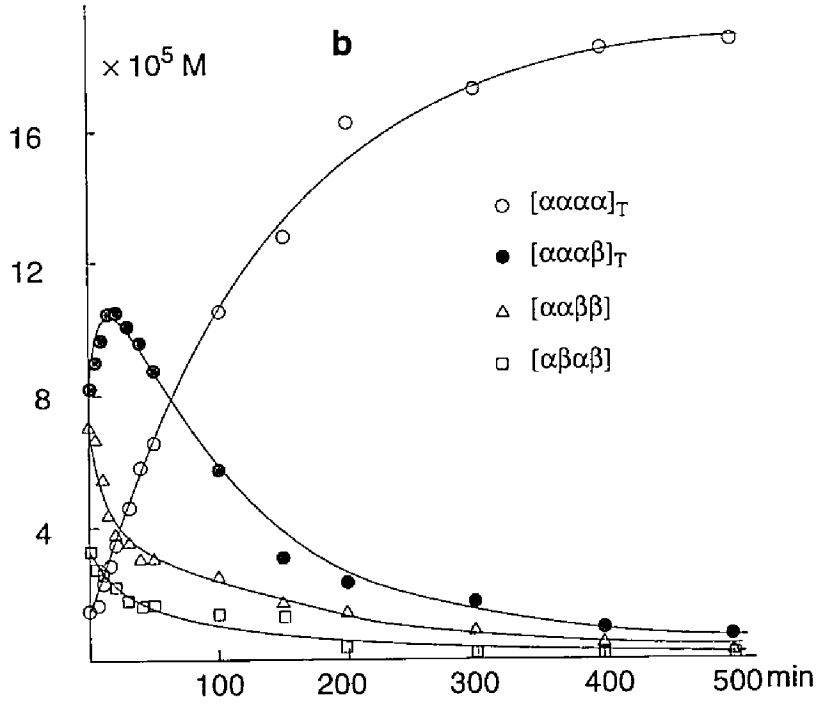

Figure 4. Fitting results for model 4. The solid lines show the theoretical curves generated by REDAP using parameters shown in Table 2. Fitting results for model 3 are very similar to those for model 4.

$$d[\alpha\alpha\alpha\alpha]_T/dt = d([\alpha\alpha\alpha\alpha]+2[(\alpha\alpha\alpha\alpha)_2])/dt = (1+4K_1[\alpha\alpha\alpha\alpha])\cdot d[\alpha\alpha\alpha\alpha]/dt$$

In these expressions, the observed concentrations of the $\alpha\alpha\alpha\alpha$ and $\alpha\alpha\alpha\beta$ isomers, $[\alpha\alpha\alpha\alpha]_T$ and $[\alpha\alpha\alpha\beta]_T$, are presented as $[\alpha\alpha\alpha\alpha]+2[(\alpha\alpha\alpha\alpha)_2]$ and $[\alpha\alpha\alpha\beta]+2[(\alpha\alpha\alpha\beta)_2]$, respectively, because, due to their rapid equilibrium, these monomer and dimer species are not observed separately by HPLC employed as the analytical method in this work. Following equations derived from the equilibrium conditions were also used as the relationship between the concentrations of these monomer and dimer species.

$$d[(\alpha\alpha\alpha\alpha)_2]/dt = 2K_1[\alpha\alpha\alpha\alpha]\cdot d[\alpha\alpha\alpha\alpha]/dt$$

$$d[(\alpha\alpha\alpha\beta)_2]/dt = 2K_2[\alpha\alpha\alpha\beta]\cdot d[\alpha\alpha\alpha\beta]/dt$$

Similar sets of differential equations are also easily written for model 2 and 3. In the calculations, all these rate and equilibrium constants were used as optimization parameters. The results of fitting by use of these kinetic models

Table 2. Optimized parameters for kinetic models of atropisomerization of **1** [a]

model	$k_{\pm1}$	$k_{\pm2}$	$k_{\pm3}$	K_1	K_2	ss [b]
	x 10^2 min^{-1}			x10^{-5} M^{-1}		x 10^{10}
2	1.3 (0.1)	—	—	1000 (3000)	—	32.6
3 [c]	1.7	5.9	0.85	530	—	7.93
	5.6	1.1	2.1			
4	1.7 (0.1)	—	—	740 (340)	0.045 (0.005)	5.50

[a]The experimental conditions ; $[1]_{Total} = 2 \times 10^{-4}$ M, at 80 °C in $CHCl_2CHCl_2$. Standard deviations are given in parentheses. [b]Residual square sum. [c]Standard deviations are not given, because optimization gives no convergent parameter.

are summarized in Figure 3, Figure 4, and Table 2.

Although model 2 roughly reproduces the trend of exclusive production of the αααα isomer at the final state, this model results in the significant deviations from the observed kinetic traces for other isomers as shown in Figure 3. Model 3 does not give a normal stable parameter set under the usual convergent conditions.[10] The parameters obtained under the more milder conditions, however, shows good fitting with the experimental data as indicated by the smaller residual square sum value, ss (the calculated curves are not shown in Figure 4 but apparently almost the same with those of Figure 4). Finally, optimization for model 4 results in normal convergence and shows excellent agreement with all kinetic traces as shown in Figure 4. It should be noted that model 4 gives better fitting (smaller ss) than model 3, even though the former is defined with much fewer parameters than the latter. Since there is no rational reason for assuming six different rate constants for rotation of each benzene ring of **1** at the present stage, the results strongly indicate that model 4 is the most plausible mechanism of atropisomerization of **1** not only from viewpoint of statistics but also from viewpoint of Ockham's razor.[11] Thus, the present results demonstrate that the combination of non-linear least square optimization and numerical integration can be utilized as a powerful tool for analyses of complex kinetic models containing equilibrium processes.

Experimental Section

REDAP (Reaction Dynamics Analysis Program) is written in C language, for execution on NEC PC9800 series computers and includes a graphic routine for presentation of results.

It is needed to obtain kinetic differential equations for all species. For the

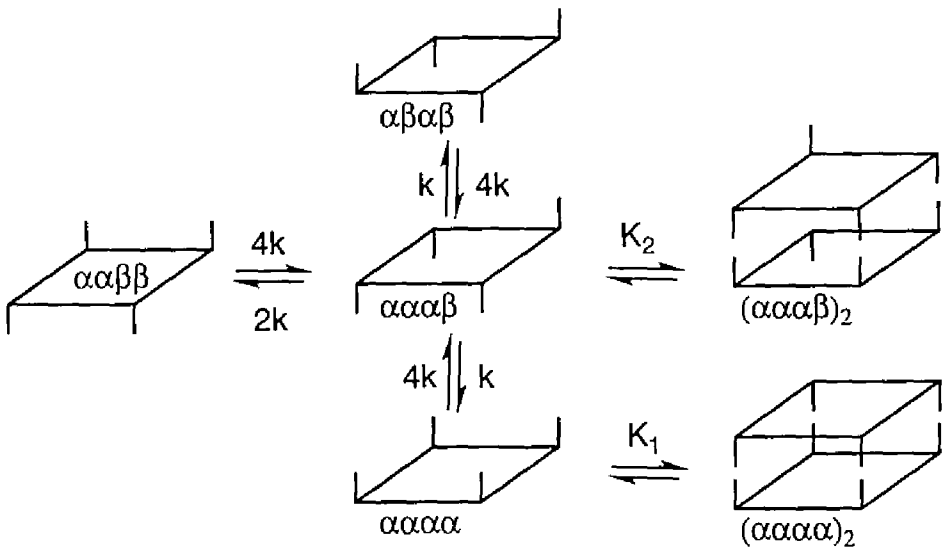

case of model 4, six species ($\alpha\beta\alpha\beta$, $\alpha\alpha\beta\beta$, $\alpha\alpha\alpha\beta$, $\alpha\alpha\alpha\alpha$, $(\alpha\alpha\alpha\beta)_2$, $(\alpha\alpha\alpha\alpha)_2$) are contained and six kinetic differential equations of $\alpha\beta\alpha\beta$, $\alpha\alpha\beta\beta$, $\alpha\alpha\alpha\beta$, $\alpha\alpha\alpha\alpha$, $(\alpha\alpha\alpha\beta)_T$, and $(\alpha\alpha\alpha\alpha)_T$ were used. In these experiments, the observed concentrations of the $\alpha\alpha\alpha\alpha$ and $\alpha\alpha\alpha\beta$ isomers, $[\alpha\alpha\alpha\alpha]_T$ and $[\alpha\alpha\alpha\beta]_T$, are presented as $[\alpha\alpha\alpha\alpha]+2[(\alpha\alpha\alpha\alpha)_2]$ and $[\alpha\alpha\alpha\beta]+2[(\alpha\alpha\alpha\beta)_2]$ respectively, because, due to their rapid equilibrium, these monomer and dimer species are not observed separately by HPLC which employed as the analytical method in this work.

From equilibrium conditions,

$K_1 = [(\alpha\alpha\alpha\alpha)_2]/ [\alpha\alpha\alpha\alpha]^2$

$[(\alpha\alpha\alpha\alpha)_2] = K_1[\alpha\alpha\alpha\alpha]^2$

$d[(\alpha\alpha\alpha\alpha)_2]/dt = 2K_1[\alpha\alpha\alpha\alpha] \cdot d[\alpha\alpha\alpha\alpha]/dt$ eq.1

$K_2 = [(\alpha\alpha\alpha\beta)_2]/ [\alpha\alpha\alpha\beta]^2$

$[(\alpha\alpha\alpha\beta)_2] = K_2[\alpha\alpha\alpha\beta]^2$

$d[(\alpha\alpha\alpha\beta)_2]/dt = 2K_2[\alpha\alpha\alpha\beta] \cdot d[\alpha\alpha\alpha\beta]/dt$ eq.2

for pure kinetic processes,

$d[\alpha\alpha\beta\beta]/dt = 2k([\alpha\alpha\alpha\beta]-2[\alpha\beta\beta])$ eq.3

$d[\alpha\beta\alpha\beta]/dt = k([\alpha\alpha\alpha\beta]-4[\alpha\beta\alpha\beta])$ eq.4

$d[\alpha\alpha\alpha\beta]/dt = 4k[\alpha\beta\alpha\beta]-k[\alpha\alpha\alpha\beta]+4k[\alpha\alpha\beta\beta]-2k[\alpha\alpha\alpha\beta]+4k[\alpha\alpha\alpha\alpha]-$

$k[\alpha\alpha\alpha\beta]-2d[(\alpha\alpha\alpha\beta)_2]/dt$ eq.5

$d[\alpha\alpha\alpha\alpha]/dt = k[\alpha\alpha\alpha\beta]-4k[\alpha\alpha\alpha\alpha]-2d[(\alpha\alpha\alpha\alpha)_2]/dt$ eq.6

substitute eq.2 into eq.5

$d[\alpha\alpha\alpha\beta]/dt = 4k([\alpha\beta\alpha\beta]+[\alpha\alpha\beta\beta]+[\alpha\alpha\alpha\alpha]-[\alpha\alpha\alpha\beta])-$

$4K_2[\alpha\alpha\alpha\beta] \cdot d[\alpha\alpha\alpha\beta]/dt$

$d[\alpha\alpha\alpha\beta]/dt = 4k([\alpha\beta\alpha\beta]+[\alpha\alpha\beta\beta]+[\alpha\alpha\alpha\alpha]-[\alpha\alpha\alpha\beta]/(1+4K_2[\alpha\alpha\alpha\beta])$ eq.7

substitute eq.1 into eq.6

$d[\alpha\alpha\alpha\alpha]/dt = k[\alpha\alpha\alpha\beta]-4k[\alpha\alpha\alpha\alpha]-4K_1[\alpha\alpha\alpha\alpha] \cdot d[\alpha\alpha\alpha\alpha]/dt$

$d[\alpha\alpha\alpha\alpha]/dt = k([\alpha\alpha\alpha\beta]-4[\alpha\alpha\alpha\alpha])/(1+4K_1[\alpha\alpha\alpha\alpha])$ eq.8

$$d[\alpha\alpha\alpha\beta]_T/dt = d([\alpha\alpha\alpha\beta]+2[(\alpha\alpha\alpha\beta)_2])/dt=$$

$$(1+4K_2[\alpha\alpha\alpha\beta])\cdot d[\alpha\alpha\alpha\beta]/dt \qquad \text{eq.9}$$

$$d[\alpha\alpha\alpha\alpha]_T/dt = d([\alpha\alpha\alpha\alpha]+2[(\alpha\alpha\alpha\alpha)_2])/dt=$$

$$(1+4K_1[\alpha\alpha\alpha\alpha])\cdot d[\alpha\alpha\alpha\alpha]/dt \qquad \text{eq.10}$$

REDAP calculates numerical integration and optimizes kinetic and thermodynamic parameters by using eq.3, eq.4, eq.7, eq.8, eq.9, and eq.10.

References and Notes

1) Kuroda, Y. Kawashima, A. Urai, T. Ogoshi, H. *Tetrahedron Lett.* **1995**, 36, 8449.

2) For example, (a) Gottwald, L. K. ; Ullman, E. F. *Tetrahedron Lett.* **1969**, 3071-3074. (b) Colleman, J. P.; Gagne, R. R.; Reed, C. A.; Halbert, T. R.; Lang, G.; Robinson, W. T. *J. Am. Chem. Soc.* **1975**, 97, 1427. (c) Hatano, K.; Anzai, K.; Nishino, A. ; Fujii, K. *Bull. Chem. Soc. Jpn.* **1985**, 58, 3653. (d) Crossley, M. J.; Field, L. D.; Forster, A. J.; Harding, M. M.; Sternhell, S. *J. Am. Chem. Soc.* **1987**, 109, 341.

3) The model 1 gives analytically integrated rate expressions.

4) REDAP (Reaction Dynamics Analysis Program) is written in C language, runs on NEC PC9800 series computers and includes a graphic routine for presentation of results.

5) A similar program was reported as OPKINE. The program treats equilibrium processes based on microscopic reversibility of kinetic processes, see (a) Baeza, J. J. B.; Romos,G. R. R.; Pla, F. P.; Mokina, R. V. *Analyst* **1990**, 115, 721 . (b) Pla, F. P.; Baeza, J. J. B.; Romos,G. R. R.; Palou, J. *J. Comp. Chem.* **1991**, 12, 283.

6) Gill, G. *Proc. Cambridge Philos. Soc.* **1951**, 47, 96.

7) Kowalik, J.; Osborne, M. R. "Methods for Unconstrained Optimization Problems", Elsevier, Amsterdam (1968).

8) Marquardt, D. W. *J. Soc. Indust. Appl. Math.* **1963**, 11, 431.

9) Fujimoto, T.; Umekawa, H.; Nishino, N. *Chem. Lett.* **1992**, 37.

10) REDAP stops the optimization procedures when change rates of the residual

square sum and the all parameters are less than 0.001% and 0.01%, respectively.

11) The present results do not exclude the possible participation of a hetero-dimer such as $\alpha\alpha\alpha\alpha \cdot \alpha\alpha\alpha\beta$. At the present stage, we should consider the K_1 and K_2 values as a kind of averaged values affected by existence of the hetero-dimer. The formation constants of such hetero-dimers, however, are reasonably expected to be as small as K_2 compared with K_1.

Molecular Recognition between Self-Organized Porphyrin Dimer Zn Complex and Bidentate Ligands.

Abstract

Atropisomerization of [5,10,15,20-tetrakis(2-carboxy-4-nonylphenyl) porphyrinato]zinc(II) (**1**) gives the αααα isomer exclusively in toluene. UV-vis, IR, NMR and vapor pressure osmometry investigations of **1** suggest that the porphyrin aggregates in nonpolar solvents and the resulting aggregate is face-to-face porphyrin dimer through the eight hydrogen bonds among four pairs of carboxylic acids. This self-assembled porphyrin dimer has a cavity between the two porphyrin faces, the distance between the porphyrin planes is 8-9 Å, furthermore, top and bottom end are zinc as the coordination site. So this self-assembled cavity is available for molecular recognition site for bidentate ligands such as pyrazine. The complexation of aromatic amines such as pyrazine, pyridine, and so on with this porphyrin dimer in CH_2Cl_2 and $CHCl_3$ were investigated using NMR and spectroscopic titration experiments. These experiments revealed that the incorporation of guests into porphyrin dimer were highly specific for pyrazine. The theoretical fitting for spectroscopic investigation suggests that the equibrium constant of porphyrin dimerization is $5x10^5M^{-1}$ and the binding constant with pyrazine is $1x10^{10}M^{-1}$.

Chapter 3

Introduction

Biological systems are composed of self-aggregation of flexible units which organized themselves into stable, well-defined structure. Self-assembly system using noncovalent intermolecular interactions such as hydrogen bond, coordination, Coulomb interaction, etc, is one of the most interesting methodology in the biomimetic chemistry and some systems were developed in the design of synthetic functional molecules.[1] As for the chemistry of porphyrin dimers, it is now well developed for their chemical and physical properties,[2] but the system using self-assembly has only begun to be exploited.[3] Recently, we reported the self-assembling system of *meso*-tetrakis(2-carboxy-4-nonylphenyl)porphyrin (**2**) for porphyrin dimer formation which is accompanied by conformational change of the monomeric porphyrin.[4] This self-assembling process is so highly selective for dimer formation that, even starting from mixture of monomeric porphyrin isomers, the system gives practically pure dimer of the αααα isomer. We report here a novel self-assembly of zinc porphyrin dimer which, unlike monomer , act as a highly selective receptor for pyrazine.

Results and discussion

The porphyrin used in this work is [*meso*-tetrakis(2-carboxy-4-nonylphenyl)porphyrinato]zinc(II) (**1**) which was prepared from zinc insertion of porphyrin **2**. It is generally known that the normal statistical distribution of tetra phenyl porphyrin is αβαβ:ααββ:αααβ:αααα = 1:2:4:1.[5] In fact, atropisomerization of [*meso*-tetrakis(2-methoxycarbonyl-4-nonylphenyl) porphyrinato]zinc(II) (**3**) in DMSO and toluene were normal as shown in Figure 1. However, atropisomerization of **1** was different. In DMSO thermodynamical equilibrium shifted from statistical distribution and the αβαβ isomer increased. In this case curve fitting using model 1which is normal atropisomerization model (Figure 1c) gave no good results but using model 2 (Figuer 2c) which contained 2 kinetic parameters gave good fitting curves with optimized parameters k_1=0.000727min^{-1} and k_2=0.00154min^{-1} as shown in Figure 2. The k_2 value which expresses kinetic constant from αααα to αααβ and from αααβ to αβαβ is two times greater than k_1. This result means that when the three neighboring carboxy groups are in same direction, central carboxy group is probably able to rotate easily to opposite porphyrin plane due to their steric hindrance or some other

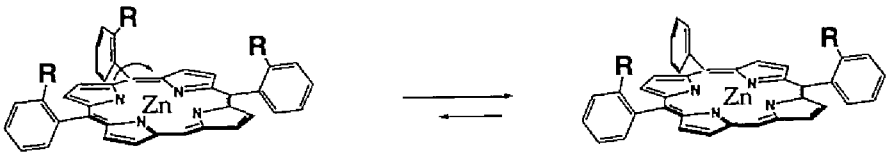

reasons.

Atropisomerization of **1** in nonpolar solvent such as toluene gives the

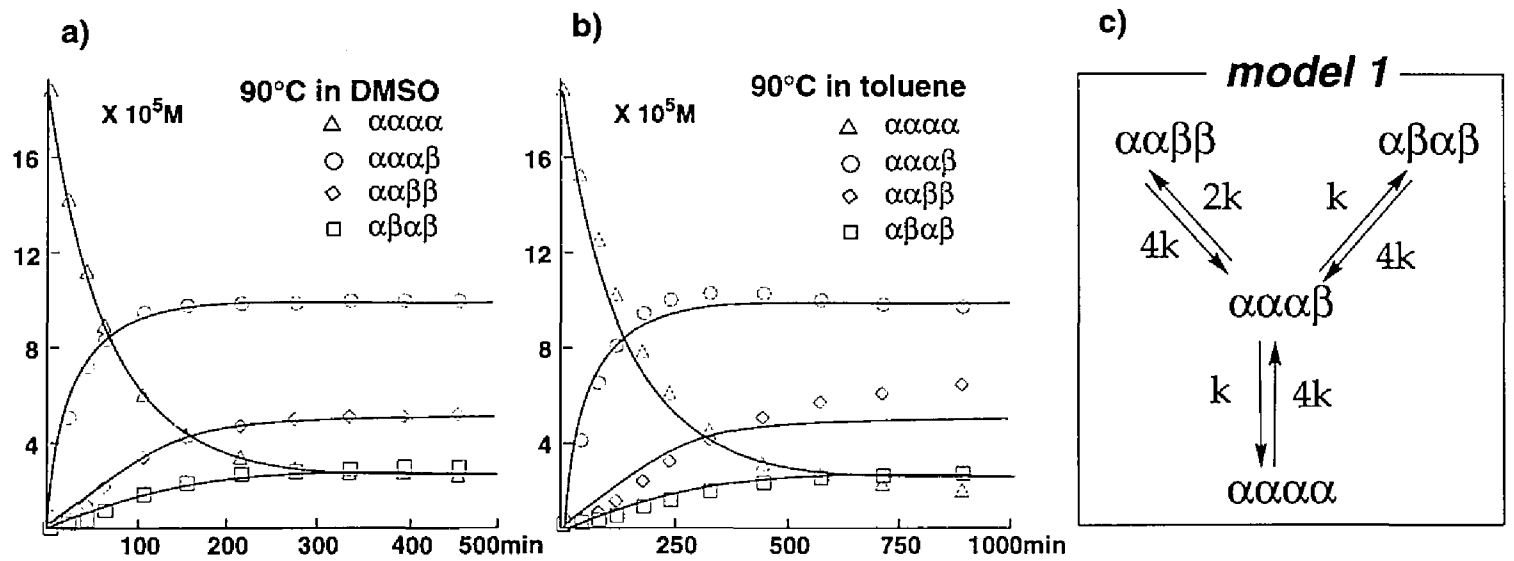

Figure 1. Thermal atropisomerization of **3** in a) DMSO and b) toluene at 90 °C. Solid lines are theoretical curves obtained by curve fitting analyses using model 1 which is standard thermal TPP atropisomerization model. k=0.0037min^{-1} in DMSO and 0.0015min^{-1} in toluene. $[\mathbf{3}]_{total}$=2x10^{-4}M.

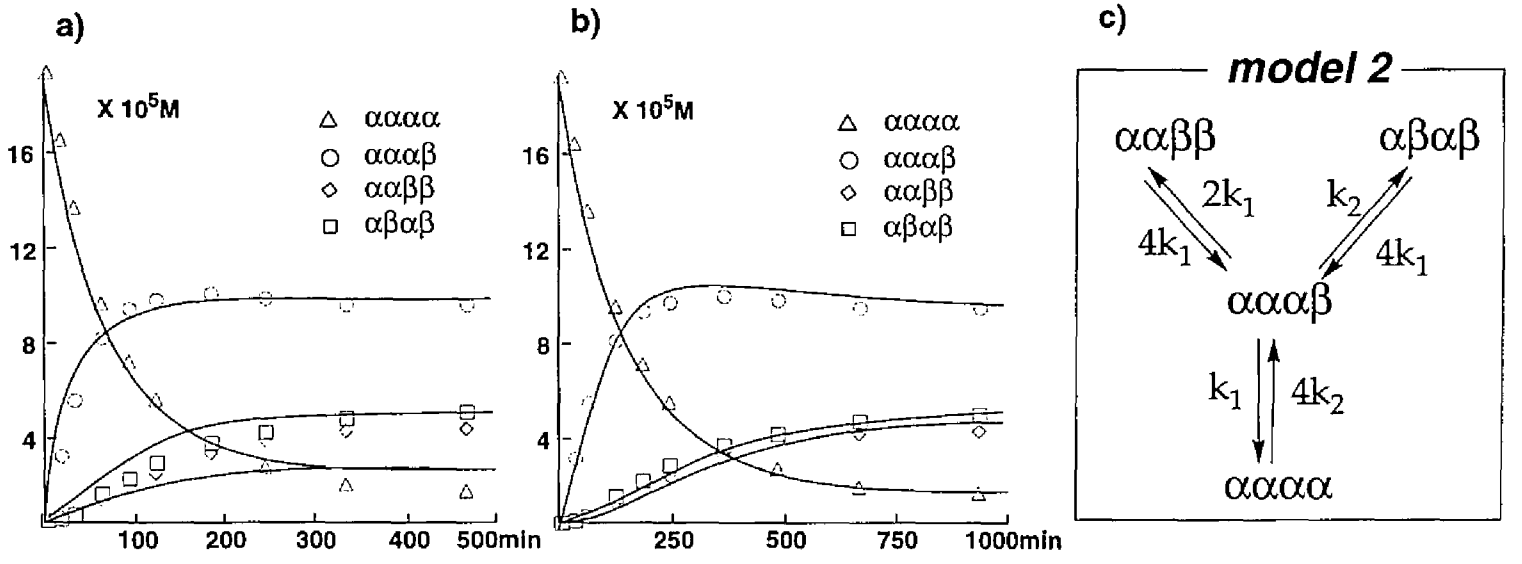

Figure 2. Thermal atropisomerization of **1** in DMSO at 90 °C. Solid lines are theoretical curves obtained by curve fitting analyses using a) model 1 and b) model 2 which contains 2 kinetic constants. $k=0.0037min^{-1}$ in model 1 and $k_1=0.000727min^{-1}$, $k_2=0.00154min^{-1}$in model 2. $[\mathbf{1}]_{total}= 2x10^{-4}M$.

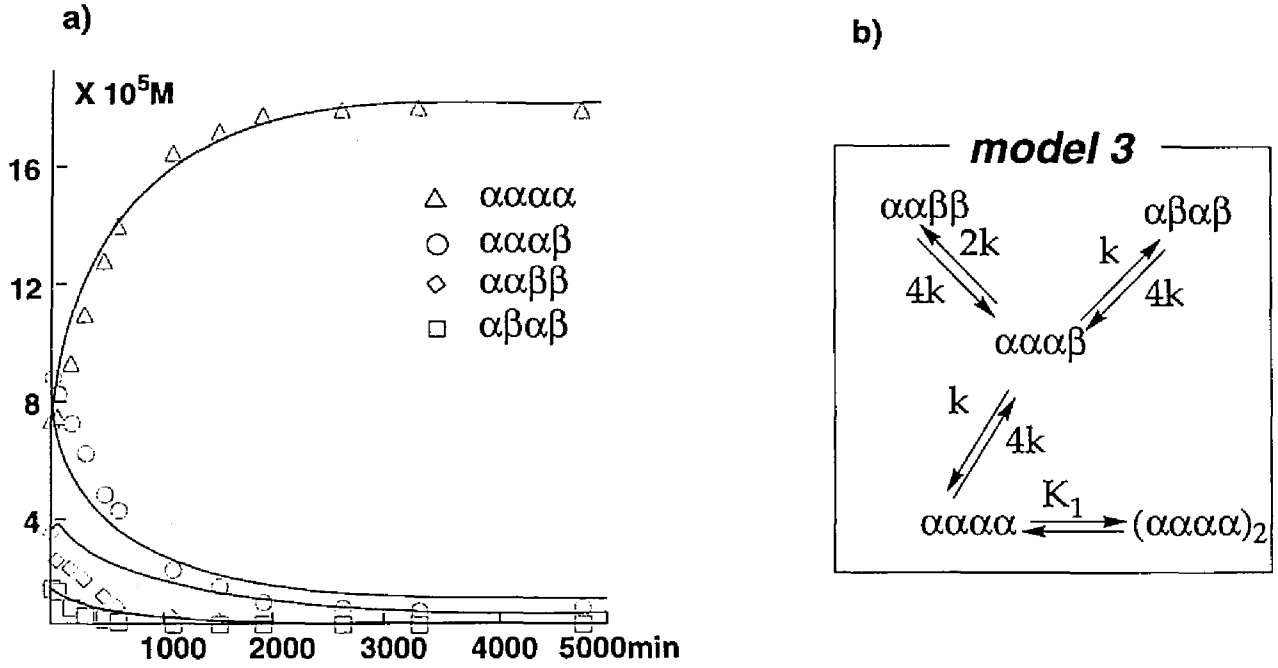

Figure 3. Thermal atropisomerization of **1** in toluene at 90 °C. Solid lines are theoretical curves obtained by curve fitting analyses using model 3 which contains 1 equilibrium constant. k= $0.00248min^{-1}$ and $K_1=1.68x10^7$. $[1]_{total}=2x10^{-4}M$. Residual square sum=$2.44x10^{-9}$.

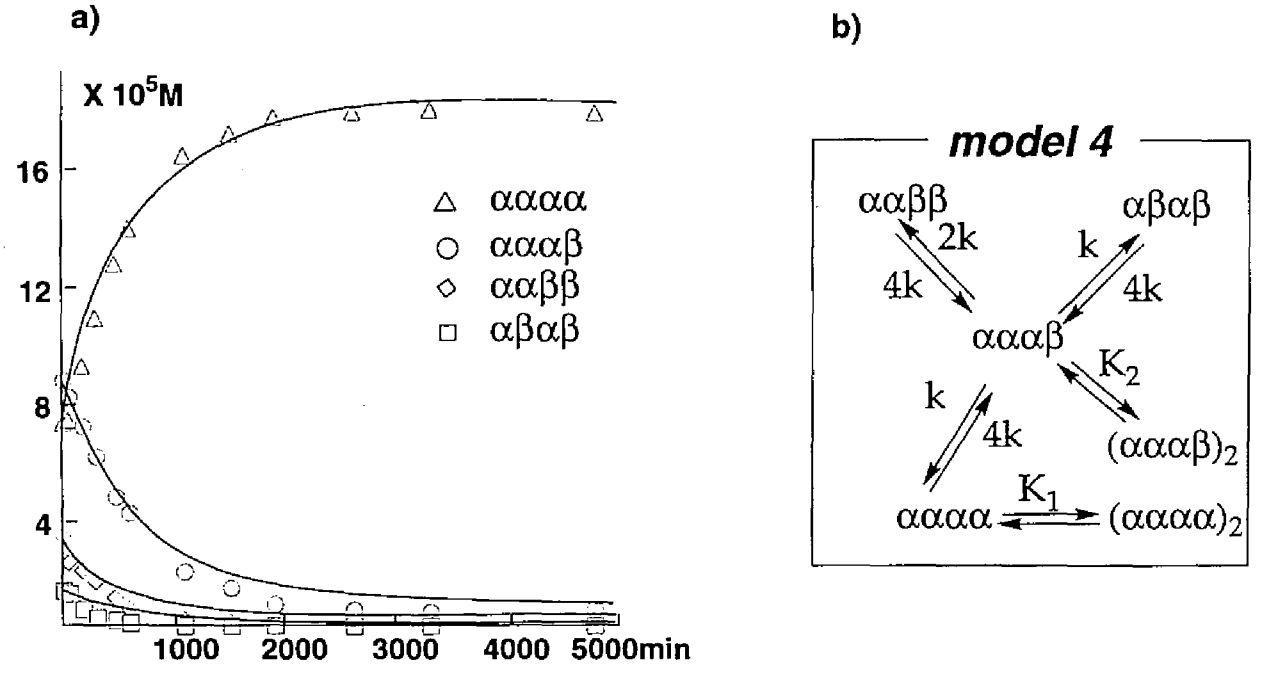

Figure 4. Thermal atropisomerization of **1** in toluene at 90 °C. Solid lines are theoretical curves obtained by curve fitting analyses using model 4 which contains 2 equilibrium constants. k= 0.00408min^{-1}, K_1=1.71x10^{7}M^{-1} and K_2=1.09x10^{4}M^{-1}. $[\mathbf{1}]_{total}$=2x10^{-4}M. Residual square sum= 8.41x10^{-10}.

αααα isomer exclusively and the final ratio of the αααα isomer is over 90%.[6] For this unusual atropisomerization we examinded curve fitting using two models, model 3 (Figure 3b) containing 1 equilibrium parameter and model 4 (Figure 4b) containing 2 equilibrium parameters. The results of fitting are summarized in Figure3 and Figure 4. Although the model 3 roughly reproduces the trend of exclusive production of the αααα isomer at the final state, this model results in the significant deviations from the observed kinetic traces for other isomers as shown in Figure 3. Optimization for the model 4 shows excellent agreement with all kinetic traces and gives better fitting (smaller ss) than the model 3 as shown in Figure 4. The optimized equilibrium constant for αααα dimerization is 1.71×10^7 and this is a major driving force for the unusual atropisomerization.

The physical major properties of αααα isomer of porphyrin **1** were investigated similary as previous work[4] by UV/vis, IR, NMR, and vapor pressure

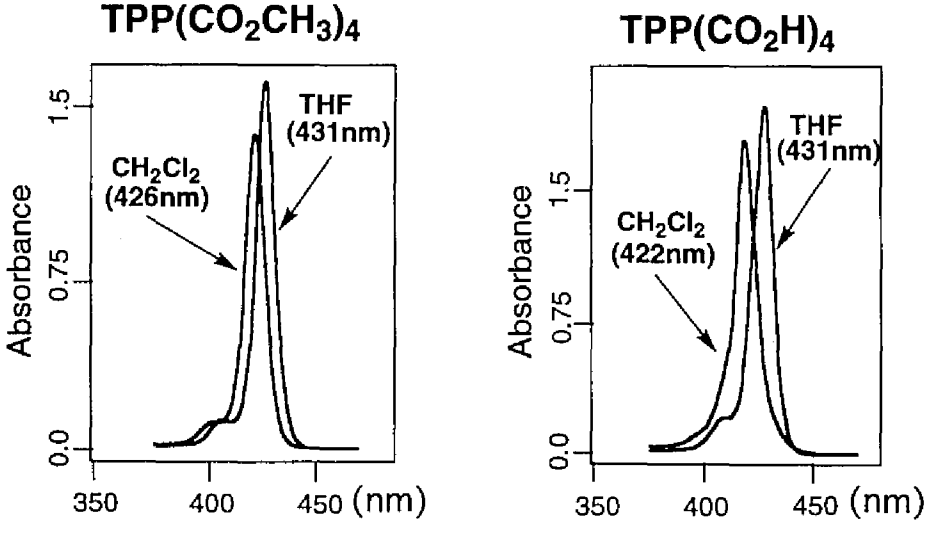

Figure 5. The absorption spectra of αααα-atropisomer of Zn $TPP(CO_2CH_3)_4$ and Zn $TPP(CO_2H)_4$.

osmometry in nonpolar solvents.

The UV-vis spectra of porphyrin **1** and **3** in THF show almost the same and each λmax is identical (431nm) as shown in Figure 5. In contrast, the Soret band for **1** in non-polar solvent, CH_2Cl_2, shifts from 426nm to 422nm compared with **3** and the shoulder peaks at 400nm-415nm disappears. These spectral changes are in agreement with the features of face-to-face porphyrin dimer which are previously reported.[7]

The infrared spectrum of C=O region of αααα-atropisomer of porphyrin **1** and **3** are shown in Table 1. In THF and CH_2Cl_2, the C=O stretching of **3** are almost the same, while that stretching of **1** are 1728cm^{-1} and 1695cm^{-1},

Table 1. Infrared spectra data of C=O region for Zn $TPP(CO_2CH_3)_4$ and Zn $TPP(CO_2H)_4$. [1],[3]=1mM.

	in THF	in CH_2Cl_2
3 $TPP(CO_2CH_3)_4$	1733cm^{-1}	1727cm^{-1}
1 $TPP(CO_2H)_4$	1728cm^{-1}	1695cm^{-1}

respectively. This result strongly indicates hydrogen bond formation between two carboxylic acid moieties in nonpolar solvent.

The ^{1}H-NMR spectra of aromatic reagion of porphyrin **1** and **3** in THF and CD_2Cl_2 are summarized in Figure 6. The chemical shifts of **3** behave very similarly both in THF and CD_2Cl_2, but for **1**, the large differences were observed. These behavior will come from ring current effect of porphyrin **1** which aggregate in nonpolar solvent.

Based on these results, we determined molecular weight of **1** in $CHCl_3$ at

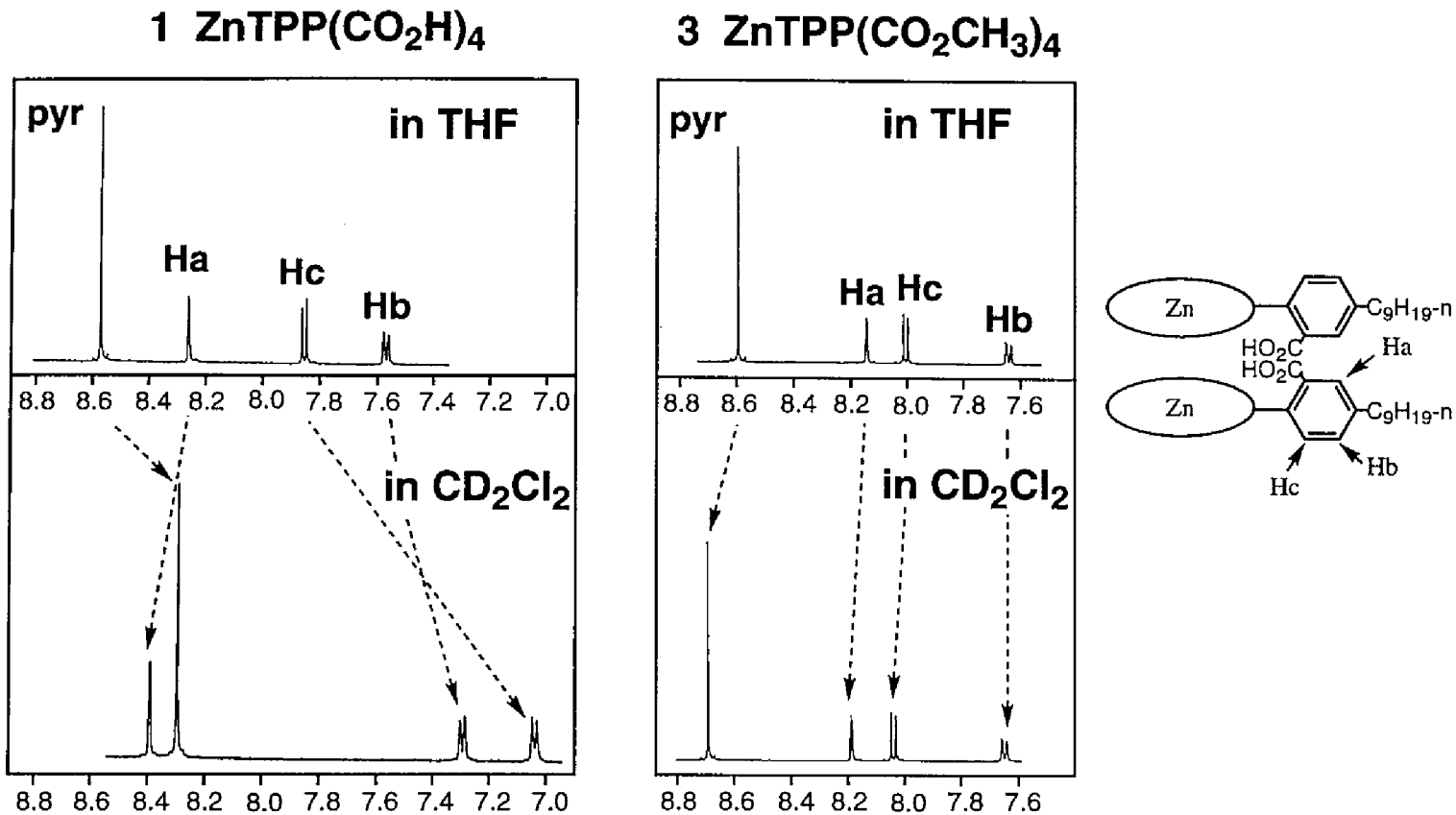

Figure 6. The ^{1}H-NMR spectra of αααα-atropisomer of porphyrin **1** and **3** in THF and CD_2Cl_2. [1],[3]=1mM.

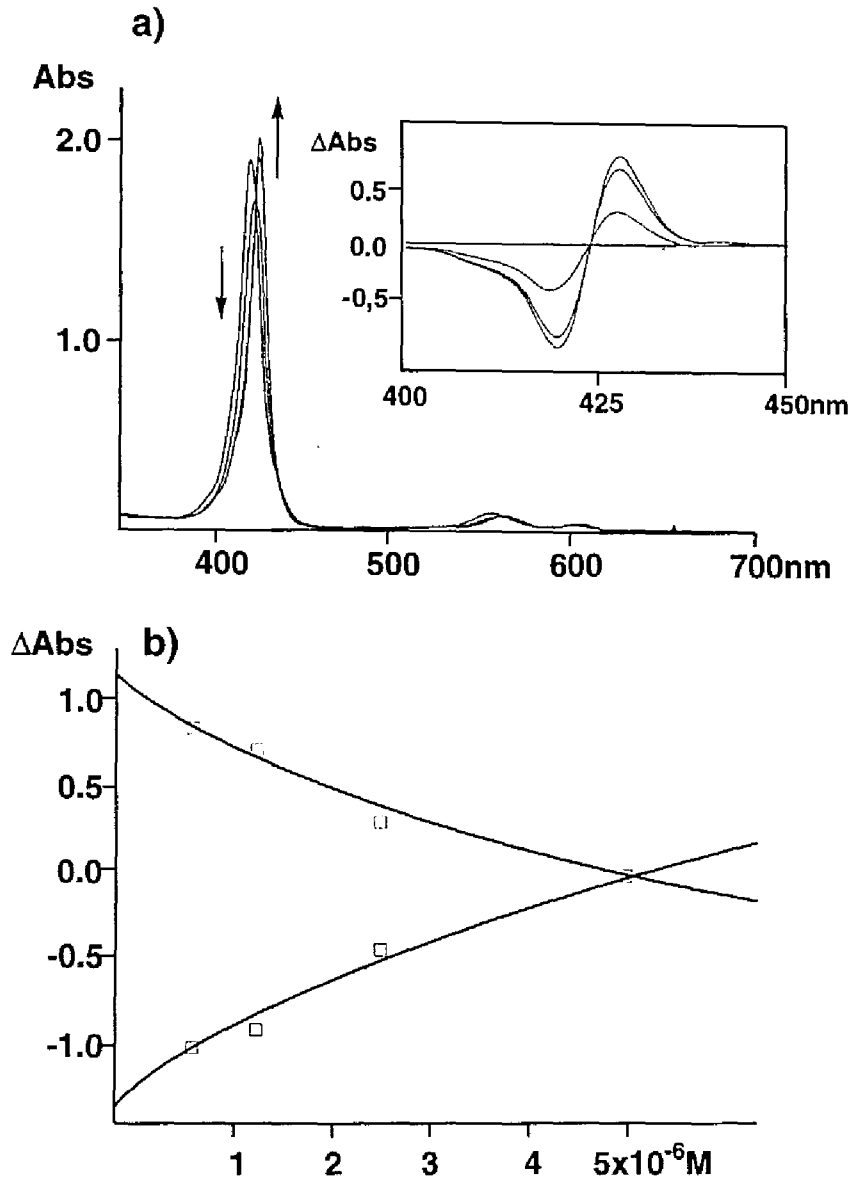

Figure 7. a) Spectral change of **1** in the concentration region of $5x10^{-6}$ to $0.625x10^{-6}$M at 20 °C in CH_2Cl_2. The spectra are corrected by multiplication for same concentration. b) Fitting result for dimer formation. The solid lines show the theoretical curves generated by REDAP with association constant K= $1x10^{6}M^{-1}$.

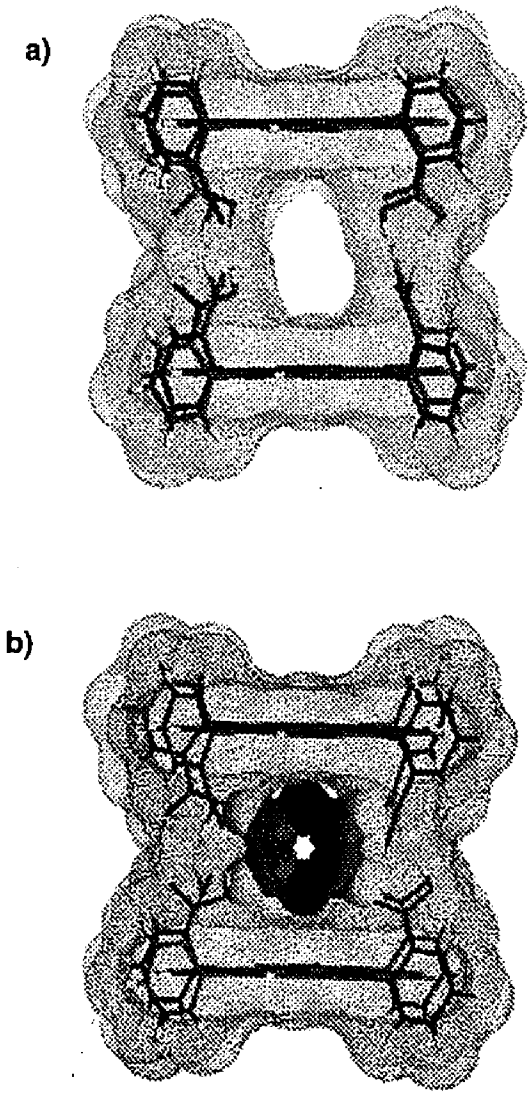

Figure 8. Schematic structures of a) Self-organized porphyrin dimer b) complex formation between porphyrin dimer and pyrazine. The figure is generated with NMRGRAPH, Molecular Simulations Inc., and dots shows the solvent accessible surfaces.

40°C using the method of vapor pressure osmometry. The results undoubtedly indicated dimer formation in $CHCl_3$, i.e., observed molecular weight of **1** in $CHCl_3$ was 2653 ± 200 which is in excellent agreement with dimer formation (M.W.=2715). All of these observations strongly suggest that **1** generates face-to-face dimer in nonpolar solvents via hydrogen bond formation between carboxylic acid moieties.

To clarify the equilibrium constant of dimer formation, we analyzed UV/vis spectral change of **1** in the concentration range of $5x10^{-6}$M to $0.625x10^{-6}$ M. The Soret band shifted from 422nm to 427nm with the concentration decreasing as shown in Figure 7-a. From this spectral change, we determined the equilibrium constant by using non-linear least square optimization method. The fitting result is shown in Figure 7-b and optimized equilibrium constant is $K=1x10^{6}M^{-1}$ in CH_2Cl_2.

Furthermore considerations of molecular models reveal the face-to-face dimer of **1** shown in Figure 8-a as a most plausible structure. This self-assembled

Scheme 1

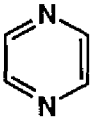

4

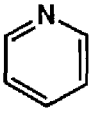

5

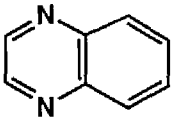

6

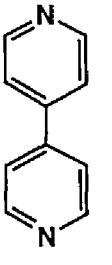

7

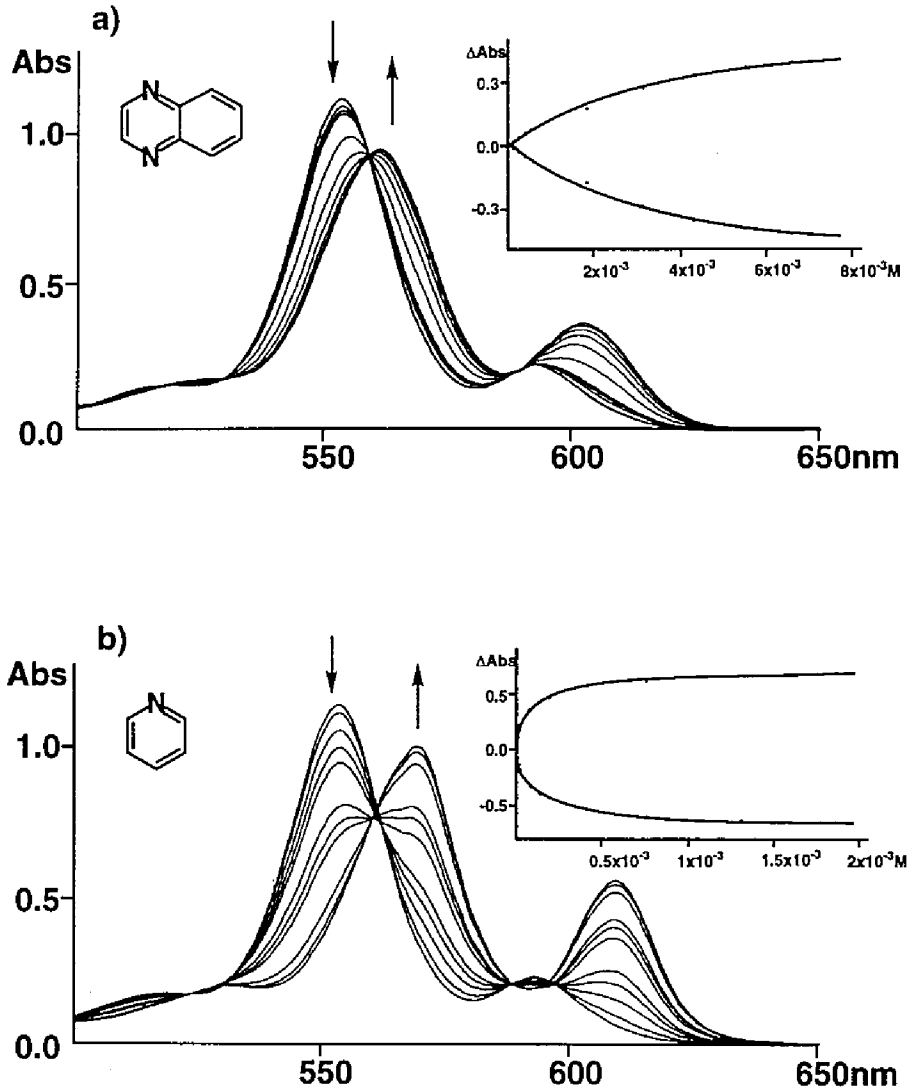

Figure 9. a) Spectral change of **1** and titration curve on addition of quinoxaline at 25°C. [**1**]=6x10^{-5}M. b) Spectral change of **1** and titration curve on addition of pyridine at 25°C. [**1**]=6x10^{-5}M.

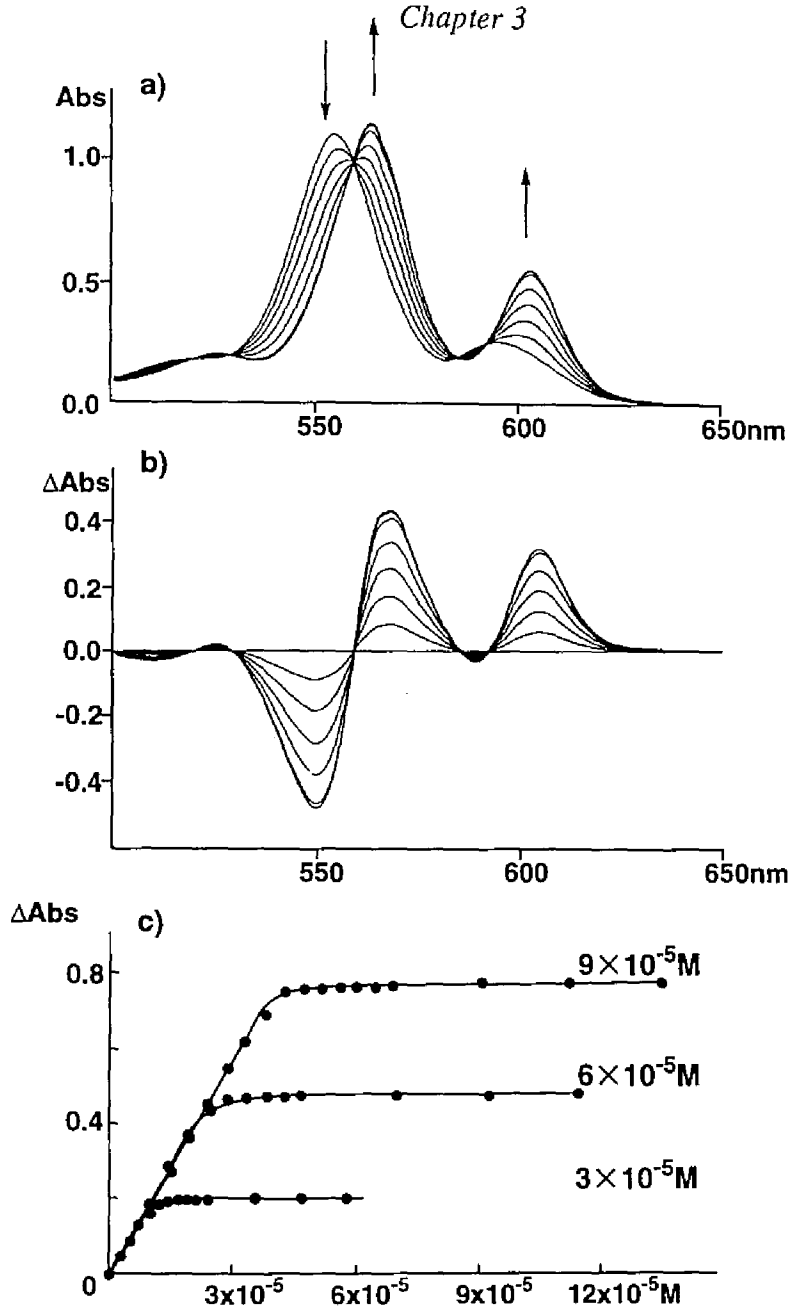

Figure 10. a) Spectral change of **1** on addition of pyrazine at 25°C. [**1**]=6x10^{-5}M. b) Difference spectra . c) Fitting result for scheme 2 on three different concentrations at 568nm. The solid lines show the theoretical curves with K_{dimer}=5x10^{5}M^{-1} and $K_{pyrazine}$=1x10^{10}M^{-1}.

porphyrin dimer has a cavity between the two porphyrin faces, the distance between the porphyrin planes is 8-9 Å, furthermore, top and bottom end are zinc as the coordination site. So this self-assembled cavity is available for molecular recognition site for bidentate ligands such as pyrazine.

Titration of guests **4-7** with porphyrin were followed by UV-visible absorption spectroscopy in CH_2Cl_2, by using the complexation shift of the Q band. The spectra did not show any significant shift by addition of 0.5 equimolar guest **5-7** which are not bidentate ligands or too large to enter the cavity, further addition of guest resulted in red shift by complexation on outer side of porphyrin dimer as shown in Figure 9. However the addition of **4**, the spectra show the significant red shift. This spectral change was linearly increased untill the guest concentration reached 0.5 equimolar, and then it was saturated (Figure 10-c). This results show that in the range of guest concentration less than 1 equimolar, only the bidentate ligands can enter the cavity of dimer. The non-linear theoretical curve fitting analyses[8] reveal that the observed data in Figure 10 show good agreement with the equilibrium model (scheme 2) containing two association constants K_{dimer} and $K_{pyrazine}$. The association constant thus obtained of porphyrin

Scheme 2

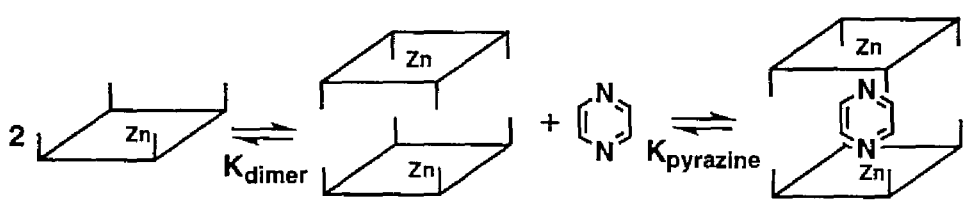

dimerization K_{dimer} was $5x10^5M^{-1}$ and the binding constant of pyrazine with the dimeric porphyrin $K_{pyrazine}$ was $1x10^{10}M^{-1}$.

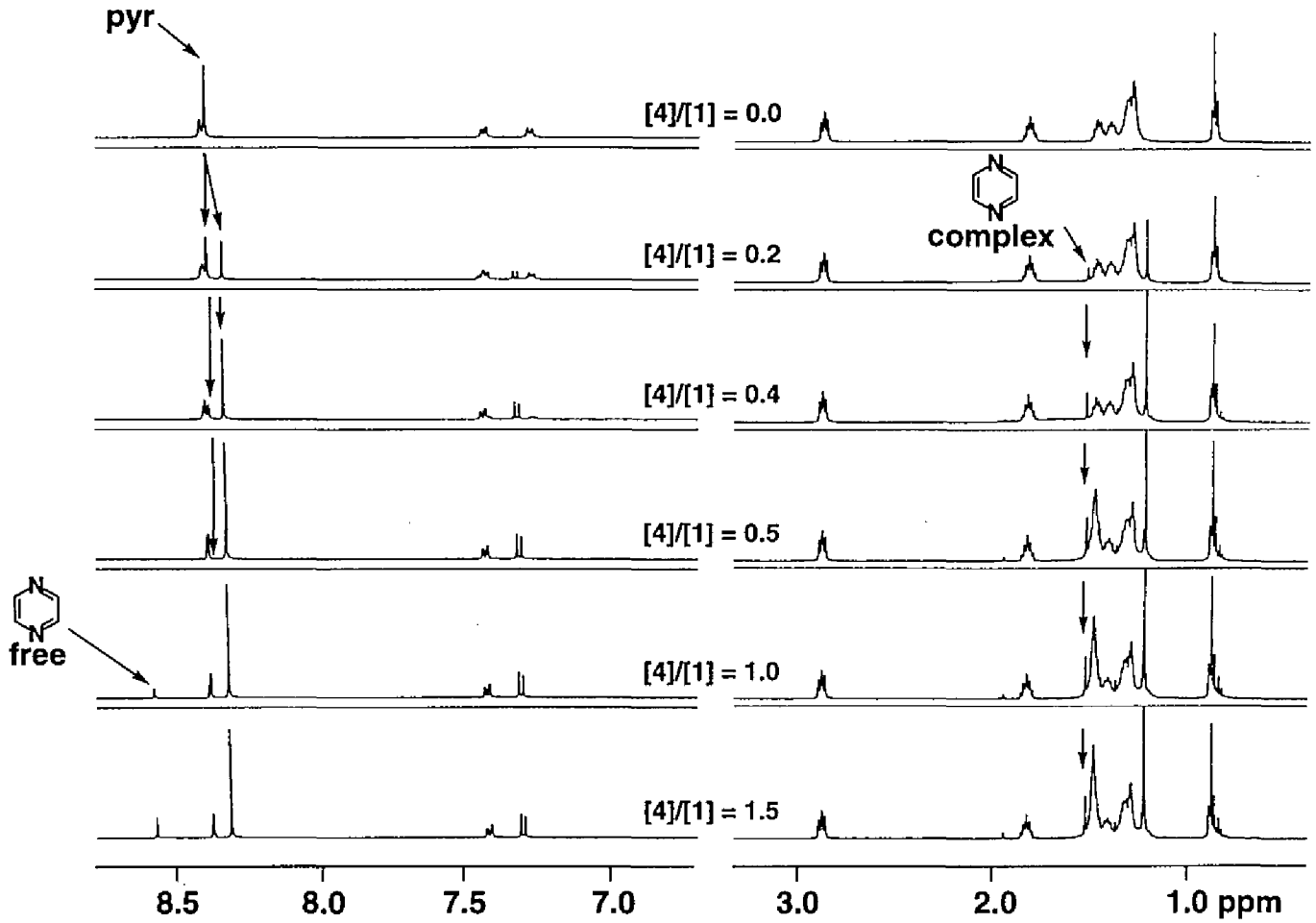

Figure 11. ^{1}H-NMR (500 MHz) spectra of titration with pyrazine in CD_2Cl_2. These spectra were recorded at 298K. The concentration of **1** was 1mM.

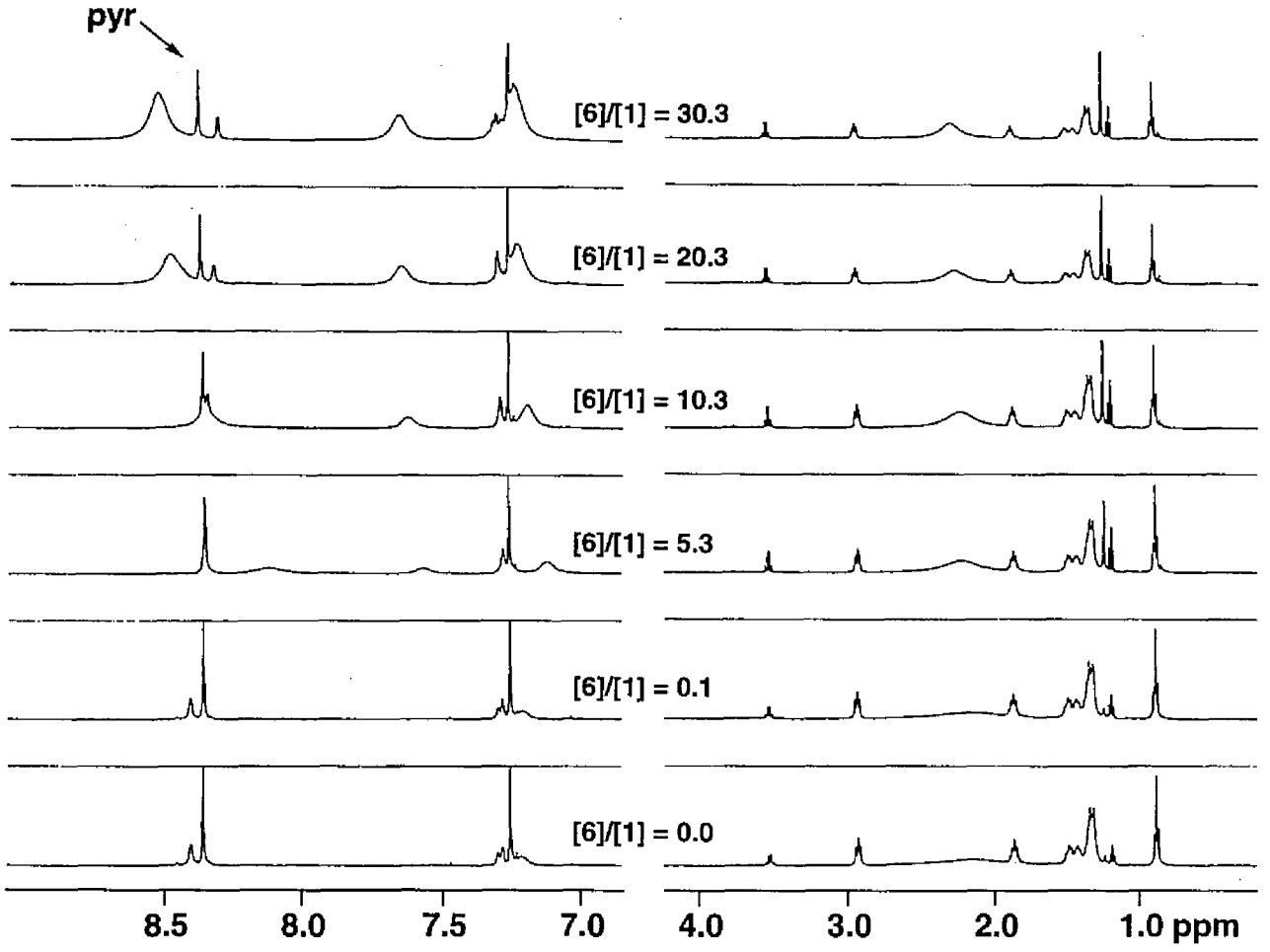

Figure 12. ^{1}H-NMR (500 MHz) spectra of titration with pyridine in $CDCl_3$. These spectra were recorded at 298K. The concentration of **1** was 1mM.

The complexation between dimer and pyrazine was detected titrimetrically by 500MHz ^{1}H NMR spectroscopy in CD_2Cl_2 (Figure 11). We observed signals of two species coming from complexing one and uncomplexing one. As a typical example, pyrrole protons of the uncomplexed dimeric porphyrin appear as a singlet signal at δ8.35 ppm. After the addition of 0.2 equimolar pyrazine, new pyrrole protons of the dimeric porphyrin complexed with pyrazine appear as a singlet signal at δ8.29 ppm. As the addition of pyrazine, the signal at δ8.35 ppm was decreased gradually and when the guest concentration was 0.5 equimolar, this signal disappeared, on the other hand, the signal at δ8.29 ppm was increased and after the guest concentration was over 0.5 equimolar, this increase stopped. The complexed pyrazine protons peak which appeared as a singlet signal at δ1.57 ppm was increased till the pyrazine concentration reached 0.5 equimolar. Beyond that concentration free pyrazine peak appeared as a singlet signal at δ8.56 ppm and was increased. These stoichiometory shows that the ratio of **1** to pyrazine in this complex was 2:1 and the upfield shift of pyrazine protons from δ8.56 to 1.57 ppm strongly support the insertion of pyrazine into the cavity of the porphyrin dimer[9] as shown in Figure 8-b. These spectral changes were not observed for other guest, for example, pyridine in $CDCl_3$, the singlet signal of pyrrole protons shifted from δ8.32 to 8.36 ppm gradually as the addition of guest and it was need more than 30 equimolar of pylidine for this shift to saturate (Figure 12).

These results show that porphyrin **1** aggregates and formes face-to-face

porphyrin dimer through the eight hydrogen bonds. This self-assembling porphyrin dimer, unlike monomer, act as a receptor which incorporates pyrazine selectively into the cavity. This high selectivity of the self-assembling receptor is available for linker to extend this self-assembling system which is powerful approach to the construction of functionalized molecules, in addition, on the basis of biomimetic interest such as photochemistry of porphyrin.

Experimental Section

General Remarks. ^{1}H-NMR spectra were recorded on a JEOL FX-90Q (90 MHz), a JEOL GX-400 (400MHz) or a JEOL α-500 (500MHz). ^{1}H-NMR chemical shifts are referenced to internal $CDCl_3$ (^{1}H δ7.25ppm) relative to Me_4Si at 0 ppm. Electronic absorption spectra were performed on a Hitachi U-3410 spectrometer, multi-channel photodiode array spectrometer, Otsuka Electronics MCPD-100 or Hewlett-Packard HP-8452A, thermostated at given temperatures with a circulation system, NESLAB Instruments, Inc. RTE-9. IR spectra were recorded on PERKIN ELMER System2000 FT-IR. Vapor pressure osmometory measurements were performed on CORONA 117. Mass spectra were obtained with a JEOL JMS DX-300 or a JEOL JMS-SX102A mass spectrometer. HPLC experiments were performed on a TOSOH HLC-837 or Waters M600E equipped with a TOSOH UV-8010 variable-wavelength detector and Waters M991 photodiode array detector.

Materials. Solvents used in spectral measurement were Spectrosol purchased from Nacalai Tesque, Inc.or Dojindo Laboratories. Other commercially available chemicals were purchased from Wako Pure Chemical Industries, Ltd. or Nacalai Tesque, Inc., or Tokyo Kasei Kogyo Co., Ltd. and employed without further purification, unless stated otherwise. Analytical thin-layer chromatography was performed with pre-coated Merck silica gel 60, F254 (0.2mm layers on glass plates). Column chromatography was performed using Merck Kieselgel 60 or WAKOgel LP-40C18.

[*meso*-Tetrakis(2-carboxy-4-nonylphenyl)porphyrinato]zinc(II) (**1**). To*meso*-tetrakis(2-carboxy-4-nonylphenyl)porphyrin in chloroform is added a saturated solution of zinc acetate in methanol. After a few minutes stirring and checking by UV-vis spectrophtometry, the mixture is washed with 1M-HCl, washed with water several times, dried over Na_2SO_4, and concentrated in vacuo. Recrystallization from CH_2Cl_2/hexane gave purple solid **1**;(αααα atropisomer):^{1}H-NMR (500 MHz, THF) δ8.56 (s, 8H), 8.25 (d, J=1.8Hz, 4H), 7.85 (d, J = 7.5Hz, 4H), 7.58 (dd, J = 7.5,1.8Hz, 4H), 2.99 (t, J=7.8Hz, 8H), 1.95 (m, 8H), 1.6-1.3 (several peaks, 48H), 0.92 (t, J = 7.0Hz, 12H); FAB MS 1359 $(M+H)^+$; Anal.Calcd for ($C_{84}H_{100}N_4O_8Zn + H_2O$) : C, 73.26; H, 7.48; N, 4.07. Found: C,73.19; H, 7.40; N, 4.02; UV-vis (THF) λmax (logε) 431nm (5.73), 563 (4.33), 604 (4.01).

HPLC analysis. The polphyrin solution $2x10^{-4}$Mwas placed in a test tube with a stirrer bar under N_2 atmosphere in a thermostated bath. The 50 μl aliquot was removed on each time and in the case of $TPP(COOH)_4$, it was added diazomethane ether solution for esterification then evaporated. The sample was dissolved in solvent and injected into HPLC. In the case of $Zn(COOH)_4$ only in toluene, the removed 50μl aliquot was diluted to 500 μl with DMSO and esterified by diazomethane ether solution. Then the mixture solution was evaporated to remove excess diazomethane, added small amount of water and extracted with ether. This extract was injected into HPLC (column YMC, A-813

C4 , eluent, methanol:water=100:1.8, detected at 420nm, flow rate=1ml/min).

Curve fitting. Curve fitting was done by REDAP (Reaction Dynamics Analysis Program) which was written in C language, for execution on NEC PC9800 series computers and included a graphic routine for presentation of results.

The association constant of dimer formation K_D was evaluated from the plot of ΔAbs against the concentration of porphyrin.

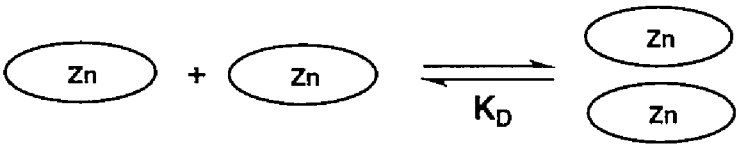

$$\frac{[P\text{-}P]}{[P][P]} = K_D \qquad (1)$$

$$\frac{[P\text{-}P_0]}{[P_0][P_0]} = K_D \qquad (2)$$

$$X=[P]+2[P\text{-}P] \qquad (3)$$

$$C=[P_0]+2[P\text{-}P_0] \qquad (4)$$

where X; total concentration of porphyrin

C; initial concentration of porphyrin

[P]; concentration of monomer porphyrin

[P-P]; concentration of dimer porphyrin

$[P_0]$; initial concentration of monomer porphyrin

$[P\text{-}P_0]$; initial concentration of dimer porphyrin

From eq 1, eq 2, eq 3, and eq 4

$$[P] = \frac{-1+\sqrt{1+8K_DX}}{4K_D} \quad (5)$$

$$[P_0] = \frac{-1+\sqrt{1+8K_DC}}{4K_D} \quad (6)$$

Initial absorbance (Abs_0) is

$$Abs_0=\varepsilon_m[P_0]+\varepsilon_D[P-P_0] \quad (7)$$

and the absorbance (Abs) is

$$Abs=\varepsilon_m[P]+\varepsilon_D[P-P] \quad (8)$$

where ε_m and ε_D are molar coefficients of monomer porphyrin and dimer porphyrin, respectively.

The concentration difference is corrected by multiplication of C/X,then eq 8 becomes

$$Abs=C/X(\varepsilon_m[P]+\varepsilon_D[P-P]). \quad (9)$$

From eq 3, eq 4, eq 7, and eq 9

$$\Delta Abs=Abs-Abs_0=\varepsilon_m(C/X[P]-[P_0])-\varepsilon_D/2(C/X[P]-[P_0])$$

$$=\Delta\varepsilon(C/X[P]-[P_0]) \quad (10)$$

where $\Delta\varepsilon=\varepsilon_m-\varepsilon_D/2$.

Since [P] and $[P_0]$ are known from eq 5 and eq 6, K_D is estimated as parameter from REDAP by using eq 10.

The association constant of dimer formatin K_D and binding constant of

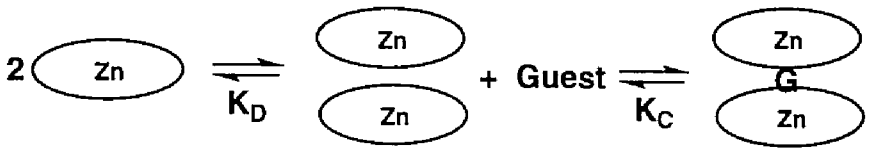

guest with porphyrin dimer K_C were evaluated from the plot of ΔAbs against the concentration of guest.

Here G_T, P_T, [G], [P], [P-P], and [P-G-P] are total concentration of guest, porphyrin, free guest, monomer porphyrin, dimer porphyrin, and complexed porphyrin dimer, respectively.

$$\frac{[P\text{-}P]}{[P][P]} = K_D \qquad (1)$$

$$\frac{[P\text{-}G\text{-}P]}{[P\text{-}P][G]} = K_C \qquad (2)$$

$$\frac{[P\text{-}P_0]}{[P_0][P_0]} = K_D \qquad (3)$$

$$G_T = [G] + [P\text{-}G\text{-}P] \qquad (4)$$

$$P_T = [P] + 2[P\text{-}P] + 2[P\text{-}G\text{-}P] \qquad (5)$$

$$P_{T0} = [P_0] + 2[P\text{-}P_0] \qquad (6)$$

and V, x, G_{T0}, P_{T0} are initial volume of solvent, added volume of solvent, initial concentration of guest, and initial concentration of porphyrin, respectively,

$$G_T = \frac{x}{V+x} G_{T0} \qquad P_T = \frac{V}{V+x} P_{T0}$$

From eq 3 and eq 6

$$[P_0] = \frac{-1+\sqrt{1+8K_DP_{T0}}}{4K_D} \quad (7)$$

$$[P\text{-}P_0]=(P_{T0}-[P_0])/2$$

from eq 1, eq 2, and eq 4

$$[P\text{-}P]=K_D[P]^2 \quad (8)$$

$$[P\text{-}G\text{-}P]=[P\text{-}P][G]K_C=K_CK_D[P]^2[G] \quad (9)$$

$$[G]=G_T-[P\text{-}G\text{-}P]=G_T-K_CK_D[P]^2[G] \quad (10)$$

from eq 10, [G] is obtained as

$$[G] = \frac{G_T}{1+K_CK_D[P]^2} \quad (11)$$

Substituting eq 8, eq 9, and eq 10 in eq 5

$$P_T=[P]+2K_D[P]^2+2K_CK_D[P]^2\frac{G_T}{1+K_CK_D[P]^2} \quad (12)$$

The guest employed here does not show electronic absorption in this experimental range, the absorbance (Abs) at given wavelength in the experiment is

$$Abs=\varepsilon_P[P]+\varepsilon_D[P\text{-}P]+\varepsilon_C[P\text{-}G\text{-}P]$$

$$=\varepsilon_P(P_T-2[P\text{-}P]-2[P\text{-}G\text{-}P]+\varepsilon_D[P\text{-}P]+\varepsilon_C[P\text{-}G\text{-}P]$$

$$=\varepsilon_PP_T+(\varepsilon_D-2\varepsilon_P)[P\text{-}P]+(\varepsilon_C-2\varepsilon_P)[P\text{-}G\text{-}P] \quad (13)$$

where ε_P, ε_D, and ε_C are molar extinction coefficients of free porphyrin, porphyrin dimer, and complexed porphyrin dimer, respectively.

Initial absorbance Abs_0 is

$$Abs_0=\varepsilon_P[P_0]+\varepsilon_D[P-P_0]$$

$$=\varepsilon_P(P_{T0}-2[P-P_0])+\varepsilon_D[P-P_0]$$

$$=\varepsilon_P P_{T0}+(\varepsilon_D-2\varepsilon_P)[P-P_0]$$

then,

$$\Delta Abs=Abs(V+x)/V-Abs_0$$

$$=\{\varepsilon_P P_T+(\varepsilon_D-2\varepsilon_P)[P-P]+(\varepsilon_C-2\varepsilon_P)[P-G-P]\}(V+x)/V-\varepsilon_P P_{T0}-(\varepsilon_D-2\varepsilon_P)[P-P_0]$$

$$=\{\varepsilon_P P_T+(\varepsilon_D-2\varepsilon_P)[P-P]+(\varepsilon_C-2\varepsilon_P)[P-G-P]\}(V+x)/V-\varepsilon_P P_T(V+x)/V-(\varepsilon_D-2\varepsilon_P)[P-P_0]$$

$$=\{(\varepsilon_D-2\varepsilon_P)[P-P]+(\varepsilon_C-2\varepsilon_P)[P-G-P]\}(V+x)/V-(\varepsilon_D-2\varepsilon_P)[P-P_0]$$

$$=(\Delta\varepsilon_1[P-P]+\Delta\varepsilon_2([P-G-P])(V+x)/V-\Delta\varepsilon_1[P-P_0] \quad (14)$$

where $\Delta\varepsilon_1=\varepsilon_D-2\varepsilon_P$ and $\Delta\varepsilon_2=\varepsilon_C-2\varepsilon_P$.

Since [P-P], [P-G-P], and $[P-P_0]$ are known from eq 7, eq 8, eq 9, and eq 12, K_C and K_D are estimated as parameter from REDAP by using eq 14.

References and Notes

(1) (a) Lehn, J. M.; Rigault, A.; Siegel, J.; Harrowfield, J.; Chevrier, B.; Moras, D. *Proc. Natl. Acad. Sci. USA.* **1987**, 84, 2565. (b) Lehn, J. M. *Angew. Chem. Int. Ed. Engl.* **1988**, 27, 89. (c) Lehn, J. M. *Angew. Chem. Int. Ed. Engl.* **1990**, 29, 1304. (d) Ghadiri, M. R.; Kobayashi, K.; Granja, J. R.; Chadha, R. K.; McRee, D. E. *Angew. Chem. Int. Ed. Engl.* **1995**, 34, 93. (e) Maverick, A. W.; Klavetter, F. E. *Inorg. Chem.* **1984**, 23, 4129. (f) Ruttimann, S.; Bernardinelli, G.; Williams, A. F. *Angew. Chem. Int. Ed. Engl.* **1993**, 32, 392. (g) Saalfrank, R. W.; Burak, R.; Breit, A.; Stalke, D.; Irmer, R. H.; Daub, J.; Porsch, M.; Bill, E.; Muther, M.; Trautwein, A.X. *Angew. Chem. Int. Ed. Engl.* **1994**, 33, 1621. (h) Seel, C.; Vogtle, F. *Angew. Chem. Int. Ed. Engl.* **1992**, 31, 528. (i) Fujita, M.; Nagao, S.; Ogura, K. *J. Am. Chem. Soc.* **1995**, 117, 1649. (j) Whitesides, G. M.; Mathias, J. P.; Seto, C. T. *Science* **1991**, 254, 1312. (k) Benniston, A. C.; Harriman, A.; Lynch, V. M. *Tetrahedron Lett.* **1994**, 35, 1473. (l) Anderson, H. L.; Anderson,S.; Sanders, J. K. M. *J. Chem. Soc., Perkin Trans. 1* **1995**, 2231. (m) Goodman, M. S.; Jubian, V.; Linton, B.; Hamilton, A. D. *J. Am. Chem. Soc.* **1995**, 117, 11610. (n) Valdes, C.; Spitz, U. P.; Toledo, L. M.; Kubik, S. W.;Rebek, J.,Jr. *J. Am. Chem. Soc.* **1995**, 117, 12733. (o) Mathias, J. P.; Seto, C. T.; Simanek, E. E.; Whitesides, G. M. *J. Am. Chem. Soc.* **1994**, 116, 1725. (p) Collin, J. P.; Harriman, A.; Heitz, V.; Odobel, F.; Sauvage, J. P. *J. Am. Chem. Soc.* **1994**, 116, 5679. (q) Chernook, A. V.; Shulga, A. M.; Zenkevich, E. I.; Rempel, U.; Borczyskowski, C. V. *J. Phys. Chem.* **1996**, 100, 1918

For original Carcerand, see; (r) Cram, D. J. *Science* **1983**, 219, 1177. (s) Cram, D. J. *Nature* **1992**, 356, 29.

(2) (a) Collman, J. P.; Wagenknecht, P. S.; Hutchison, J. E. *Angew. Chem. Int. Ed. Engl.* **1994**, 33, 1537. (b) Chang, C. K. *J. Chem. Soc., Chem. Commun.* **1977**, 800-801. (c) Osuka, A.; Maruyama, K. *J. Am. Chem. Soc.* **1988**, 110, 4454-4456. (d) Sessler, J. L.; Capuano, V. L.; Harriman, A. *Ibid.* **1993**, 115, 4618-4628. (e) Overfield, R. E.; Scherz, A.; Kaufmann, K. J.; Wasielewski, M. R. *Ibid.* **1983**, 105, 4256-4260. (f) Dubowchik, G. M.; Hamilton, A. D. *J. Chem. Soc., Chem. Commun.* **1986**, 1391-1394. (g) Ogoshi, H.; Sugimoto, H.; Yoshida, Z. *Tetrahedron Lett.* **1977**, 169-172.

(3) (a) Sessler, J. L.; Wang, B.; Harriman, A.; *J. Am. Chem. Soc.* **1995**, 117, 704. (b) Hunter, C. A.; Sarson, L. D. *Angew. Chem. Int. Ed. Engl.* **1994**, 33, 2313. (c) Segawa, H.; Takehara, C.; Honda, K.; Shimidzu, T.; Asahi, T.; Mataga. N. *J. Phys. Chem.* **1992**, 96, 503. (d) Drain, C. M.; Fischer, R.; Nolen, E. G.; Lehn, J. M. *J. Chem. Soc., Chem. Commun.* **1993**, 243-245. (e) Kobuke, Y.; Miyaji, H. *J. Am. Chem. Soc.* **1994**, 116, 4111-4112. (f) Aoyama, Y.; Kamohara, T.; Yamagishi, A.; Toi, H.; Ogoshi, H. *Tetrahedron Lett.* **1987**, 28, 2143-2146.

(4) Kuroda, Y.; Kawashima, A.; Urai, T.; Ogoshi, H. *Tetrahedron Lett.* **1995**, 36, 8449.

(5)Gottwald, L. K. ; Ullman, E. F. *Tetrahedron Lett.* **1969**, 3071-3074.

(6)As there was no appropriate direct method to analyze an distribution of **1**, after the esterification of **1** with diazomethane at room temperature without disturbance of the original distribution, it was determing by using usual reverse phase HPLC column. HPLC column : YMC-Pack C4, eluent : methanol /water =100:3.

(7) (a) Osuka, A.; Maruyama, K. *J. Am. Chem. Soc.* **1988**, 110, 4454-4456. (b)

Collman, J, P.; Bencosme, C, S.; Barnes, C, E.; Miller, B, D. *J. Am. Chem. Soc.* **1983**, 105, 2704-2710.

(8) Kuroda, Y.; Kawashima, A.; Ogoshi, H. *Chem. Lett.* **1996**, 57.

(9) (a) Marvaud, V.; Launay, J. P. *Inorg. Chem.* **1993**, 32, 1376. (b) Uemori, Y.; Nakatsubo, A.; Imai, H.; Nakagawa, S.; Kyuno, E. *Inorg. Chem.* **1992**, 31, 5164.

Self-Organized Porphyrin Dimer as Highly Specific Receptor for Pyrazine Derivatives

Abstract

Complex formation between pyrazine derivatives having large side moieties and dimeric self-assembly of αααα-isomer of [*meso*-tetrakis(2-carboxy-4-nonylphenyl)porphyrinato]zinc(II) (**1**) leading to connection between binding pocket and outer space was investigated. ^{1}H NMR and UV-vis titration experiments for this dimeric assembly with pyrazine derivatives revealed highly specific 1:2 complex formation of pyrazine having long alkyl chains and **1**. The equilibrium constants for porphyrin dimer formation and 4-(2-pyrazinyl)-N-benzoylbutanamide (**5**) binding are estimated to be ca. 5 x 10^5 and ca. 2 x 10^7 M^{-1}, respectively. The most characteristic feature of the present ternary system, $(\mathbf{1})_2$• pyrazine, is that the pyrazine derivative having large side moiety such as benzoyl group can coordinate to two zinc atoms inside the dimer cavity by sticking the side moiety out of a window formed between hydrogen bond pillars of the complex.

Introduction

It is of current interest to construct large scale three dimensional chemical structures by using non-covalent interactions which give the systems abilities of reversible self-assembling.[1] Self-assembling abilities in such systems sometimes play an essential role from a viewpoint of not only reversibility but also molecular design of the system, because the abilities make it possible to construct highly complicated structures which are difficult to prepare by usual synthetic procedures. We have recently found a self-assembling system consisted of (**1**), which performs self-induced conformational change to give a carcerand-like porphyrin dimer assembly. [2,3] This assembly has a characteristic inner space available to incorporate and/or to be coordinated by another organic molecule such as pyrazine as a third component of the assembly. Here we report the complex formation between porphyrin dimer and pyrazine derivatives having a side chain to pass through the window formed between hydrogen bond pillars of carcerand-like porphyrin dimer assembly. This opens the possibility to extend this self assembling system to higher order assembling systems.

Results and Discussion

This carcerand-like porphyrin dimer has windows formed between hydrogen bond pillars. For making inside-outside connection, side chains of pyrazine derivatives need pass through this window. We examined three pyrazine derivatives having different types of side chains, i.e. 2-methylpyrazine (**2**), propyl pyrazinecarboxylate (**3**), and N-butylpyrazinamide (**4**) (Scheme 1). Titration of **2**-**4** with porphyrin **1** were followed by UV-visible absorption

Scheme 1

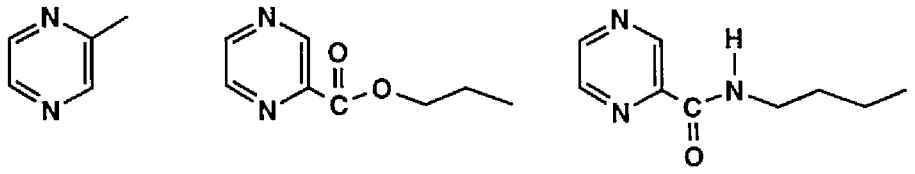

2 **3** **4**

spectroscopy in CH_2Cl_2 by using the complexation shift of the Q band. On the addition of **2**, the spectra show the significant red shift as shown in Figure 1 and absorption at 568 nm was linearly increased until the guest concentration was reached 0.5 equimolar, and further addition of **2** did not show any absorption change. This sharp saturation at the concentration ratio of **1/2** =2/1 (Figure 1-c) is similar to that of pyrazine (chapter 3). This result shows that **2** was incorporated into the cavity of porphyrin dimer. In the case of guest **3** and **4**, however, the spectra did not show any significant shift by addition of 0.5 equivalent of guests, further excess addition of titrants resulted in red shift by complexation on outer side of porphyrin dimer as shown in Figure 2. These observations are noteworthy, because the facts suggest that the methyl group at the 2-position of pyrazine does

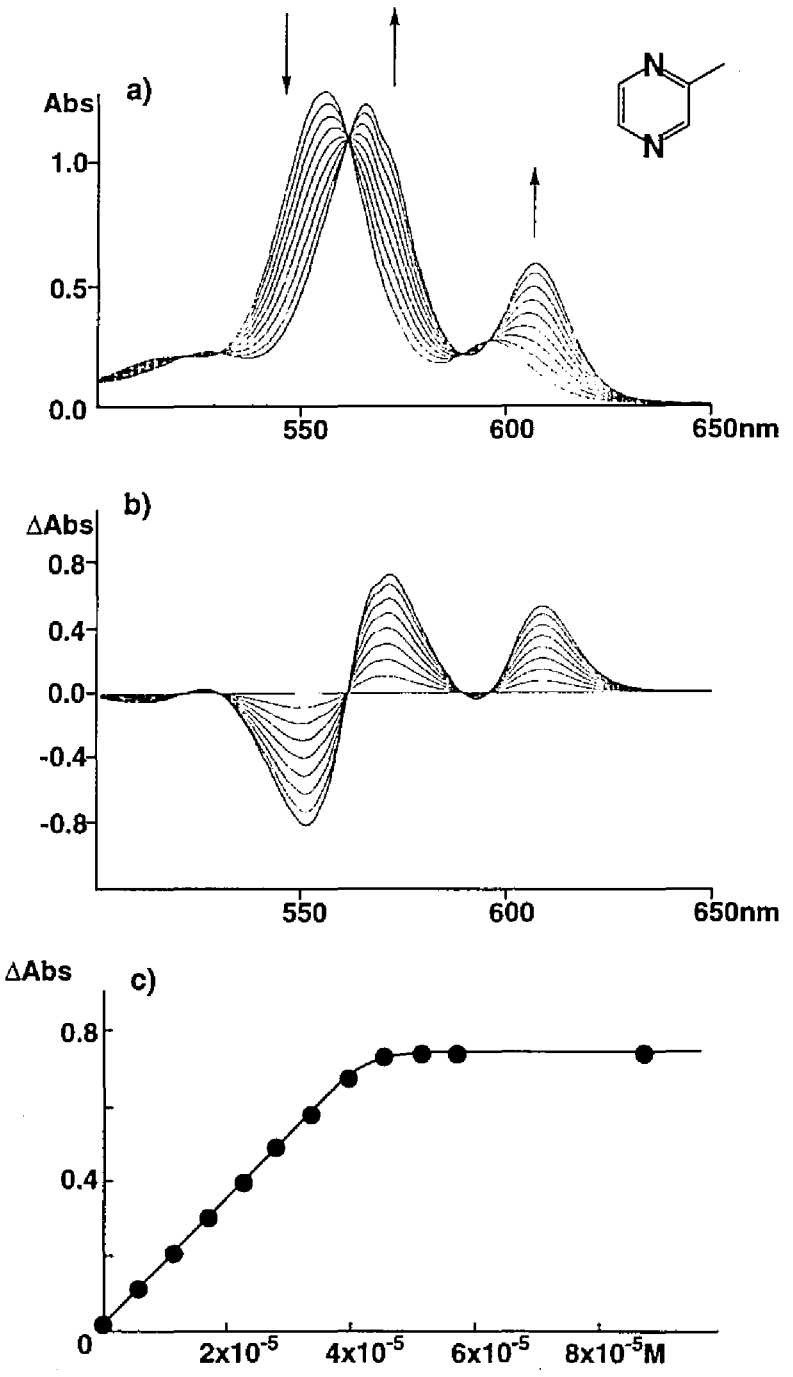

Figure 1. a) Spectral change of **1** on addition of **2** at 25°C. [**1**]=9x10^{-5}M. b) Difference spectra . c) Titration curve at 568 nm.

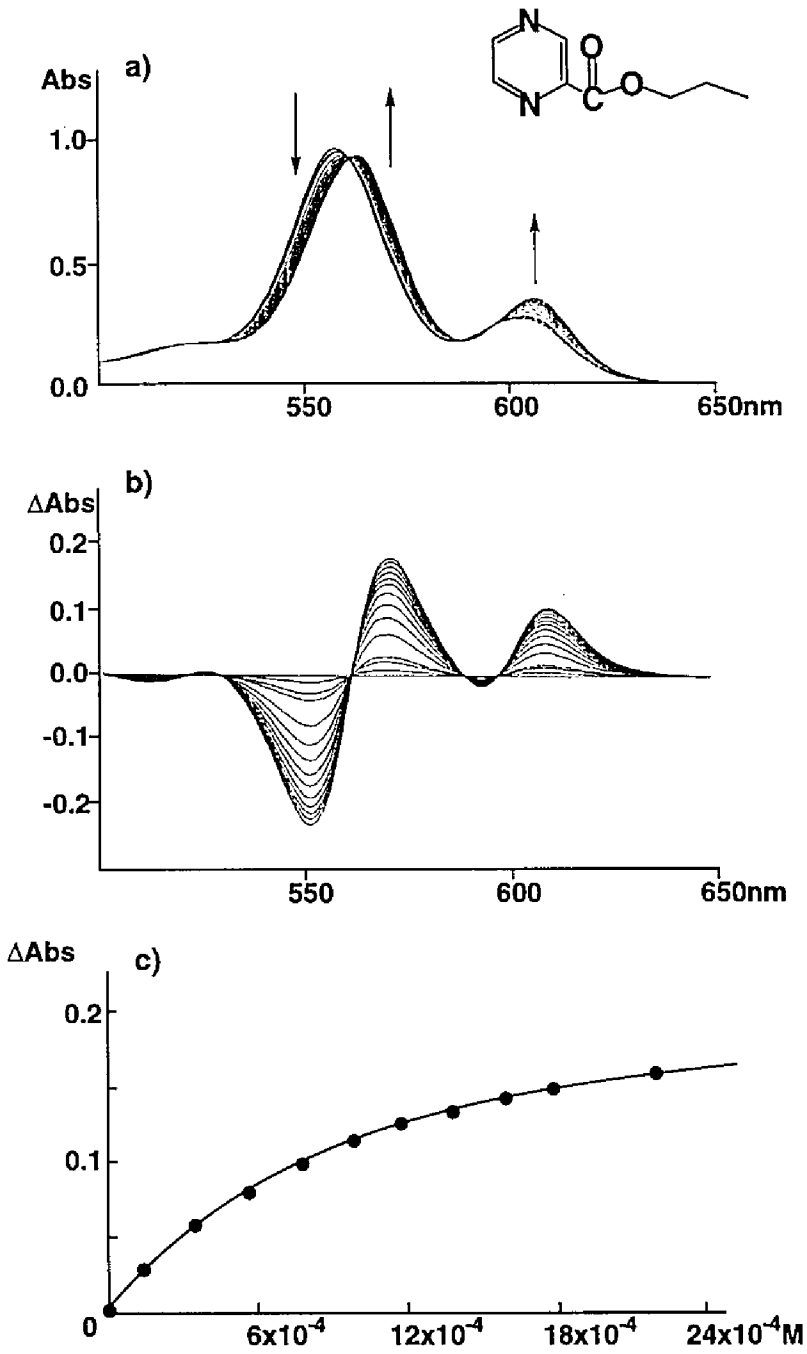

Figure 2. a) Spectral change of **1** on addition of **3** at 25°C. [**1**]=6x10^{-5}M. b) Difference spectra . c) Titration curve at 568 nm.

not hinder present coordination severely. On the other hand ester and amide groups are too large to pass thorough the windows formed by hydrogen bond

Scheme 2

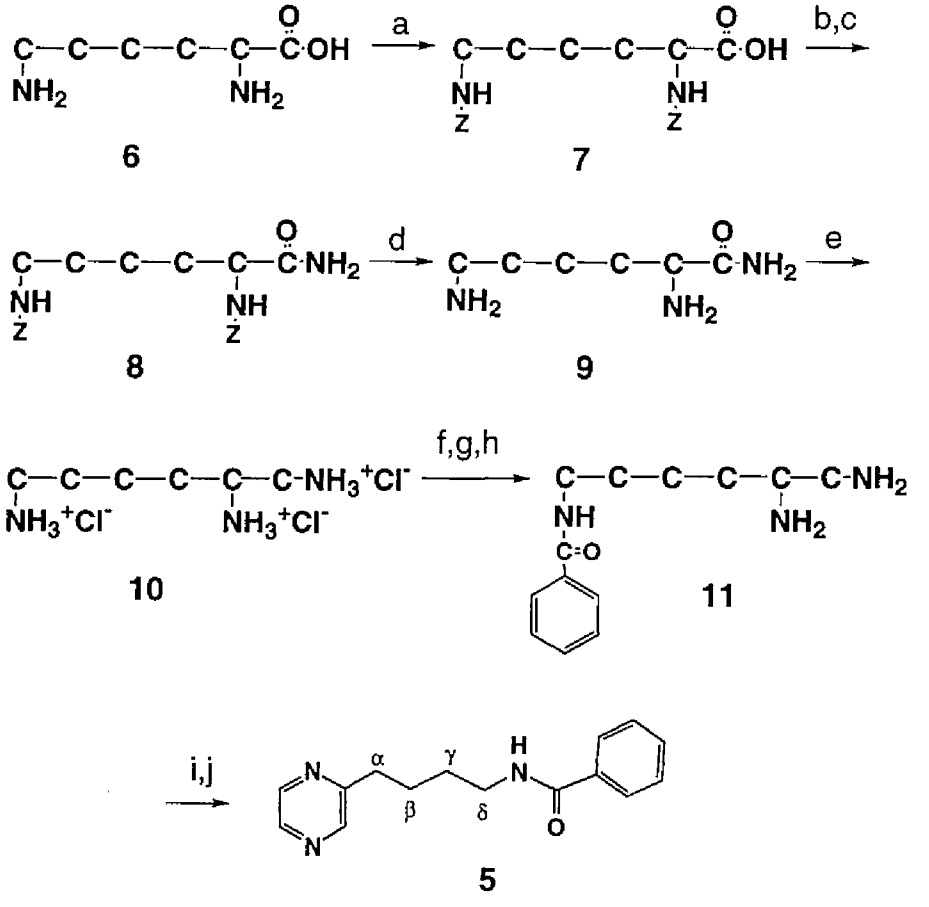

Reagents: (a) Z-Cl, NaOHaq. (b) $HC(CH_3)_2COCl$/THF. (c) NH_4OH. (d) 10% Pd-C/H_2. (e) BH_3.THF. (f) $CuCO_3 \cdot Cu(OH)_2$. (g) Benzoyl chloride. (h) H_2S. (i) Glyoxal, NaOH. (j) air.

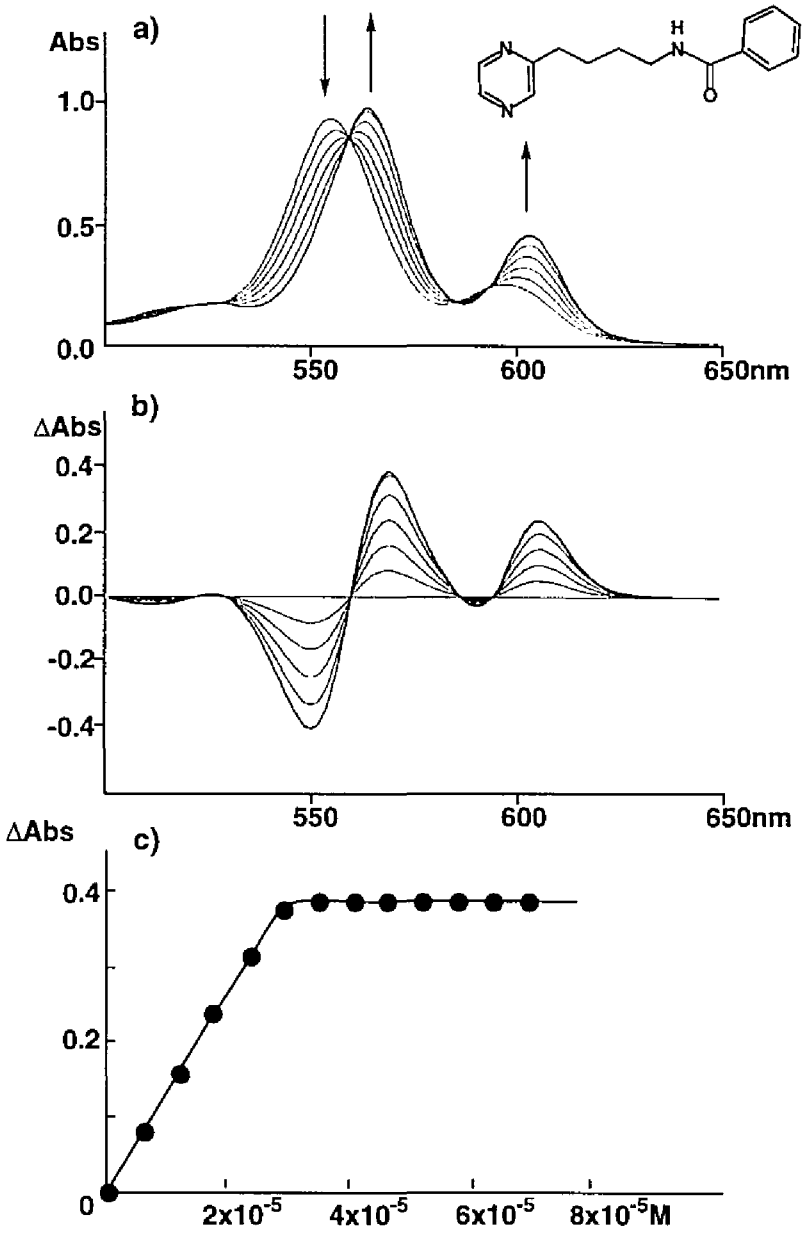

Figure 3. a) Spectral change of **1** on addition of **5** at 25°C. [**1**]=6x10^{-5}M. b) Difference spectra . c) Fitting result for complex formation at 568 nm. The solid line shows the theoretical curves with K_{dimer}=5x10^{5}M^{-1} and $K_{pyrazine}$= 2x10^{7}M^{-1}.

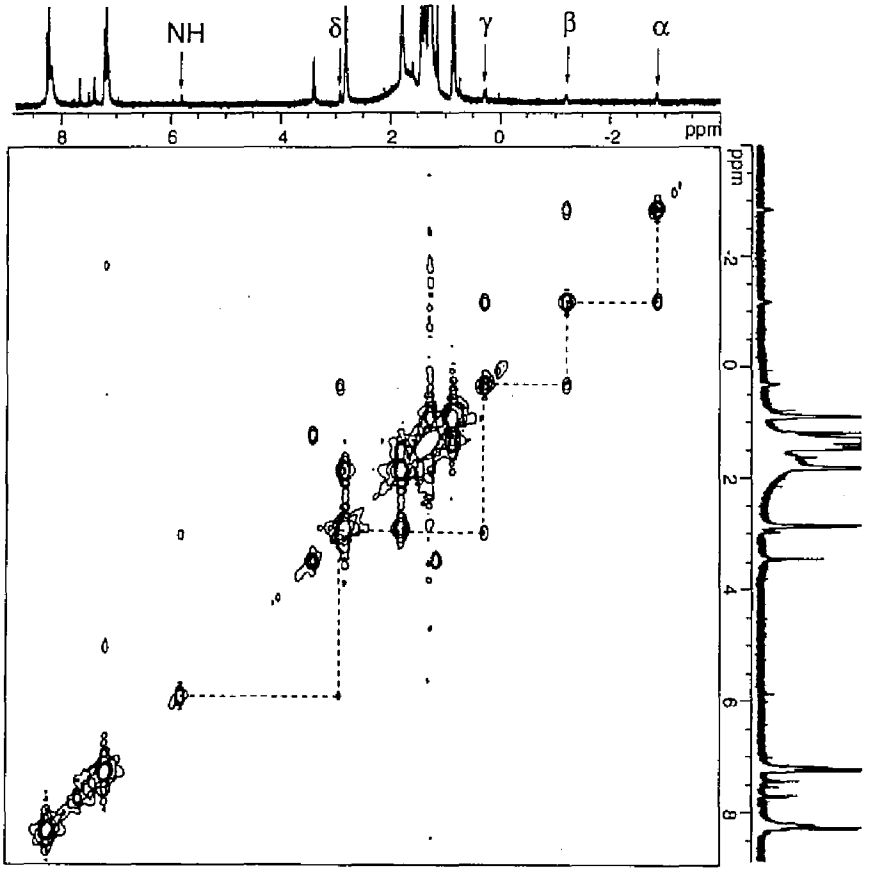

Figure 4. The COSY spectrum (500 MHz) of the assembly consisted of **1** (1 mM) and the pyrazine derivative **5** (0.5 mM) in $CDCl_3$ at 298 K.

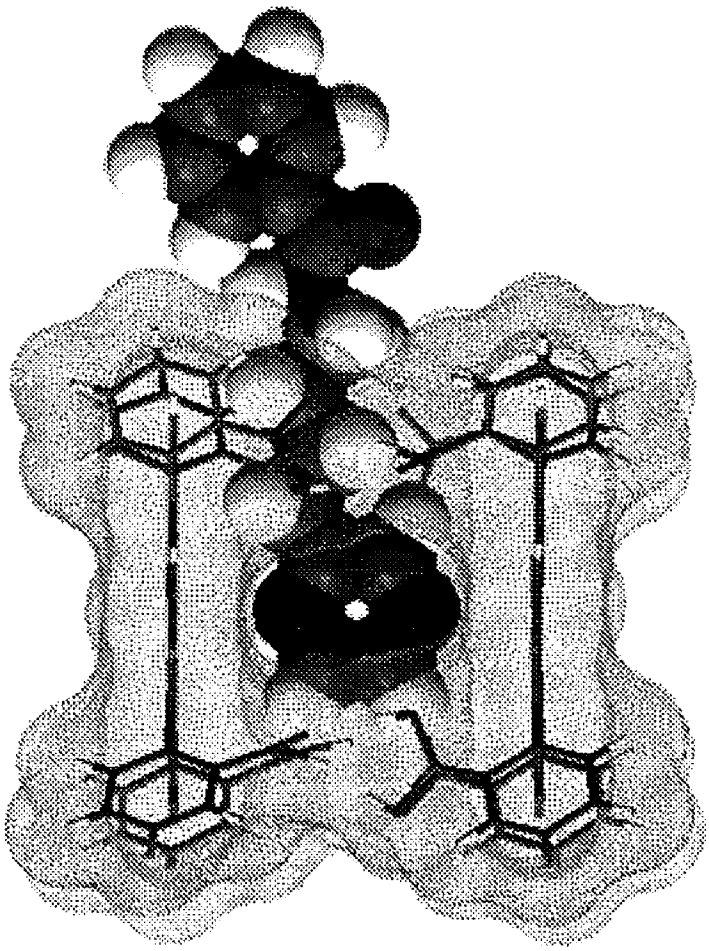

Figure 5. A schematic structure of the assembly, $(\mathbf{1})_2 \bullet \mathbf{5}$. The figure is generated with NMRGRAPH, Molecular Simulations Inc., and dots shows the solvent accessible surfaces of $(\mathbf{1})_2$.

pillars.

We attempted to take advantage of this observation for the purpose of construction of a further new type of self-assembling system. We designed a new ligand having side chain to pass through the window, 4-(2-pyrazinyl)-*N*-benzoylbutanamide (**5**) and prepared it according to Scheme 2.

In spite of its side chain which is evidently too large for the inner space of the **1** dimer, the UV-vis spectroscopic titration experiments of **1** with **5** show normal 2:1 complex formation (Figure 3). The binding constant of porphyrin with **5** determined by using non-linear theoretical curve fitting analyses[4] was K_2 = ca. $2x10^7$ M^{-1}.[5]

This interesting situation is clarified by examination of ^{1}H-COSY spectra of the 1:2 mixture of **1** and **5** shown in Figure 4. Although detailed analyses of the spectra are still incomplete due to line broadening and the lack of symmetry, characteristic upfield shifts of the side chain of **5** on complexation are obvious[6], i.e., α, β, γ, δ and amide protons of **5** originally observed at 2.88, 1.88, 1.70, 3.52 and 6.32 ppm shift to -2.84, -1.19, 0.32, 2.98 and 5.87 ppm, respectively. The benzoyl protons of **5**, however, show no significant shifts and appear at the normal aromatic region (δ 7.49, 7.58 and 7.75 ppm) even in the complexed form.

These observations are fully consistent with the unique structure of the present complex, $(\mathbf{1})_2$• **5** shown in Figure 5, where the pyrazine moiety coordinates to the two zinc atoms extending the methylene side chain along the surface of porphyrins and the benzoyl moiety is stuck out of a window formed between hydrogen bond pillars of the complex.

The present complex may provide not only a porphyrin dimer which have

unique "inside-outside" connection but also a basic component for more large scale self-assemblies which consist of several other assemblies connected to each other.

Experimental Section

General Remarks. ^{1}H-NMR spectra were recorded on a JEOL FX-90Q (90 MHz), a JEOL GX-400 (400MHz) or a JEOL α-500 (500MHz). ^{1}H-NMR chemical shifts are referenced to internal $CDCl_3$ (1H d7.25ppm) relative to Me_4Si at 0 ppm. Electronic absorption spectra were performed on a Hitachi U-3410 spectrometer, Multi-channel Photodiode Array Spectrometer, Otsuka Electronics MCPD-100 or Hewlett-Packard HP-8452A, thermostated at given temperatures with a circulation system, NESLAB Instruments, Inc. RTE-9. IR spectra were recorded on PERKIN ELMER System2000 FT-IR. Vapor pressure osmometory measurement were performed on CORONA 117. Mass spectra were obtained with a JEOL JMS DX-300 or a JEOL JMS-SX102A mass spectrometer. HPLC experiments were performed on a TOSOH HLC-837 or Waters M600E equipped with a TOSOH UV-8010 variable-wavelength detector and Waters M991 Photodiode Array Detector.

Materials. Solvents used in spectral measurement were Spectrosol purchased from Nacalai Tesque, Inc.or Dojindo Laboratories. Other commercially available chemicals were purchased from Wako Pure Chemical Industries, Ltd. or Nacalai Tesque, Inc., or Tokyo Kasei Kogyo Co., Ltd. and employed without further purification, unless stated otherwise. Analytical thin-layer chromatography was performed with pre-coated Merck silica gel 60, F254 (0.2mm layers on glass plates). Column chromatography was performed using Merck Kieselgel 60 or WAKOgel LP-40C18.

Propyl pyrazinecarboxylate (**3**). In a 30-ml two necked flask equipped with a reflux condenser and septam was placed 1 g (8 mM) of pyrazinecarboxylic acid. Thionyl chloride 1.765 ml (24 mM) was dropwise added with stirring by a magnetic stirrer under nitrogen atmosphere. The flask was placed in an oil bath and heated at 80°C for 1 h. The reflux condenser is then replaced by a distillation head and the mixture was distilled. The cooled residual acid chloride is transfered with 20 ml of anhydrous THF to a dropping funnel which is attached to a 50 ml flask. A solution of 1.2 ml (0.016 M) of *n*-propyl alchol and 0.65 ml (8 mM) of pyridine with 10 ml of anhydrous THF was introduced into the flask. The acid chloride was added slowly to the vigously stirred solution under nitrogen atmosphere. The mixture was then stirred at room temperature for 3 h. The reaction mixture was extracted with ethyl acetate, dried over Na_2SO_4, and concentrated in vacuo. The resulting residue was loaded on silica gel column eluting with ethyl acetate to give 0.63 g (48 %) of b as a liquid; R_f 0.69 (ethyl acetate); ^{1}H NMR (500 MHz, $CDCl_3$) δ9.24, 8.70, 8.67 (pyr, 3H), 4.35, 1.80 (CH_2, 4H), 0.97 (CH_3, 3H); FAB MS 167 $(M+H)^+$.

N-Butylpyrazinamide (**4**). In a 30-ml two necked flask equipped with a reflux condenser and septam was placed 1 g (8 mM) of pyrazinecarboxylic acid. Thionyl chloride 1.765 ml (24 mM) was dropwise added with stirring by a magnetic stirrer under nitrogen atmosphere. The flask was placed in an oil bath and heated at 80°C for 1 h. The reflux condenser was then replaced by a distillation head and the mixture was distilled. The cooled residual acid chloride was transferred with 20 ml of anhydrous THF to a dropping funnel which was

attached to a 50-ml flask. A solution of 1.58 ml (0.016 M) of butylamine with 10 ml of anhydrous THF wais introduced into the flask. The acid chloride was added slowly to the vigously stirred solution under nitrogen atmosphere. The mixture was then stirred at room temperature for 3 hours. The reaction mixture was extracted with ethyl acetate, dried over Na_2SO_4, and concentrated in vacuo. The resulting residue was loaded on silica gel column eluting with ethyl acetate to give 0.8 g (56 %) of **4** as a white solid; R_f 0.66 (ethyl acetate); ^{1}H NMR (500 MHz, $CDCl_3$) δ9.29, 8.62, 8.41 (pyr, 3H), 7.80 (NH, 1H), 3.37, 1.51, 1.29 (CH_2, 6H), 0.84 (CH_3, 3H); FAB MS 180 $(M+H)^+$.

N-α-N-ε-Dibenzyloxycarbonyl-lysine (**7**). A 100ml-flask was charged with 1.46 g (0.01M) of lysine hydrochloride and 20 ml 1M NaOH. The mixture was stirred vigorously with magnetic stirrer and was dropwise added carbobenzoxychloride 3.7 ml (0.026 M) and 26 ml of 1M NaOH simultaneously at 0°C for 30 min and then stirred at room temperature for 1.5 h. The reaction mixture was washed with ether and then acidified and extracted with ethyl acetate. The resulting solution was dried over Na_2SO_4 and evaporated in vacuo to give 3.7 g (90%) colorless liquid. ^{1}H-NMR (CD_3OD) δ7.35-7.2 (m, 10H), 5.05 (s, 2H), 5.02 (s, 2H), 4.15 (m, 1H), 3.06 (m, 2H), 1.9-1.3 (several peaks, 6H).

N-α-N-ε-Dibenzyloxycarbonyl-lysinamide (**8**). A solution of 10 g of **7** in 50 ml dry THF and 3.9 ml dry Et_3N was stirred for 10 min at -15°C. To the solution was added 3.44ml of isobutyl chloroformate. After 10 min 64 ml of 28% NH_4OH was

added to the mixture and stirred for 30 min at –15°C. Then the reaction mixture was stirred at r.t. for 1.5 h. The precipitate was filtered and the filtrate was extracted with ethyl acetate and evaporated. The resulting solid and precipitate were combined and dried in vacuo. Recrystallization from methanol yielded 9.6 g (96%). ^{1}H-NMR (DMSO) δ7.4–7.2 (m, 10H), 5.02 (s, 2H), 4.98 (s, 2H), 3.85 (m, 1H), 2.95 (m, 2H), 1.6-1.1 (several peaks, 6H).

Lysineamide (**9**). A flask charged with 4.6 g of **8**, 120 ml of methanol and 500 mg of 10% Pd-C was equipped with a hydrogen insert tube. The solution was stirred with hydrogen bubbling for 6 h. The reaction mixture was filtered with sunction through Celite and washed with methanol. The filtrate was concentrated under reduced pressure to give 1.6 g (98%) of a white solid. ^{1}H-NMR ($CDCl_3$) δ7.12 (s, 1H), 6.14 (s, 1H), 3.30 (m, 1H), 2.63 (t, 2H), 1.8-1.3 (several peaks, 10H), ; FAB MS 146$(M+H)^+$.

Hexane-1,2,6-triamine trihydrochloride (**10**). A two-necked round bottomed flask equipped with a reflux condenser was charged with 8 g of **9**, 170 ml of THF and 450ml of 1M BH_3 THF solution under N_2 atmosphere. The solution was stirred at 70°C for 6 h. The reaction mixture was cooled to r.t. and evaporated. To the resulting solution was added carefully 280ml of 6M HCl in an ice-bath and concentrated under reduced pressure. Reprecipitation with methanol/ethyl acetate gave 9.0 g (68%) white oil. ^{1}H-NMR (CD_3OD) δ 3.44 (m, 1H), 3.13 (d, 2H), 2.80 (m, 2H), 1.8-1.3 (several peaks, 6H), ; ^{13}C NMR (CD_3OD) δ 50.8, 42.3, 40.3,

31.2, 27.0, 23.0, ; FAB MS (Hexane-1,2,6-triamine)132 $(M+H)^+$.

N-(5,6-Diaminohexyl)benzamide (**11**). Copper (II) carbonate [$CuCO_3 \cdot Cu(OH)_2$] (456 mg, 0.0019 mol) was addded to a solution of triamine **10** (1 g, 0.0076 mol) in 15.3 ml of 0.5M NaOH solution and the solution stirred at 90°C for 30 min. The solution was filtered and the filtrate was cooled to 0°C. Benzoyl chloride (1.329 ml, 0.011 mol) was added to the cooled blue solution with vigorous stirring over 30 min, with simultaneous addition of $NaHCO_3$ (962 mg, 0.011 mol) to maintain the basic pH. After being stirred for a further 4 h, the solution was treated with hydrogen sulphide gas for 10 min to give a brown precipitate. This was filtered off to leave a yellow solution. This solution was evaporated under reduced pressure and small amount of 6M KOH solution was added. After continuous extraction with CH_2Cl_2, the organic layer was dried with Na_2SO_4 and evaporated under reduced pressure to give a clear oil (532 mg, 30%). This material was used without further purification.

^{1}H NMR ($CDCl_3$) δ 7.72 (d, 2H), 7.40 (t, 1H), 7.33 (t, 2H), 6.64 (s, 1H), 3.57 (m, 1H), 2.8-2.6 (several peaks, 3H), 2.40 (m, 1H), 1.6-1.2 (several peaks, 10H), ; ^{13}C-NMR ($CDCl_3$) δ 167.5, 134.7, 131.1, 128.3, 126.8, 53.3, 48.5, 39.7, 35.0, 29.5, 23.4, ; FAB MS 236 $(M+H)^+$.

4-(2-Pyrazinyl)-N-benzoylbutanamide (**5**) A solution of 100 mg(0.43 mmol) of **11** in 1 ml 1M KOH MeOH solution was stirred at 0°C in an ice bath and 1 ml H_2O solution of 121 mg (0.43 mmol) glyoxal sodium hydrogen sulfite

monohydrate was added. The solution was allowed to warm to r.t. and stirred overnight. Air was bubbled through the solution for 3 h. The reaction mixture was extracted with ethyl acetate, the organic layer was dried over Na_2SO_4 and evaporated under reduced pressure to yield a white solid 22 mg (20%).

^{1}H NMR ($CDCl_3$) δ 8.48 (s, 2H, pyrazine), 8.41 (d, 1H, pyrazine), 7.76 (d, 2H, phenyl), 7.49 (t, 1H, phenyl), 7.43 (t, 2H, phenyl), 6.32 (s, 1H, amide), 3.52 (q, 2H, CH_2), 2.88 (t, 2H, CH_2), 1.88 (m, 2H, CH_2), 1.70 (m, 2H, CH_2), ; FAB MS 256 $(M+H)^+$.

References and Notes

1) (a) Whitesides, G. M.; Mathias, J. P.; Seto, C. T. *Science* **1991**, 254, 1312. (b) Lehn, J. M. *Science* **1993**, 260, 1762. (c) Benniston, A. C.; Harriman, A.; Lynch, V. M. *Tetrahedron Lett.* **1994**, 35, 1473. (d) Anderson, H. L.; Anderson,S.; Sanders, J. K. M. *J. Chem. Soc., Perkin Trans. 1* **1995**, 2231. (e) Goodman, M. S.; Jubian, V.; Linton, B.; Hamilton, A. D. *J. Am. Chem. Soc.* **1995**, 117, 11610. (f) Valdes, C.; Spitz, U. P.; Toledo, L. M.; Kubik, S. W.;Rebek, J.,Jr. *J. Am. Chem. Soc.* **1995**, 117, 12733. (g) Mathias, J. P.; Seto, C. T.; Simanek, E. E.; Whitesides, G. M. *J. Am. Chem. Soc.* **1994**, 116, 1725. (h) Collin, J. P.; Harriman, A.; Heitz, V.; Odobel, F.; Sauvage, J. P. *J. Am. Chem. Soc.* **1994**, 116, 5679. (i) Chernook, A. V.; Shulga, A. M.; Zenkevich, E. I.; Rempel, U.; Borczyskowski, C. V. *J. Phys. Chem.* **1996**, 100, 1918. (j) Fujita, M.; Nagao, S.; Ogura, K. *J. Am. Chem. Soc.* **1995**, 117, 1649.

2) (a) Kuroda, Y.; Kawashima, A.; Urai,T.; Ogoshi, H. *Tetrahedron Lett.* **1995**, 46, 8449. (b) Chapter 3 in this thesis.

3) For other spontaneous dimeric porphyrin formation systems, see (a) Aoyama, Y.; Kamohara, T.; Yamagishi, A.; Toi, H.; Ogoshi, H. *Tetrahedron Lett.* **1987**, 28, 2143. (b) Segawa, H.; Takehara, C.; Honda, K.; Shimidzu, T.; Asahi, T.; Mataga. N. *J. Phys. Chem.* **1992**, 96, 503. (c) Drain, C. M.; Fischer, R.; Nolen, E. G.; Lehn, J. M. *J. Chem. Soc., Chem. Commun.* **1993**, 243. (d) Kobuke, Y.; Miyaji, H. *J. Am. Chem. Soc.* **1994**, 116, 4111. (e) Hunter, C. A.; Sarson, L. D. *Angew. Chem. Int. Ed. Engl.* **1994**, 33, 2313. (f) Sessler, J. L.; Wang, B.; Harriman, A. *Ibid.* **1995**, 117, 704.

4) Kuroda, Y.; Kawashima, A.; Ogoshi, H. *Chem.Lett.* **1996**,57.

5) Since the titration curves are almost linear indicating the very large K_1 and K_2 values, the curve-fitting analyses, in spite of excellent agreement between experimental and theoretical curves, results in poor standard deviations (over 50 %) for these parameters. Therefore, only these orders of magnitude are meaningful.

6) Following examples of large upfield shifts of bidentate ligands sandwitched by porphyrins are reported. (a) For 4,4'-bipyridyl - covalently linked face-to face porphyrin systems, see Uemori, Y.; Nakatsubo, A.; Imai, H.; Nakagawa, S.; Kyuno, E. *Inorg. Chem.* **1992**, 31, 5164. (b) For pyrazine - polymeric porphyrin systems, see Marvaud, V.; Launay, J. P. *Inorg. Chem.* **1993**, 32, 1376.

Molecular Recognition of Amines by Tetracarboxynaphthylporphyrin

Abstract

A novel functional porphyrin, *meso*-tetrakis(2-carboxy-1-naphthyl) porphyrin (**1**), was designed to have four carboxylic acids. These acids on naphthyl rings were fixed since isomerization of porphyrin **1** is difficult due to the steric hindrance of naphthyl rings at meso position. In polar solvents such as THF, porphyrin **1** is monomer. The interactions of various amines with porphyrin **1** were investigated by UV-vis absorption spectroscopy and association constants were determined by non linear least square optimization analysis from the absorbance changes of Soret band. Three stoichiometric ratios, porphyrin **1** /amine = 1/1, 1/2, and 2/1, were observed and they depend on the basicity and structure of each amine.

Introduction

Porphyrin derivatives are suitable for the physiochemical studies of the molecular recognition and there are some examples to study molecular recognition behavior,[1] because porphyrins have rigid structure to be need for spatial arrangement of the recogniton groups and have macrocyclic aromatic chromophore to provide several characteristic spectroscopic detection methods such as NMR, UV-vis, CD, fluorescence, and so on. Here we report the synthesis of a novel functional porphyrin, *meso*-tetrakis(2-carboxy-1-naphthyl) porphyrin (**1**), which was designed to have four carboxylic acids as recognition site for amines. Interactions of various amines with porphyrin **1** in THF were investigated by UV-vis absorption spectroscopy.

Results and discussion

The novel functional porhyrin **1** was prepared according to Scheme 1. 2-Methoxycarbonyl-1-naphthaldehyde (**9**) as a precursor of porphyrin **1** was prepared from 1-bromo-2-methylnaphthalene (**3**) in six steps. This aldehyde **9** is so sensitive to acid that appropriate condensation method of porphyrin is Lindsey's method.[2] Condensation of **9** and pyrrole gave meso-tetra(2-methoxycarbonyl-1-naphthyl)porphyrin (**2**) as a mixture of 4 atropisomers in 10 % yield. Each atropisomer was separated by HPLC[3] and identified by ^{1}H NMR and FAB mass spectroscopy. Atropisomerization of tetraphenylporphyrin normally gives four atropisomers and the ratio is αβαβ:ααββ:αααβ:αααα= 1:2:4:1.[4] However atropisomerization of porphyrin **2** arising from rotation of the naphthyl rings was not detected at 70°C in tetrachloroethane for 24h. The αααα atropisomer of porphyrin **2** was separated by silica gel column chromatography (CH_2Cl_2/Et_2O=25/1) and hydrolyzed in aq. 15M NaOH/THF solution to afford αααα atropisomer of **1** in 70% yield.

Complex formation between host **1** and a series of amines (Table 1) were followed by UV-vis spectrophotometric titration in THF at 20°C. The association constants were determined by non linear least square optimization analysis[5] of complexation shifts of Soret band.

Spectroscopic titration of **1** with pyridine (**10**) showed red shift with clear an isosbestic point at 426 nm, which indicates 1:1 complex formation between **1** and **10** as shown in Figure 1. From this spectral change, association constant was estimated as 0.6 M^{-1}. Similar spectral change for complexation of **1** with guest **11-12** were observed and estimated association constants are summalized in

Scheme 1

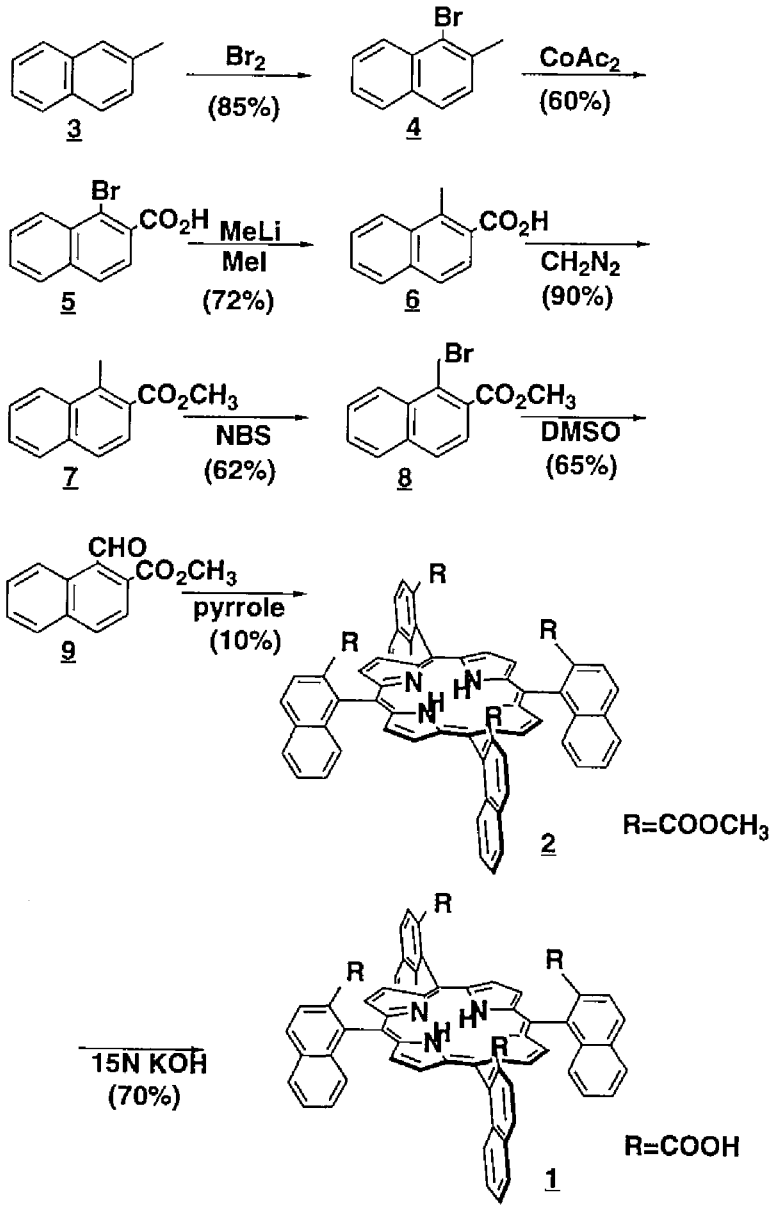
Br
Br2
(85%)
CoAc2
(60%)
3
4
CO2H
MeLi
MeI
(72%)
CH2N2
(90%)
5
6
CO2CH3
NBS
(62%)
DMSO
(65%)
7
8
CHO
pyrrole
(10%)
9
R
N
H
2
R=COOCH3
15N KOH
(70%)
1
R=COOH

Scheme 2

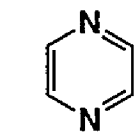

10

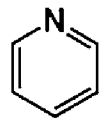

11

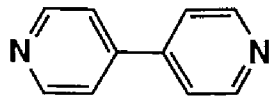

12

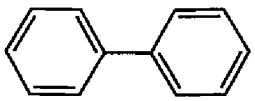

13

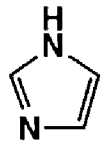

14

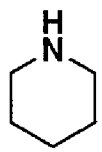

15

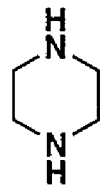

16

$H_2N(CH_2)_3NH_2$

17

$H_2N(CH_2)_6NH_2$

18

$H_2N(CH_2)_3NH(CH_2)_4NH_2$

19

$H_2N(CH_2)_3NH(CH_2)_4NH(CH_2)_3NH_2$

20

Table 1. Reference guest **13** do not show any spectral change arising from the complex formation in electronic absorption spectra. These results show that guest **10-12** whose basicity are low form 1:1 complexation with **1** due to the interaction between amines and carboxylic acid of **1** and these association constants are very small in THF.

In contrast to guest **10-12**, guest **14** showed different spectral changes. The initial λmax of Soret band was 426 nm. It showed blue shift with the addition of **14** gradually, and on further addition, it changed to red shift as shown in Figure 2. In this case, no clear isosbestic point was found in Soret region and

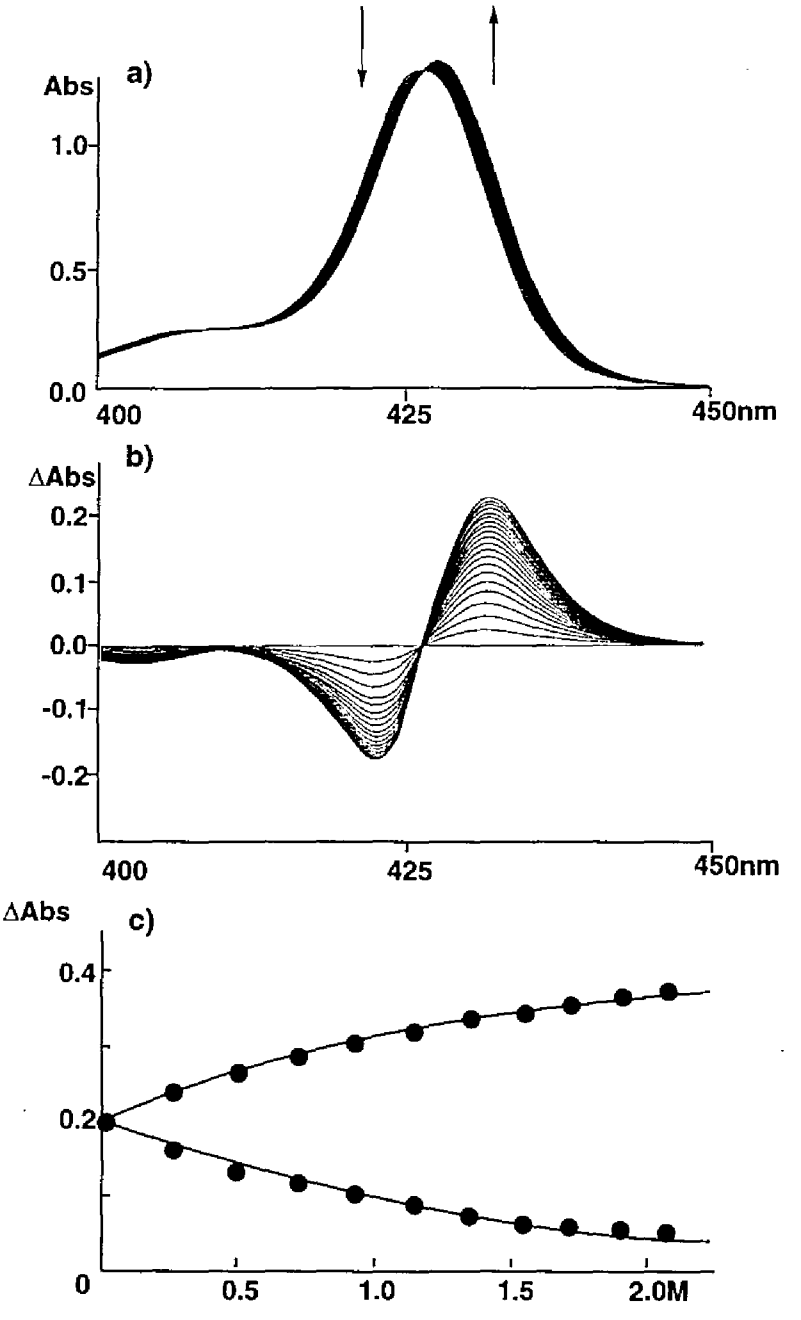

Figure 1. a) Spectral change of **1** on addition of **10** at 20°C. [**1**]=4.2x10^{-6}M. b) Difference spectra . c) Fitting results for complex formation at 422 and 432nm. The solid lines show the theoretical curves with K=5.6x10^{-1}M^{-1}.

Table 1. Optimized association constants of complexation between **1** and amines in THF at 20°C.

	K_1 (s.d.) M^{-1}	K_2 (s.d.) M^{-1}
10[a]	0.56 (3.4×10^{-2})	
11[a]	6.9×10^{-2} (1.3×10^{-2})	
12[a]	1.5 (0.34)	
13[d]	———	
14[b]	350 (44)	17 (1.8)
15[b]	3.8×10^{5} (4.6×10^{4})	68 (15)
16[b]	5.9×10^{5} (5.1×10^{4})	300 (28)
17[b]	2.7×10^{5} (3.3×10^{4})	1.1×10^{4} (1.4×10^{3})
18[e]	———	
19[c]	2.2×10^{7} (1.7×10^{6})	4.5×10^{5} (4.5×10^{4})
20[c]	6.6×10^{7} (2.2×10^{7})	4.5×10^{6} (1.4×10^{6})

a) Porphyrin / amine = 1:1 complexation
b) Porphyrin / amine = 1:2 complexation
c) Porphyrin / amine = 2:1 complexation
d) no spectral change
e) We could not fit the spectral change to neither 1:2 nor 2:1 complexation model.

biphasic absorption change was observed which indicate that this system contains not only 1:1 but also 1:2 complex formation. For this spectral change, we examined curve fitting using the following scheme for the complexation. The

$$\mathbf{1} + \mathbf{14} \overset{K_1}{\rightleftharpoons} \mathbf{1 \cdot 14} \overset{\mathbf{14},\, K_2}{\rightleftharpoons} \mathbf{1 \cdot (14)_2}$$

results of fitting shows excellent agreement with experimental one as shown in Figure 2-c. The optimized association constants for 1:2 complexation are K_1= 353 M^{-1} and K_2=17 M^{-1} respectively. Titration of guest **15-17** with **1** also showed similar spectral changes to **14** and fitting results for 1:2 complexation are summarized in Table 1. K_1 of each amine is 20 times larger than K_2 and this results show that the second complexation is interfered by electrostatic repulsion and/or steric hindrance of 1:1 complex. However basicity of these amines **14-17** are stronger than those of **10-12** and interactions between amines of **14-17** and carboxylic acids of **1** are strong enough to make 1:2 complex formation overcoming electrostatic repulsion and steric hindrance on porphyrin face.

The titration experiment of guest **19** showed the same spectral change as titration of **14-17**; initial blue shift followed by red shift, with no clear isosbestic point in Soret region. However added guest concentration is very different. In the case of **14**, first saturation of spectral change i.e. turing point from blue shift to red shift, was observed at 5×10^{-3} M of **14** concentration , on the other hand, spectral change of **19** showed first saturation at 3×10^{-6} M. This spectral change of **19** cannot be fitted by equation of 1:2 complexation since the first saturation was observed at low guest concentration which is smaller than equimolar of **1**.

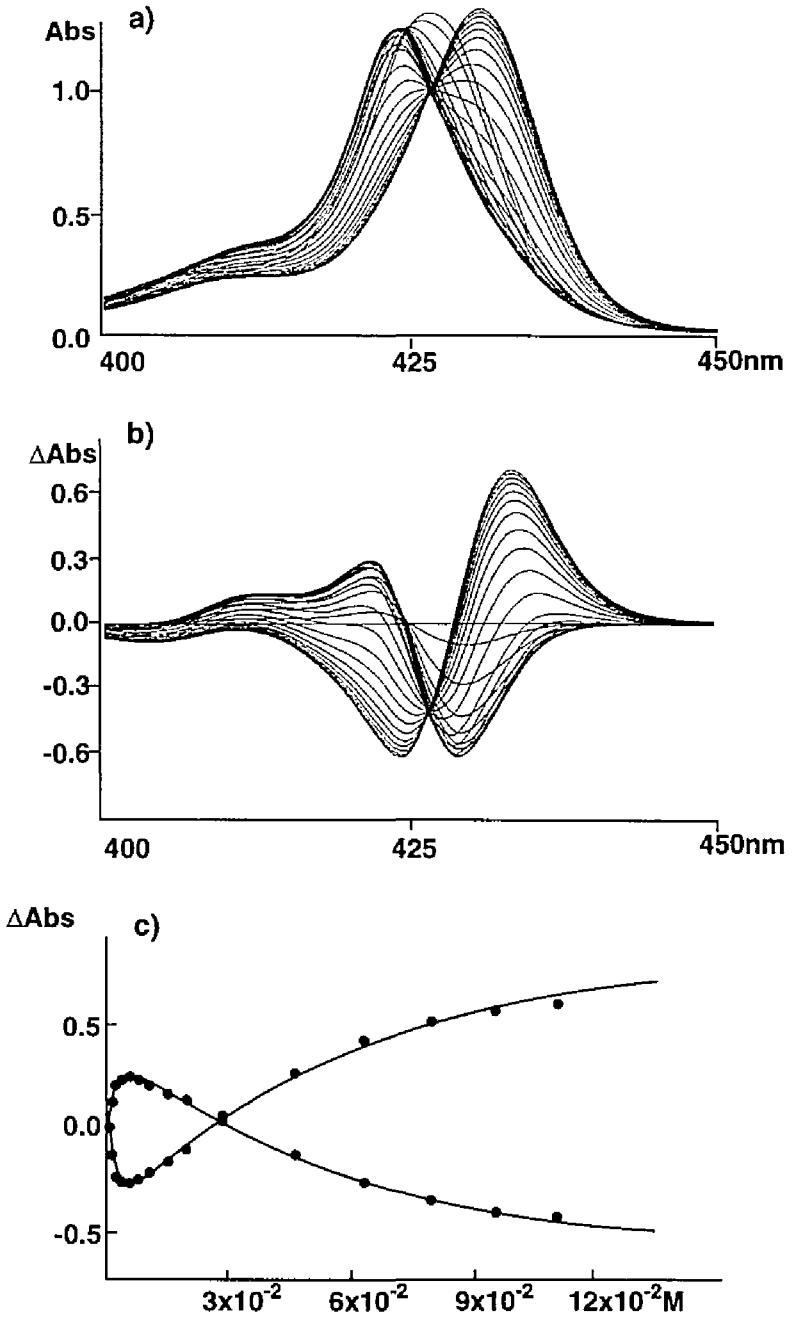

Figure 2. a) Spectral change of **1** on addition of **14** at 20°C. [**1**]=4.5x10^{-6}M. b) Difference spectra . c) Fitting results for complex formation at 422 and 432nm. The solid lines show the theoretical curves with K_1=353M^{-1} and K_2=17M^{-1}.

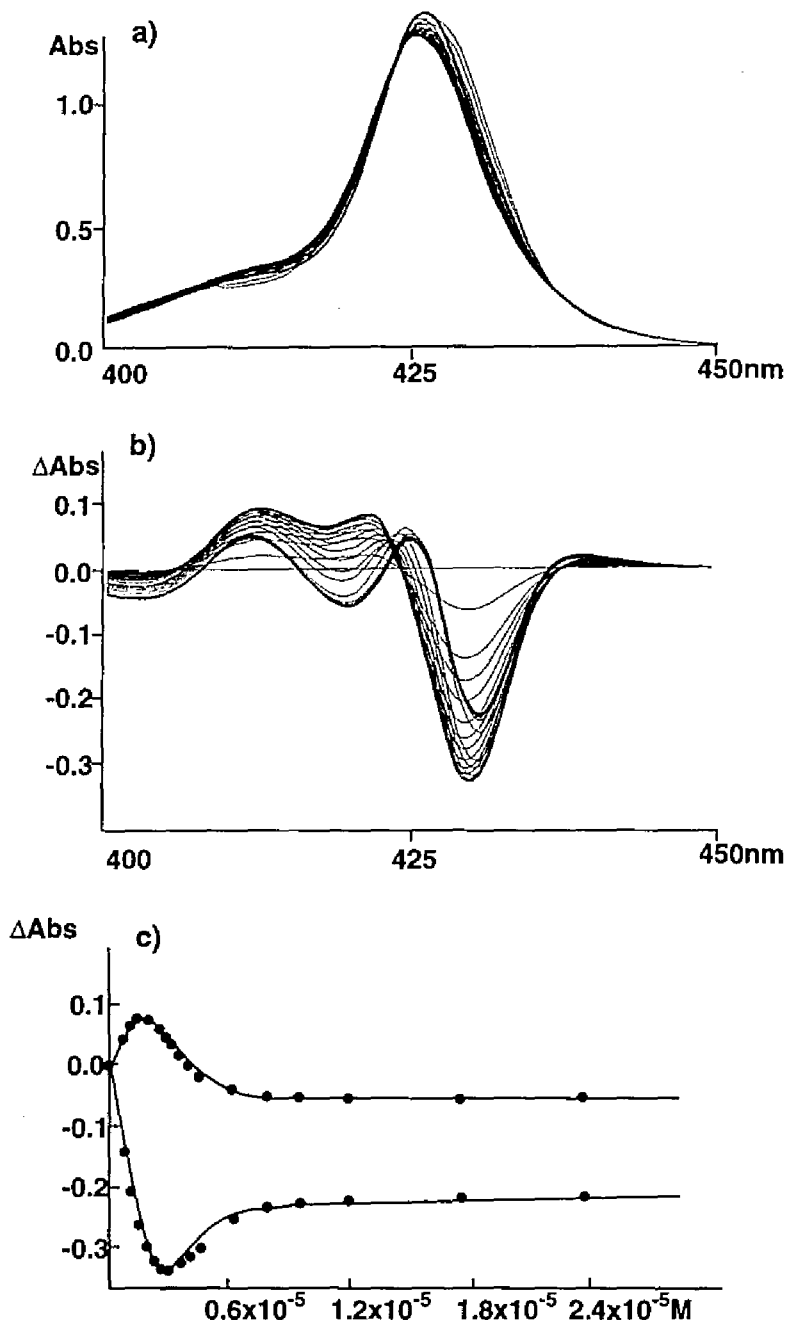

Figure 3. a) Spectral change of **1** on addition of **19** at 20°C. [**1**]=4.7x10^{-6}M. b) Difference spectra . c) Fitting results for complex formation at 419 and 429nm. The solid lines show the theoretical curves with K_1=2.0x10^{7}M^{-1} and K_2= 3.6x10^{5}M^{-1}.

Structure of **19** is linear with two amino groups at the both ends, so **19** is likely to bound with 2:1 stoichiometric ratio. For this spectral change, we analyzed by using 2:1 complexation as the following scheme. The result of fitting shows

$$\mathbf{1} + \mathbf{19} \overset{K_1}{\rightleftharpoons} \mathbf{1 \cdot 19} \overset{\mathbf{1}, K_2}{\rightleftharpoons} (\mathbf{1})_2 \cdot \mathbf{19}$$

excellent agreement with experimental one as shown in Figure 3-c. The optimized association constants for 2:1 complexation are $K_1 = 2.2 \times 10^7\ M^{-1}$ and $K_2 = 4.5 \times 10^5\ M^{-1}$ respectively. Titration of **20** with **1** also showed similar spectral changes to **19** and fitting results for 2:1 complexation are summarized in Table 1. 2:1 complexation is favorable because **19** and **20** have long alkyl chains and their structure are linear.

Titration result of **18** showed similar spectral change to **19**, but we could not fit the spectral change to neither 1:2 nor 2:1 complexation. Length of **18** is in between **17** and **19**. It is considered that in the case of **18**, both complexation of 1:2 and 2:1 are formed and we could not get good fitting result. These results show that length of amine affect whether complexation is 1:2 or 2:1.

These results show that **1** forms three types of complexation with amines and they depends on basicity and structure of amine. This means that we can estimate structure and basicity of amine by analyzing spectral change of **1** on addition of amine.

Experimental Section

General Remarks.^{1}H-NMR spectra were recorded on a JEOL FX-90Q (90 MHz), a JEOL GX-400 (400MHz) or a JEOL α-500 (500MHz). ^{1}H-NMR chemical shifts are referenced to internal $CDCl_3$ (1H d7.25ppm) relative to Me_4Si at 0 ppm. Electronic absorption spectra were performed on a Hitachi U-3410 spectrometer, Multi-channel Photodiode Array Spectrometer, Otsuka Electronics MCPD-100 or Hewlett-Packard HP-8452A, thermostated at given temperatures with a circulation system, NESLAB Instruments, Inc. RTE-9. IR spectra were recorded on PERKIN ELMER System2000 FT-IR. Vapor pressure osmometory measurement were performed on CORONA 117. Mass spectra were obtained with a JEOL JMS DX-300 or a JEOL JMS-SX102A mass spectrometer. HPLC experiments were performed on a TOSOH HLC-837 or Waters M600E equipped with a TOSOH UV-8010 variable-wavelength detector and Waters M991 Photodiode Array Detector.

Materials. Solvents used in spectral measurement were Spectrosol purchased from Nacalai Tesque, Inc.or Dojindo Laboratories. Other commercially available chemicals were purchased from Wako Pure Chemical Industries, Ltd. or Nacalai Tesque, Inc., or Tokyo Kasei Kogyo Co., Ltd. and employed without further purification, unless stated otherwise. Analytical thin-layer chromatography was performed with pre-coated Merck silica gel 60, F254 (0.2mm layers on glass plates). Column chromatography was performed using Merck Kieselgel 60 or WAKOgel LP-40C18.

1-Bromo-2-methyl naphthalene (**4**) was prepared from 2-methyl naphthalene (**3**) and bromine according to the literature, [6] 85% yield colorless liquid. ^{1}H-NMR ($CDCl_3$) δ8.39-8.21(m,1H) δ 7.78-7.08(m,5H) δ 2.59(s,3H).

1-Bromo-2-naphthoic acid (**5**) was prepared as a following literature.[7] To a solution of 100 g of **4** in 800 ml acetic acid were added 24g of cobalt (II) acetate-tetrahydrate and 10 g of 2-butanon. The flask was heated to 100-120 °C and bubbled oxygen for 9 hours. To the reaction mixture was added 750 g of ice and acidified with concentrated HCl. The precipitate was separated, thoroughly washed with water,and dried under vacuum at 80°C for 12h. Recrystallization from toluene yielded 68 g (60%). ^{1}H-NMR ($CDCl_3$) δ10.70(s,1H),δ 8.64-8.37 (m,1H),δ 8.00-7.56 (m,5H) ; MS m/e 251 (M^+).

1-Methyl-2-naphthoic acid (**6**) was prepared in a similar manner as described in a literature.[8] An oven-dried 500 ml flask was fitted with a dropping funnel, N_2 bubbler, low-temperature thermometer and magnetic stirrer. 1-Bromo-2-naphthoic acid 18.0g(0.07mol) was taken up in 220ml of dry ether and 270ml of dry THF. The solution was cooled to -95°C in a bath of ether-liquid N_2 bath. Methyllithium in ether (0.14mol) was added slowly, maintaining the temperature below -92°C with subsequent stirring for 0.75 h at this temperature. Dry methyl iodide (0.14mol) was then added and the solution was allowed to come to room temperature overnight. The product was extracted into 5% NaOH, which was in

turn acidified to pH 1. The resulting precipitate was taken up in ether, dried over $MgSO_4$ and evaporated to give 9.6 g (72%) light yellow solid. ^{1}H-NMR (DMSO-d_6) δ 8.10-7.29(m,6H), 2.65(s,3H); MS m/e 186 (M^+).

Methyl 1-methyl-2-naphthoate (**7**). The mixture of potassium hydroxide 2.5 g , water 4 ml, and ethanol 12 ml was stirred and added slowly the 50ml ether solution of N-methyl-N-nitroso-p-toluenesulfonamide 10 g in an oil bath at 50°C. The exit gases were passed through a 30ml of ether cooled below 0°C.
To 4.6 g of **6** in ether was added the diazomethane ether solution with stirring, untill the N_2 gas evolution was ceased. The reaction mixture was evaporated and purified by column chromatography with dichloromethane.

Yield 90%. ^{1}H-NMR($CDCl_3$) δ 8.27-8.05(m,1H) 7.94-7.35(m,5H) 3.97(s,3H) 2.92(s,3H); MS m/e 200 (M^+).

Methyl 1-bromomethyl-2-naphthoate (**8**) ; A stirred suspension of **7** (12 g), N-bromosuccinimide (10.6 g), and dibenzoyl peroxide(40 mg) in 70 ml of dry CCl_4 was refluxed for 3 h while being irradiated. Completion of the reaction was indicated by the presence of only succinimide which covers the surface of solution. The hot mixture was filtered and the collected precipitate was extracted twice with portions of CCl_4. Evaporation of the combined filtrates under reduced pressure left a brownish solid which was recrystallized from hexane-CH_2Cl_2 to give 62% of colorless cubic crystals.

^{1}H-NMR ($CDCl_3$) δ 8.37-8.21(m,1H) 8.05-7.46(m,5H) 5.46(s,2H) 4.00(s,3H);

MS m/e 279 (M^+).

2-Methoxycarbonyl-1-naphthaldehyde (**9**) ;To the mixture of sodium hydrogen carbonate (2 g) and **8** (1 g) were added dimethylsulfoxide (22.3 ml) with stirring under Ar atmosphere at 65°C for 30 min. Then the reaction mixture was cooled in an ice bath and extracted with CH_2Cl_2. Evaporation of the solution left a light brownish solid which was purified by column chromatography (Florisil) with CH_2Cl_2 and recrystallized from hexane-CH_2Cl_2 yielding white solid 65%.

^{1}H-NMR($CDCl_3$) δ 10.80(s,1H) 8.54-8.37(m,1H) 8.10-7.51(m,5H) 4.00(s,3H); MS m/e 214 (M^+).

meso-Tetra(2-methoxycarbonyl-1-naphthyl)-porphyrin (**2**). A three-necked flask fitted with a septum, reflux condenser, and nitrogen inlet port was charged with 50ml of CH_2Cl_2 (distilled from CaH_2) , **9** (107mg,10^{-2}M), and pyrrole (35ml, 10^{-2}M). After the solution was purged with N_2 for 5 minutes, 21ml ($3.3x10^{-3}$M) of $BF_3.OEt_2$ was added. The room temperature reaction was monitored by removing 50 μl aliquots and oxidizing with excess amount of DDQ, followed by absorption spectrophotometry. At the end of 80 min the reaction mixture was treated with DDQ. Then equimolar ($3.3x10^{-3}$M) of triethylamine was added to the mixture and evaporated in vacuo. The residue was purified by column chromatography on a silica gel and on an ODS column, and then the 4 atropisomers were separated with HPLC.

Table 2.Proton NMR data of atropisomers of meso-tetrakis(o-methoxycarbonylnaphthyl)porphyrins in $CDCl_3$.

Assignment	αβαβ	ααββ	αααβ	αααα
Internal NH	-1.80(s,2H)	-1.87(s,2H)	-1.88(s,2H)	-1.91(s,2H)
Methyl ester H	3.02(s,12H)	2.86(s,12H)	2.68(s,3H) 2.98(s,3H) 2.99(s,6H)	2.88(s,12H)
Naphthalene H_a	6.78(d,4H)	7.05(m,8H)	6.84(d,4H)	6.86(d,4H)
Naphthalene H_b	6.95(t,4H)		6.97(t,4H)	6.97(t,4H)
Naphthalene H_c	7.48(t,4H)	7.51(t,4H)	7.48(t,4H)	7.47(t,4H)
Naphthalene H_d	8.08(d,4H)	8.09(d,4H)	8.07(d,4H)	8.08(d,4H)
Naphthalene H_e	8.29(d,4H)	8.29(d,4H)	8.29(d,4H)	8.29(d,4H)
Naphthalene Hf	8.38(d,4H)	8.36(d,4H)	8.39(d,4H)	8.38(d,4H)
Pyrrole H	8.28(s,8H)	8.27(d,8H)	8.27(m,8H)	8.27(s,8H)

FAB Mass, $(M+H)^+$ 1047

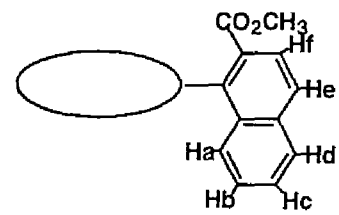

meso-Tetrakis(2-carboxy-1-naphthyl)porphyrin (**1**). A 20 ml of flask fitted with reflux condenser was charged with 57.4 mg of **2**, 5.7 ml of THF, and 5.7 ml of 15M KOH aq. The reaction mixture was heated at 60°C under N_2 atmosphere with vigorously stirring. At the end of 2 days, the reaction mixture was cooled and made acidic (pH≈1) with 1M HCl, extracted with ethyl acetate, washed with water, dried over Na_2SO_4, and concentrated in vacuo. The residue was purified by recrystallization with hexane/THF to give 38.5 mg (70%) of product as a purple solid.; **1**(αααα atropisomer):^{1}H-NMR (500MHz, DMSO) δ 8.45 (d, 4H), 8.37 (d, 4H), 8.23 (d, 8H), 8.21 (d, 4H), 7.53 (t, 4H),7.07 (t, 4H), 6.64 (d, 4H), -2.01 (s, 2H); FAB Mass 991$(M+H)^+$.

Spectroscopic Titration. To a solution of ca. 4.5×10^{-6} M of **1** in THF was added a solution of amine in THF at 20°C and absorbance changes of Soret band were monitored by UV-vis spectrophotometry. The association constants were determined by non linear least square optimization analysis from the plot of ΔAbs against the concentration of porphyrin.

$$\mathbf{1} + \text{amine} \underset{}{\overset{K_1}{\rightleftharpoons}} \mathbf{1 \cdot amine} \overset{\text{amine, } K_2}{\rightleftharpoons} \mathbf{1 \cdot amine_2}$$

$$K_1 = \frac{[\text{Por}\cdot\text{A}]}{[\text{Por}]\,[\text{A}]} \qquad K_2 = \frac{[\text{Por}\cdot\text{A}_2]}{[\text{Por}\cdot\text{A}]\,[\text{A}]}$$

In the case of 1:2 complexation, following equations were used.

$$[\text{Por}\cdot\text{A}] = K_1[\text{Por}][\text{A}] \quad (1)$$

$$[\text{Por}\cdot\text{A}_2] = K_2[\text{Por}\cdot\text{A}][\text{A}] = K_1K_2[\text{Por}][\text{A}]^2 \quad (2)$$

$$c = [\text{Por}]_{total} = [\text{Por}]+[\text{Por}\cdot\text{A}]+[\text{Por}\cdot\text{A}_2] \quad (3)$$

$$x = [\text{A}]_{total} = [\text{A}]+[\text{Por}\cdot\text{A}]+2[\text{Por}\cdot\text{A}_2] \quad (4)$$

where c; taoal concentration of porphyrin

x; total concentration of amine

[Por]; concentration of free porphyrin

[A]; concentration of free amine

[Por·A]; concentration of 1:1 complex

[Por·A_2]; concentration of 1:2 complex

$$\Delta Abs = Abs - Abs_0 = \varepsilon_0[Por]+\varepsilon_1[Por\cdot A]+\varepsilon_2[Por\cdot A_2] - \varepsilon_0[Por]_{total}$$

$$= (\varepsilon_1-\varepsilon_0)[Por\cdot A]+(\varepsilon_2-\varepsilon_0)[Por\cdot A_2]$$

$$= (\varepsilon_1-\varepsilon_0)K_1[Por][A] + (\varepsilon_2-\varepsilon_0)K_1K_2[Por][A]^2 \quad (5)$$

where ε_0, ε_1, and ε_2 are molar coefficients of free porphyrin and 1:1 complex, 1:2 complex, respectively.

from eq.(1), (2), and (3)

$$[Por] = c/(1 + K_1[A] + K_1K_2[A]^2) \quad (6)$$

$$\Delta Abs = \{(\varepsilon_1-\varepsilon_0)K_1[A] + (\varepsilon_2-\varepsilon_0)K_1K_2[A]^2\}c/(1 + K_1[A] + K_1K_2[A]^2) \quad (7)$$

from eq.(1), (2), and (4)

$$[A] = x-[Por\cdot A]-2[Por\cdot A_2]$$

$$= x-K_1[Por][A] -2K_1K_2[Por][A]^2 \quad (8)$$

[A] is given from eq. (6) and (8) and K_1, K_2 are estimated as parameters from the computer calculation using eq. (7).

References and Notes

1) (a) Ogoshi, H.; Masai, N.; Yoshida, Z.; Takemoto, J.; Nakamoto,K. *Bull. Chem. Soc. Jpn.* **1971**, 44, 49. (b) Aoyama, Y.; Asakawa, M.; Matsui, Y.; Ogoshi, H. *J. Am. Chem. Soc.* **1991**, 113, 6233. (c) Ogoshi, H.; Hatakeyama, H.; Kotani, J.; Kawashima, A.; Kuroda, Y. *J. Am. Chem. Soc.* **1991**, 113, 8181. (d) Lindsey, J. S.; Kearney, P. C.; Duff, R. J.; Tjivikua, P. T.; Rebek, J. Jr. *J. Am. Chem. Soc.* **1988**, 110, 6575. (e) Aoyama, Y.; Yamagishi, A.; Asagawa, M.; Toi, H.; Ogoshi, H.; *J. Am. Chem. Soc.* **1988**, 110, 4076.

2) Lindsey, J. S.; Wagner, R. W. *J. Org. Chem.* **1989**, 54, 828.

3) HPLC column : YMC-Pack C18 (AM-313, 4.6x250 mm), eluent : CH_3CN, flow rate: 1.0 ml/min, detected at 420 nm. Retention time of 4 atropisomers; αβαβ=11.3 min, ααββ=11.9 min, αααβ=13.2 min, αααα=22.2 min.

4) For example, (a) Gottwald, L. K. ; Ullman, E. F. *Tetrahedron Lett.* **1969**, 3071-3074. (b) Colleman, J. P.; Gagne, R. R.; Reed, C. A.; Halbert, T. R.; Lang, G.; Robinson, W. T. *J. Am. Chem. Soc.* **1975**, 97, 1427. (c) Hatano, K.; Anzai, K.; Nishino, A. ; Fujii, K. *Bull. Chem. Soc. Jpn.* **1985**, 58, 3653. (d) Crossley, M. J.; Field, L. D.; Forster, A. J.; Harding, M. M.; Sternhell, S. *J. Am. Chem. Soc.* **1987**, 109, 341.

5) Kuroda, Y.; Kawashima, A.; Ogoshi, H. *Chem. Lett.* **1996**, 57.

6) Adams, R.; Binder, L. O. *J. Am. Chem. Soc.* **1941**, 63, 2774 .

7) Hellwinkel, D.; Bohnet, S.; *Chem. Ber.* **1987**, 120, 1151.

8) Cornejo, J. J.; Ghodsi, S.; Johnson, R. D.; Woodling, R. ; Rickborn, B.; *J. Org. Chem.*. **1983**, 48, 3869.

List of Publications

Chapter 1. Self-induced Porphyrin Dimer Formation *via* Unusual Atropisomerization of Tetraphenylporphyrin Derivative.
Kuroda, Y.; Kawashima, A.; Urai, T.; Ogoshi, H.
Tetrahedron Lett. **1995**, 36, 8449.

Chapter 2. Computer Analyses of Complex Kinetics Containing Equilibrium Processes. Example of Application for Unusual Atropisomerization of a Tetraphenylporphyrin Derivative.
Kuroda, Y.; Kawashima, A.; Ogoshi, H.
Chem. Lett. **1996**, 57.

Chapter 3. Molecular Recognition between Self-Organized Porphyrin Dimer Zn Complex and Bidentate Ligands.
Kuroda, Y.; Kawashima, A.; Hayashi, H.; Ogoshi, H.
To be submitted.

Chapter 4. Self-Organized Porphyrin Dimer as Highly Specific Receptor for Pyrazine Derivatives.
Kuroda, Y.; Kawashima, A.; Hayashi, H.; Ogoshi, H.
Submitted to *J. Am. Chem. Soc.*

Chapter 5. Molecular Recognition of Amines by Tetracarboxynaphthylporphyrin.
Kuroda, Y.; Kawashima, A.; Ikeda, K.; Ogoshi, H.
To be submitted.

List of Other Publications

Electronic Structures of Dative Metal-Metal Bonds: Ab Initio Molecular Orbital Calculations of $(OC)_5Os$-$M(CO)_5$ (M=W, Cr) in Comparison with $(OC)_5M$-$M(CO)_5$ (M=Re, Mn).
Nakatsuji, H.; Hada, M.; Kawashima, A.
Inorg. Chem. **1992**, 31, 1740.

New Mode of Porphyrin Complexation with Nucleobase.
Ogoshi, H.; Hatakeyama, H.; Kotani, J.; Kawashima, A.; Kuroda, Y.
J. Am. Chem. Soc. **1991**, 113, 8181.

List of Presentations

Self-Assembling Porphyrin Dimerization Based on Multipoint Molecular Recognition.

Kuroda, Y.; Kawashima, A.; Urai, T.; Ogoshi, H.

The 69th Annual Meeting of Chemical Society of Japan, Kyoto, April, 1995.

Porphyrin Dimerization Based on Multipoint Molecular Recognition.

Kuroda, Y.; Kawashima, A.; Urai, T.; Ogoshi, H.

The 1995 International Chemical Congress of Pacific Basin Societies, Hawaii, December, 1995.

Self-Assembling Zinc Porphyrin Dimerization Based on Multipoint molecular Recognition.

Kuroda, Y.; Kawashima, A.; Hayashi, Y.; Ogoshi, H.

The 70th Annual Meeting of Chemical Society of Japan, Tokyo, April, 1996.

Unusual Atropisomerization of Tetracarboxyphenylporphyrin Derivative.

Kuroda, Y.; Kawashima, A.; Ogoshi, H.

The 11th Symposium on Biofunctional Chemistry, Fukuoka, October, 1996.

List of Other Presentations

Theoretical Study of Electronic Structures of Dative Metal-Metal Bonds$(OC)_5Os$-$M(CO)_5$ (M=W, Cr).

Nakatsuji, H.; Hada, M.; Kawashima, A.

The 61st Annual Meeting of Chemical Society of Japan, Yokohama, April, 1991.